

Orbiting Carbon Observatory-2 & 3 (OCO-2 & OCO-3)



Data Product User's Guide, Operational Level 2 Lite Files

Version 3.0

Revision B

April 2, 2024

Data Release: 11.2 (OCO-2 Level 2 Lite Files), 10/10.4 (OCO-3 Level 2 Lite Files)

National Aeronautics and
Space Administration



Jet Propulsion Laboratory

California Institute of Technology

Pasadena, California

Preparers

| | |
|---------------------|---------------------------|
| Vivienne Payne | Jet Propulsion Laboratory |
| Abhishek Chatterjee | Jet Propulsion Laboratory |
| Robert Rosenberg | Jet Propulsion Laboratory |
| Matthäus Kiel | Jet Propulsion Laboratory |
| Brendan Fisher | Jet Propulsion Laboratory |
| Kacie Shelton | Jet Propulsion Laboratory |
| Le Kuai | Jet Propulsion Laboratory |
| Christopher O'Dell | Colorado State University |
| Tommy Taylor | Colorado State University |
| Gregory Osterman | Jet Propulsion Laboratory |

Document History

| Revision Date | Changes | Author |
|---------------------------------------|--|--------------------------------|
| A – April 11, 2014 | Initial release, prelaunch release of simulated data | G. Osterman and team |
| B – June 16, 2014 | Update to prerelease, correcting MaxMS values | G. Osterman and team |
| C – December 30, 2014 | Updated for release with L1B data | R. Granat and team |
| D – March 30, 2015 | Updated for version 6 release with initial L2 data | R. Granat and team |
| E – June 19, 2015 | Updated for version 7 release | R. Granat and team |
| F – 10 September 10, 2015 | Updated with information on lite files and warn levels | G. Osterman and team |
| G – June 30, 2016 | Updated to provide more information on use of L1b data, add details on aerosol fields. New notes in gray background. | G. Osterman and team |
| H – October 1, 2017 | Updated for new data release: V8 | G. Osterman and team |
| I – December 15, 2017 | Updated to include missing BRDF Table | G. Osterman and team |
| J – October 10, 2018 | Updated for the Version 9 (V9) Release | G. Osterman and team |
| Version 1, Revision A – June 8, 2020 | Version 2 combines OCO-2 and OCO-3 information | G. Osterman and team |
| Version 2, Revision A – July 5, 2022 | Updated for OCO-2 v11 and OCO-3 v10.4 data releases | G. Osterman and team |
| Version 3, Revision A – June 1, 2023 | Updated for the new OCO-2 lite file release, v11.1 | C O'Dell, G. Osterman and team |
| Version 3, Revision B – April 2, 2024 | Updated for OCO-2 Level 2 Lite file release, v11.2 | G. Osterman and team |

The research described in this document was carried out at the Jet Propulsion Laboratory, California Institute of Technology, under a contract with the National Aeronautics and Space Administration.

© 2024. All rights reserved.

TABLE OF CONTENTS

| | | |
|------|--|----|
| 1 | Introduction..... | 1 |
| 1.1 | Quick Summary of What is New with the OCO-2 and OCO-3 Data Products..... | 1 |
| 1.2 | Document Overview..... | 1 |
| 1.3 | Data Products..... | 1 |
| 1.4 | Data Usage Policy | 4 |
| 2 | Mission Overviews | 5 |
| 2.1 | Scope of Document | 5 |
| 2.2 | Observing Modes for OCO-2 | 6 |
| 2.3 | Observing Modes for OCO-3 | 6 |
| 2.4 | More Information on Missions..... | 6 |
| 3 | What is New in OCO-2 v11/v11.1/v11.2..... | 9 |
| 3.1 | Updates for v11.2 | 9 |
| 3.2 | Updates for OCO-2 v11.1 Lite Files | 10 |
| 3.3 | OCO-2 Updates for Version 11r Full Physics Products..... | 10 |
| 4 | What is New OCO-3 v10/v10.4..... | 12 |
| 4.1 | Radiometric errors | 12 |
| 4.2 | Geolocation errors | 13 |
| 4.3 | OCO-3 v10.4 Lite File Update | 14 |
| 5 | OCO-2 v11. 2/v11.1 Lite Files: Description, Data Filtering and Bias Correction | 16 |
| 5.1 | Quality Filtering | 16 |
| 5.2 | Bias Correction..... | 16 |
| 5.3 | CO ₂ scale change..... | 31 |
| 6 | OCO-3 v10: Description, Data Filtering and Bias Correction..... | 32 |
| 6.1 | Quality Filtering and Bias Correction | 32 |
| 7 | Overview of OCO-2 v11 and OCO-3 v10 Data Products..... | 37 |
| 7.1 | File Naming Conventions..... | 37 |
| 7.2 | Data Files Content | 40 |
| 8 | OCO-2 and OCO-3 L2 Standard Data Products..... | 41 |
| 8.1 | Data Description and User Alerts..... | 41 |
| 8.2 | The RetrievalHeader Folder | 41 |
| 8.3 | RetrievalGeometry Folder | 42 |
| 8.4 | RetrievalResults..... | 45 |
| 8.5 | Aerosols | 46 |
| 8.6 | L1B Spectral Parameters | 47 |
| 9 | ABO2 Preprocessor | 48 |
| 9.1 | Prescreening of OCO-2 Soundings for Cloud and Aerosol..... | 48 |
| 9.2 | Key ABO2 Preprocessor Data Fields in Preprocessing Results Folder | 48 |
| 10 | IMAP-DOAS Preprocessor..... | 52 |
| 10.1 | Advanced Cloud and Aerosol Screening..... | 52 |
| 10.2 | Retrievals of Solar-Induced Chlorophyll Fluorescence..... | 52 |
| 10.3 | Key Science Data Fields..... | 52 |

| | | |
|-------|---|-----|
| 11 | Format Specification for OCO-2 v11 and OCO-3 v10 Lite Files..... | 55 |
| 11.1 | Overview | 55 |
| 11.2 | File Structure & Fields | 55 |
| 12 | Full Data Tables for OCO-2 and OCO-3 Level 2 Standard Files (L2Std) | 67 |
| 12.1 | OCO-2 and OCO-3 L2Std Metadata Group..... | 67 |
| 12.2 | Aerosol Results Group..... | 71 |
| 12.3 | Albedo Results Group | 71 |
| 12.4 | BRDF Results | 72 |
| 12.5 | Dispersion Results | 76 |
| 12.6 | L1BSc Sounding Reference Fields..... | 77 |
| 12.7 | L1BSc Spectral Parameter Fields..... | 78 |
| 12.8 | L2 Preprocessing Fields..... | 80 |
| 12.9 | L2 Retrieval Geometry Fields | 82 |
| 12.10 | L2 Retrieval Header Fields..... | 85 |
| 12.11 | L2 Retrieval Results | 85 |
| 12.12 | L2 Spectral Parameters Group..... | 89 |
| 13 | Full Data Tables for OCO-2 and OCO-3 Level 2 Lite Files (LtCO2)..... | 91 |
| 13.1 | OCO-2 and OCO-3 Lite File Main Group Fields..... | 91 |
| 13.2 | OCO-2 and OCO-3 Lite File Preprocessor Group Fields..... | 92 |
| 13.3 | OCO-2 and OCO-3 Lite File Retrieval Group Fields..... | 92 |
| 13.4 | OCO-2 and OCO-3 Lite File Sounding Group Fields..... | 94 |
| 13.5 | OCO-2 and OCO-3 Lite File Meteorology Group Fields..... | 95 |
| 14 | Tools and Data Services..... | 96 |
| 14.1 | HDFView..... | 96 |
| 14.2 | Panoply | 96 |
| 14.3 | Goddard DAAC user interface. | 96 |
| 14.4 | NASA Earth Data Search Client | 96 |
| 15 | Contact Information | 97 |
| 16 | Acknowledgements and References | 98 |
| 16.1 | Acknowledgements | 98 |
| 16.2 | Additional Resources..... | 98 |
| 17 | References..... | 99 |
| 18 | Acronyms..... | 103 |

LIST OF FIGURES

| | |
|---|----|
| Figure 3-1: Differences in X_{CO_2} between the new v11.2 data including GEOS-IT and Copernicus DEM and the v11.1 data using GEOS FPIT. The left figure show the global differences and the right figure shows histograms of the difference for the all the data (black curve), land data (green) and ocean data (blue). The average difference is -0.021 ppm with a standard deviation of 0.244. All comparisons are for July 2023 | 10 |
| Figure 4-1: Lamp radiance trends relative to prelaunch over the course of the OCO-3 mission. The three panels are for the ABO ₂ , WCO ₂ , and SCO ₂ channels. Within each panel, different colors indicate different lamps. Lamp 3 is used roughly 12 times per day, Lamp 2 is used roughly 3 times per day, and Lamp 1 is used roughly 1 time per week. | 12 |
| Figure 4-2: L2 dP values from OCO-3 v10 test data from Aug 2019 to Dec 2020..... | 13 |
| Figure 4-3: Showing the updated bias correction and the improvement in dxco ₂ . Compare the value of dxco ₂ at the top of the figure (prior to the new bias correction) to that at the bottom (corrected). The middle of the figure shows the OCO-3 ZLO and the adjustment in X_{CO_2} with time (orbit number)..... | 15 |
| Figure 5-1: Sounding density maps and time series of soundings for the three v11 training data sets..... | 17 |
| Figure 5-2: Footprint Bias per viewing mode. The land nadir and glint biases were set to be the same in the end, as they were statistically indistinguishable, but the ocean glint footprint biases were statistically different and hence set to their own values..... | 18 |
| Figure 5-3: Plot of X_{CO_2} errors relative to TCCON (ggg2020) for v11.1 land nadir & glint observations. The regression coefficients for a simultaneous fit of all terms are given in blue ("ALL"), bottom left of each panel..... | 22 |
| Figure 5-4: Same as Figure 4-3 but for Land Target Observations..... | 23 |
| Figure 5-5: Same as Figure 5-4 but for Ocean Glint Observations..... | 24 |
| Figure 5-6: Linear Fit of OCO-2 v10 to TCCON X_{CO_2} for a subset of land (ND+GL) mode overpasses of TCCON sites. Both Quality Filtering as well as the feature and footprint biases have been applied..... | 25 |
| Figure 5-7: Bias & Stddev of error as a function of selected outlier filtering variables for land observations. Here, the error is derived using the model comparison..... | 29 |
| Figure 5-8 Sample linear Fit of OCO-2 v11.1 Land ND+GL minus TCCON(ggg2020) vs. time, binned monthly, to determine possible spurious time trend. Bias-corrected X_{CO_2} differences are shown in (Blue); raw X_{CO_2} differences are shown in (Red). In this case, there is an apparent negative trend, but it is only significant at 2.4σ . Comparisons vs models and other viewing modes yield a range of results..... | 30 |
| Figure 8-1: Data folders in the L2Std file..... | 41 |
| Figure 8-2: Variables in the Retrieval Header folder..... | 41 |
| Figure 8-3: Variables in the Retrieval Geometry folder for an OCO-2 file..... | 43 |
| Figure 8-4: Variables in the Retrieval Geometry folder for an OCO-3 file..... | 44 |
| Figure 8-5: Variable in the Retrieval Results folder of the L2Std file..... | 45 |
| Figure 8-6: Variables in the AerosolResults folder..... | 46 |
| Figure 8-7: Variables in the L1BSCSpectralParameters folder..... | 47 |
| Figure 9-1: Screenshot of an HDFView look at the ABO ₂ preprocessor file..... | 49 |

LIST OF TABLES

| | |
|--|----|
| Table 1-1: List of the OCO-2 Level 2 data product types available. The L2 lite file products are recommended for the vast majority of users interested in OCO-2 X_{CO_2} . | 2 |
| Table 3-1: Differences between v11.2 and v11.1 OCO-2 Lite Data Products | 9 |
| Table 5-1: Features used in the OCO-2 v11.2/v11.1 Land Nadir (ND) + Glint (GL) bias correction, with reduction in unexplained variance in parentheses. Note SAA in this table is “Small Area Analysis”. Coefficient uncertainties are 1σ . | 18 |
| Table 5-2: Features used in the OCO-2 v11.2/v11.1 Land Target (TG) bias correction, with reduction in unexplained variance in parentheses. Coefficient uncertainties are 1σ . | 19 |
| Table 5-3: Features used in the OCO-2 v11.2/v11.1 Ocean Glint (GL) bias correction, with reduction in unexplained variance in parentheses. Note SAA in this table is “Small Area Analysis”. Coefficient uncertainties are 1σ . | 21 |
| Table 5-4: Bias Correction formulation for OCO-2 v11.2/v11.1 | 25 |
| Table 5-5: OCO-2 v11.2/v11.1 Quality Filter Thresholds and bit numbers for the associated bit-flags. Range denotes allowed ranges for each variable. All variables must pass for a given sounding to be considered “good” ($xco2_quality_flag = 0$). | 27 |
| Table 5-6: Bit definitions in <code>xco2_qf_simple_bitflag</code> . | 28 |
| Table 5-7: Time Drifts vs. Models & TCCON | 31 |
| Table 6-1: Overview of the truth proxy training datasets for OCO-3 v10. | 32 |
| Table 6-2: Filter variables and limits for the X_{CO_2} quality flag definition in OCO-3 v10. For the definitions of the individual variables see Section 9 or O’Dell et al. (2018), Kiel et al. (2019). | 33 |
| Table 6-3: Bias Correction Parameters for OCO-3 v10. | 34 |
| Table 6-4: Features used in land bias correction, with reduction in unexplained variance in parentheses. Coefficient uncertainties are 1σ . | 35 |
| Table 6-5: Same as Table 6-4 but for glint measurements over water. | 36 |
| Table 7-1: Example L2 filenames for OCO-2 and OCO-3 | 39 |
| Table 12-1: Metadata in Level 2 Standard Data file (L2Std). | 67 |
| Table 12-2: Aerosol Results data in Level 2 Standard Data file (L2Std). | 71 |
| Table 12-3: Albedo Results data in Level 2 Standard Data file (L2Std). | 71 |
| Table 12-4: BRDF Results data in Level 2 Standard Data file (L2Std) and Diagnostic file (L2Dia). | 72 |
| Table 12-5: Dispersion Results fields in Level 2 Standard Data file (L2Std) and Diagnostic file (L2Dia). | 76 |
| Table 12-6: L1BSc sounding reference in Level 2 Standard Data file (L2Std) and Diagnostic file (L2Dia). | 77 |
| Table 12-7: L1BSc SpectralParameters in Level 2 Standard Data file (L2Std) and Diagnostic file (L2Dia). | 78 |
| Table 12-8: Preprocessing Results data in Level 2 Standard Data file (L2Std) and Diagnostic file (L2Dia). | 80 |
| Table 12-9: Retrieval Geometry in Level 2 Standard Data file (L2Std). | 82 |
| Table 12-10: Retrieval Header data in Level 2 Standard Data file (L2Std). | 85 |
| Table 12-11: Retrieval Results data in Level 2 Standard Data file (L2Std). | 85 |
| Table 12-12: Spectral Parameters data in Level 2 Standard Data file (L2Std). | 89 |
| Table 13-1: Provides a description of the fields in the OCO-2 and OCO-3 Lite Data Product files. | 91 |

Table 13-2: Contains description of the fields in the “Preprocessor” folder of the Lite files..... 92
Table 13-3: Contains description of the fields in the “Retrievals” folder of the Lite files. 92
Table 13-4: Contains description of the fields in the “Sounding” folder of the Lite files..... 94
Table 13-5: Fields in the “Meteorology” folder of the OCO-2, OCO-3 Lite files. 95

1 Introduction

1.1 Quick Summary of What is New with the OCO-2 and OCO-3 Data Products

This update to the Data User's Guide is to provide information on the latest Orbiting Carbon Observatory-2 (OCO-2) Level 2 (L2) data products. The Orbiting Carbon Observatory-3 (OCO-3) data products have not changed since the release of the previous version of this document.

OCO-2 is releasing a new version of the L2 Lite File data products, v11.2. This data product update reflects a change in the meteorological products used as inputs to the L2 retrievals as well as a change to the way that the Digital Elevation Map (DEM) is used as input. More information is provided in Section 3.1.

There are no changes to the OCO-3 data products, at this time.

1.2 Document Overview

This document provides a brief overview of the OCO-2 and OCO-3 missions and then discusses the content of the publicly available Level 2 (L2) "Standard" data products. The data versions are the OCO-2 Level 2 (L2) release version 11 (v11) and the OCO-3 L2 data (v10).

The document also describes the data in the L2 "Lite" files, which are different from the L2 Standard products in that they are daily products with additional post processing data fields. They also include screened and bias corrected X_{CO_2} values using the bias corrections described later in this document. The OCO-3 Lite data product is labeled as v10.4.

Much of the mission description and background information that was contained in previous versions has been removed to improve the utility of this document as a starting point for use of the data products. Some of the key references for background information are highlighted in Section 2.4 and the full list of references are in Section 15.

1.3 Data Products

The primary product delivered by both OCO-2 and OCO-3 are the spatially resolved estimates of the column-averaged dry air mole fraction of carbon dioxide (CO_2). This quantity, called X_{CO_2} by members of the atmospheric carbon science community, quantifies the average concentration of carbon dioxide in a column of dry air extending from Earth's surface to the top of the atmosphere. Estimates of X_{CO_2} are derived by taking the ratio of the column integrated number densities of carbon dioxide and molecular oxygen along the optical path between the Sun, the surface footprint, and the instrument, and then multiplying these results by the column-averaged oxygen concentration (0.20935). These carbon dioxide and oxygen number densities are estimated from high-resolution spectra of reflected sunlight, collected by the Observatory's instrument at wavelengths (colors) within the 0.765-micron molecular oxygen A band and two carbon dioxide bands centered at wavelengths near 1.61 and 2.06 microns. In addition, OCO-2 and OCO-3 are able to make measurements of steady-state Solar-Induced chlorophyll Fluorescence (SIF).

Both missions produce different levels of data product for the user community that will provide comprehensive mission data results. These results can be summarized as:

- Level 1A – full orbits or fractions of orbits of calibrated and geographically located science and calibration data with quality control flags set.
- Level 1B – full orbits or fractions of orbits of calibrated and geographically located spectral radiances from the spectral channels centered on the 0.765-micron molecular oxygen A band and the carbon dioxide bands at wavelengths near 1.61 and 2.06 microns. This product contains a unique record of every sounding the instrument collects while viewing Earth during a single spacecraft orbit—approximately 74,000 soundings. Each sounding consists of collocated (observing the same location) spectra from the three spectrometer channels.
- Level 2 – full orbits or fractions of orbits of geographically located estimates of the column-averaged dry air mole fraction of carbon dioxide (also called X_{CO_2}) and several atmospheric and geophysical properties collected during each spacecraft orbit. This product typically includes more than 4,000 retrievals of the concentration of atmospheric carbon dioxide in cloud-free scenes, as well as surface pressure, surface albedo, aerosol content and water vapor and temperature profiles. Estimates of the solar-induced chlorophyll fluorescence are provided in a preprocessor file (L2IDP).

The Level 1B and L2 are available at the NASA Goddard Earth Science Data and Information Services Center (GES DISC). More information on obtaining the data is provided in Sections 12 and 14.

Each mission produces several different types of L2 data products that are summarized in Table 1-1. It is important to note that the latest changes in data products that are detailed in this update to the User's Guide involve changes to the OCO-2 L2 Lite data files. There were no updates to the OCO-3 data products at the time this document was released (V3.0, Revision B, April 2, 2024).

In addition, OCO-2 and OCO-3 both produce data products from two different production streams; “Forward Processing” and “Retrospective Processing”. It is recommended that data from the Retrospective data processing stream be used for scientific analysis. It is also recommended that the Lite File data products can be utilized by most data users for scientific analysis.

Table 1-1: List of the OCO-2 Level 2 data product types available. The L2 lite file products are recommended for the vast majority of users interested in OCO-2 X_{CO_2} .

| Data Product Name | Description | OCO-2 Data Product Label | Latest OCO-2 Version | OCO-3 Data Product Label | Latest OCO-3 Version |
|---|--|--------------------------|----------------------|--------------------------|----------------------|
| L2 Full Physics Lite Retrospective Processing | The L2 data products, screened and bias corrected. Data fields selected for the general data user. | OCO2_L2_Lite_FP | v11.2 | OCO3_L2_Lite_FP | v10.4 |

| Data Product Name | Description | OCO-2 Data Product Label | Latest OCO-2 Version | OCO-3 Data Product Label | Latest OCO-3 Version |
|---|--|--------------------------|--|--------------------------|----------------------|
| L2 Full Physics Standard Retrospective Processing | The Standard data products contain a more extensive list of variables for the more experienced data user. There is no prescreening or bias correction, though all variable needed to perform screening or bias correction are included | OCO2_L2_Standard | v11r | OCO3_L2_Standard | v10.4r |
| L2 Full Physics Diagnostic Retrospective Processing | These files contain all the fields in the standard product files but also include additional fields for more advanced analysis | OCO2_L2_Diagnostic | v11r | OCO3_L2_Diagnostic | v10r |
| L2 Meteorological Retrospective Processing | These files contain the meteorological fields used as inputs to the L2 retrievals. | OCO2_L2_Met | v11r (prior to April 1, 2024) v11.2 (after April 1, 2024) | OCO3_L2_Met | v10r |
| L2 IMAP Retrospective Processing | Provides data from the L2 preprocessing step using the IMAP/DOAS preprocessor | OCO2_L2_IMAPDOAS | v11r | OCO3_L2_IMAPDOAS | v10r |
| L2 A-band Retrospective Processing | Provides data from the L2 preprocessing step using the A-Band preprocessor | OCO2_L2_ABand | v11r | OCO3_L2_ABand | v10r |

| Data Product Name | Description | OCO-2 Data Product Label | Latest OCO-2 Version | OCO-3 Data Product Label | Latest OCO-3 Version |
|---|--|--------------------------|----------------------|--------------------------|----------------------|
| L2 CO ₂ Prior Retrospective Processing | Provide data for the a priori information on CO ₂ used in the L2 retrievals | OCO2_L2_CO2Prior | v11r | OCO3_L2_CO2Prior | v10r |

1.4 Data Usage Policy

These data have been produced by the OCO-2 and OCO-3 projects and are provided freely to the public. In order to improve our products and have continued support for this work, we need user feedback and user acknowledgement of data usage. Therefore, we request that when publishing using OCO-2 and/or OCO-3 data, please acknowledge NASA and the individual projects.

- Include OCO-2 and/or OCO-3 as a keyword to facilitate subsequent searches of bibliographic databases if it is a significant part of the publication.
- Include a bibliographic citation for OCO-3 and/or OCO-2 data. Some of the most relevant citations currently are listed in Section 2.4.
- Include the following acknowledgements:
 - “These data were produced by the OCO-2 project at the Jet Propulsion Laboratory, California Institute of Technology, and obtained from the OCO-2 data archive maintained at the NASA Goddard Earth Science Data and Information Services Center.”
 - “These data were produced by the OCO-3 project at the Jet Propulsion Laboratory, California Institute of Technology, and obtained from the OCO-2 data archive maintained at the NASA Goddard Earth Science Data and Information Services Center.”
- We recommend sending courtesy copies of publications to the OCO-2 Project Scientist/OCO-3 Deputy Project Scientist, Vivienne Payne (Vivienne.H.Payne@jpl.nasa.gov), OCO-3 Project Scientist/OCO-2 Deputy Project Scientist, Abhishek Chatterjee (Abhishek.Chatterjee@jpl.nasa.gov).

2 Mission Overviews

The Orbiting Carbon Observatory–2 (OCO-2) is NASA's first dedicated CO₂ monitoring satellite. OCO-2 is a “carbon copy” of the Orbiting Carbon Observatory (OCO), which was lost in 2009, when its launch vehicle malfunctioned and failed to reach orbit. A general description of the OCO mission is given in Crisp et al. [2004, 2008]. Most of the information is valid for OCO-2, but a few changes were needed to address known problems, replace obsolete hardware, or address operational changes. Changes that affect the OCO-2 data products are highlighted below.

The OCO-2 spacecraft carries and points a single instrument that incorporates 3, co-bore sighted, imaging, grating spectrometers. This instrument collects high-resolution spectra of reflected sunlight in the molecular oxygen (O₂) A band, centered near 765 nm, and in the CO₂ bands centered near 1610 and 2060 nm. Each spectrometer collects 24 spectra per second, yielding about a million observations each day over the sunlit hemisphere. Coincident measurements from the three spectrometers are combined into “soundings” and analyzed with a “full-physics” retrieval algorithm to yield estimates of X_{CO_2} . Clouds and optically thick aerosols preclude observations of the full atmospheric column in many regions, but this approach is expected to yield over 100,000 full-column X_{CO_2} estimates each day.

OCO-2 was successfully launched from Vandenberg Air Force Base on a Delta-II 7320 launch vehicle at 2:56 AM PDT on July 2, 2014. The Observatory completed its in-orbit check-out phase in October 2014 and is now routinely collecting almost 1 million soundings over the sunlit hemisphere each day. More than 10% of these measurements are sufficiently cloud free to yield precise estimates of the column-averaged CO₂ dry air mole fraction, X_{CO_2} .

The Orbiting Carbon Observatory-3 (OCO-3) continues NASA's carbon dioxide measurements from space, also measuring X_{CO_2} and solar-induced fluorescence (SIF) from space. OCO-3 was launched from the Kennedy Space Center on May 4, 2019 via a Space-X Falcon 9 and Dragon capsule. The instrument was installed as an external payload on the Japanese Experimental Module Exposed Facility (JEM-EF) of the International Space Station (ISS) with a nominal mission lifetime of 3 years. The precessing orbit of the ISS allows for viewing of the Earth at all latitudes less than approximately 52 degrees, with a ground repeat cycle that is much more complicated than the polar-orbiting satellites that so far have carried all of the instruments capable of measuring carbon dioxide from space. The spectrometer used in OCO-3 is a direct copy of the OCO-2 spectrometer. As such, OCO-3 has similar instrument sensitivity and performance characteristics to OCO-2, making measurements of X_{CO_2} with precision better than 1 ppm at 3 Hz, with each viewing frame containing eight footprints approximately 1.6 km by 2.2 km in size. However, the physical configuration of the instrument aboard the ISS, as well as the use of a new pointing mirror assembly (PMA), will alter some of the characteristics of the OCO-3 data compared to OCO-2. Specifically, there will be significant differences from day to day in the sampling locations and time of day. In addition, the flexible PMA system allows for a much more dynamic observation-mode schedule.

Descriptions of the instrument properties and the data fields/products provided in this document for OCO-2 applies to OCO-3 except where noted otherwise.

2.1 Scope of Document

This document is intended to get the user started with the OCO-2 and/or OCO-3 Level 2 data. The document contains information on using data for both instruments that are contained within the Level 2 (L2) Standard files (L2Std) and the Level 2 Lite files (Lite). The document contains

the full data tables for both files with brief descriptions of each variable in the data. A description is provided for the recommended data screening for both instruments and also a method for bias correcting the retrieved X_{CO_2} data. The Lite data files provide both the retrieved value for X_{CO_2} (called `xco2` in the L2Std file and `xco2_raw` in the Lite file) and an X_{CO_2} value that has been through the recommended data screening and bias corrected (`xco2` in the Lite files).

2.2 Observing Modes for OCO-2

The OCO-2 spacecraft carries and points a 3-channel imaging grating spectrometer designed to record high-resolution spectra of reflected sunlight in O₂ and CO₂ bands as it flies over the sunlit hemisphere. It makes observations in three modes; nadir, glint and target. The nadir and glint observation cadence has evolved over the life of the mission. During the first year of observations the instrument observed 16 days in glint mode followed by 16 days of nadir observations (note the OCO-2 cycle for a near repeat of observations is 16 days or 233 orbits). After the first year, the observation strategy changed to glint only observations over the majority of the Pacific and Atlantic oceans and alternating nadir/glint observations on all other orbits.

Target mode observations are taken primarily for purposes of validating the instrument performance against ground-based observations from the Total Carbon Column Observation Network (TCCON) (Wunch et al., 2010). The validation strategy and findings have been described in Wunch et al. (2011 and 2017) and Kiel et al. (2019). Target mode observations are also used for evaluating the OCO-2 SIF products.

2.3 Observing Modes for OCO-3

The nominal planned viewing strategy of OCO-3 is to take down-looking nadir viewing measurements over land to minimize the probability of cloud and aerosol contamination. Over water measurements will be taken near the specular reflection spot (glint viewing) to maximize the signal over the low reflectivity surface.

However, unlike OCO-2, which performs complex maneuvers of the entire satellite bus to observe ground targets, the OCO-3 instrument is fitted with an agile 2-D pointing mechanism, i.e., a pointing mirror assembly (PMA). This allows for rapid transitions between nadir and glint mode (less than 1 minute). The PMA also allows for target mode observations, similar to those taken by OCO-2; mostly TCCON ground sites for use in validation. The PMA provides the ability to scan large contiguous areas (order 80 km by 80 km), such as cities and forests, on a single overpass. These are known as “snapshot” mode and provide for fine scale spatial sampling of CO₂ and SIF variations unlike any current satellite system. Together with OCO-2, the OCO-3 snapshot mode can be used to gather a significant fraction of overlapping data. More details are contained in Eldering et al. (2018).

2.4 More Information on Missions

Mission background information is available in the OCO-2/OCO-3 Algorithm Theoretical Basis Documents (ATBD). There are separate ATBDs for the Level 1B algorithm and the Level 2 algorithm. A mission description is included in both documents. These documents are available at GES DISC (<https://disc.gsfc.nasa.gov/information/documents?keywords=OCO-2&title=OCO-2%20Documents>).

Listed below are some of the primary publications that provide information on different aspects of the missions. A full list of mission publications are available on the project web sites (<https://ocov2.jpl.nasa.gov/science/publications/>) and (<https://ocov3.jpl.nasa.gov/science/publications/>):

- OCO-2 Early Mission Performance:
 - Crisp D. et al. (2017), The on-orbit performance of the Orbiting Carbon Observatory-2 (OCO-2) instrument and its radiometrically calibrated products, *Atmos. Meas. Tech.*, 10, 59–81, 2017, <https://doi.org/doi:10.5194/amt-10-59-2017>
 - Eldering A. et al., (2017), The Orbiting Carbon Observatory-2 early science investigations of regional carbon dioxide fluxes, *Science*, 358, 2017, <http://dx.doi.org/10.1126/science.aam5745>.
- OCO-2 Algorithm and Validation:
 - Kiel M. et al. (2019), How bias correction goes wrong: measurement of X_{CO_2} affected by erroneous surface pressure estimates, 12, <https://doi.org/10.5194/amt-12-2241-2019>.
 - Wunch D. et al. (2011a), The Total Carbon Column Observing Network, *Phil. Trans. R. Soc. A*, 369, 2087–2112, 2011, <https://doi.org/doi:10.1098/rsta.2010.0240>.
 - Wunch D. et al. (2011b), A method for evaluating bias in global measurements of CO₂ total columns from Space, *Atmos. Chem. Phys.*, 11, 20899-20946, 2011, <https://doi.org/doi:10.5194/acp-11-12317-2011>.
 - Wunch D. et al. (2017), Comparisons of the Orbiting Carbon Observatory-2 (OCO-2) X_{CO_2} Measurements with TCCON, *Atmos. Meas. Tech.*, 10, 2209-2238, 2017, <https://doi.org/doi:10.5194/amt-10-2209-2017>.
 - Jacobs N. et al. (2024), The importance of digital elevation model accuracy in X_{CO_2} retrievals: improving the Orbiting Carbon Observatory 2 Atmospheric Carbon Observations from Space version 11 retrieval product, *Atmos Meas. Tech.*, 17, 1375-1401, <https://doi.org/10.5194/amt-17-1375-2024>.
 - Taylor, T. E. et al : Evaluating the consistency between OCO-2 and OCO-3 X_{CO_2} estimates derived from the NASA ACOS version 10 retrieval algorithm, *Atmos. Meas. Tech.*, 16, 3173–3209, <https://doi.org/10.5194/amt-16-3173-2023>, 2023.
- OCO-3:
 - Eldering A. et al. (2019), The OCO-3 mission: measurement objectives and expected performance based on 1 year of simulated data, *Atmos. Meas. Tech.*, 12, 4, 2341-2370, 2019, <https://doi.org/doi:10.5194/amt-12-2341-2019>.
 - Taylor T.E. et al. (2020), OCO-3 early mission operations and initial (vEarly) X_{CO_2} and SIF retrievals, *Rem. Sens. Env.*, 251, 112032, <https://doi.org/10.1016/j.rse.2020.112032>.
- SIF:
 - Doughty, R. et al. (2022), Global GOSAT, OCO-2, and OCO-3 solar-induced chlorophyll fluorescence datasets, *Earth Syst. Sci. Data*, 14, 1513–1529, <https://doi.org/10.5194/essd-14-1513-2022>, 2022.

- Sun Y. et al. (2018), Overview of Solar-Induced chlorophyll Fluorescence (SIF) from the Orbiting Carbon Observatory-2: Retrieval, cross-mission comparison, and global monitoring for GPP, *Rem. Sens. Env.*, 209, 808-823, 2018, <https://doi.org/10.1016/j.rse.2018.02.016>.
- Frankenberg C. et al. (2014), Prospects for chlorophyll fluorescence remote sensing from the Orbiting Carbon Observatory-2, *Rem. Sens. Env.*, 147, 1-12, 2014, <https://doi.org/doi:10.1016/j.rse.2014.02.007>.

3 What is New in OCO-2 v11/v11.1/v11.2

3.1 Updates for v11.2

Version 11.2, which will be in place for all data produced on and after April 1, 2024 includes two significant changes:

- A transition in the meteorological data products used as inputs to the L2 retrievals
- A continuation of the transition to a new Digital Elevation Model first introduced in the v11.1 Lite data products.

The primary change involves the meteorological data inputs that are used for the OCO-2 and OCO-3 L2 retrievals. The Global Modeling and Assimilation Office (GMAO) has recently switched from the [GEOS FP-IT](#) product to the [GEOS-IT](#) product. OCO-2 has made the decision to switch to using the GEOS-IT products in the forward processing and retrospective processing on April 1, 2024 and switch to the new data label of V11.2. All OCO-2 products prior to April 1, 2024 will remain as V11.1 products that use the GEOS FP-IT meteorological data as input for the retrievals.

In v11.1 products, the Copernicus GLO90 DEM¹ was introduced for modification of the ‘dP’ term in the bias correction. This would show up in the v11.1 Lite files in the X_{CO2} product that is bias corrected. In v11.2, the new DEM is also used for determining the elevation of the OCO-2 footprints. This will be true for both the complete L2 Full Physics data products and the v11.2 Lite products. Table 3-1 summarizes the changes between v11.1 and v11.2. A description of the DEMs and the effects that the changes in the DEM can have on X_{CO2} data is discussed in Jacobs et al. (2024).

Table 3-1: Differences between v11.2 and v11.1 OCO-2 Lite Data Products

| Processing Date | Data Product | Meteorological Data | DEM |
|----------------------------|------------------------------|---------------------|------------------|
| Prior to April 1, 2024 | v11 L2 Full Physics Products | GEOS FP-IT | NASADEM+ |
| | v11.1 Lite Files | GEOS FP-IT | Copernicus GLO90 |
| On and after April 1, 2024 | v11.2 Full Physics Products | GEOS-IT | Copernicus GLO90 |
| | v11.2 Lite Files | GEOS-IT | Copernicus GLO90 |

The transition to the new GMAO-IT data products will lead to a noticeable discontinuity in the X_{CO2} data record from OCO-2. The effect is small, but varies regionally as can be seen in Figure 3-1. This discontinuity should be kept in mind when using the OCO-2 data for time periods that stretch beyond April 1, 2024.

¹ The Copernicus WorldDEM™-90 Digital Elevation Model, 90m horizontal resolution (copyright DLR e.V., 2010-2014, Airbus Defence and Space GmbH 2014-2018) was provided under Copernicus by the European Union and ESA; all rights reserved.
<https://spacedata.copernicus.eu/collections/copernicus-digital-elevation-model> .

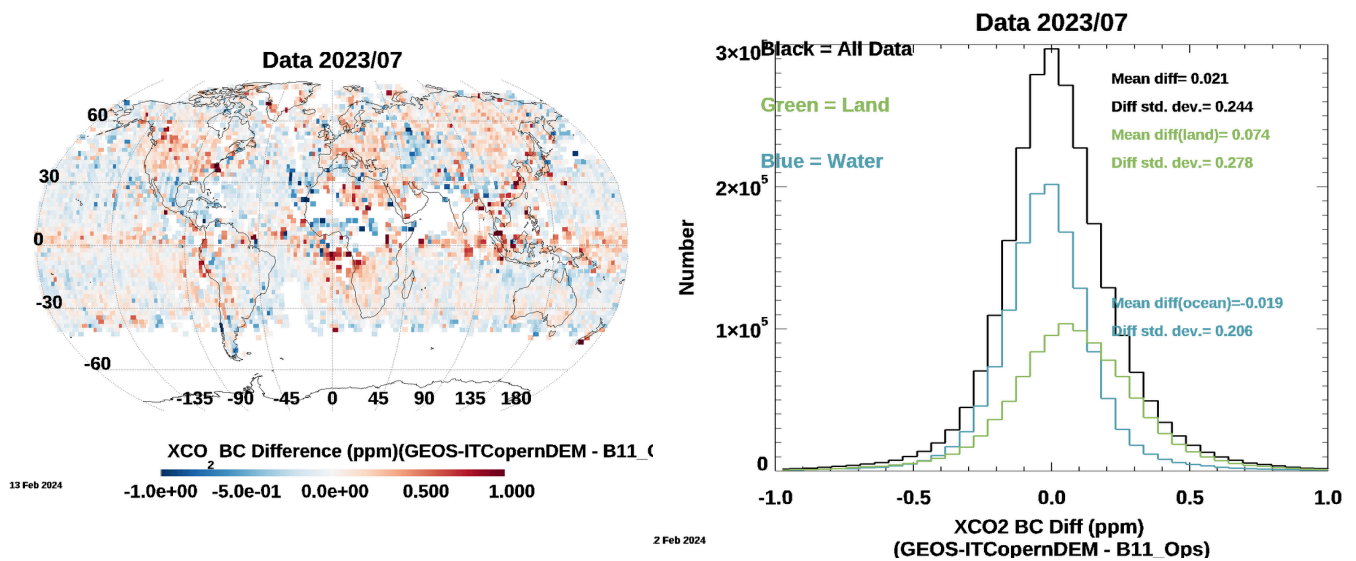


Figure 3-1: Differences in XCO₂ between the new v11.2 data including GEOS-IT and Copernicus DEM and the v11.1 data using GEOS FPIT. The left figure show the global differences and the right figure shows histograms of the difference for the all the data (black curve), land data (green) and ocean data (blue). The average difference is -0.021 ppm with a standard deviation of 0.244. All comparisons are for July 2023

3.2 Updates for OCO-2 v11.1 Lite Files

Version 11.1 is a minor update to version 11 in which only the filtering and bias corrected values of XCO₂ were changed, along with a few other variables. The primary change was related to modifications of surface elevation (which in turn modifies surface pressure). This process is described in detail in Jacobs et al. (2024). Specifically, the v11.1 changes include:

- Modification to ‘dP’ terms in the bias correction using the Copernicus GLO90 DEM², as this was found to be significantly more accurate than the previous DEM.
- Filter variables ‘co2_ratio’ and ‘h2o_ratio’ have now been bias corrected, and the latter has been scaled according to its uncertainty. The bias-corrected versions (‘co2_ratio_bc’ and ‘h2o_ratio_bc’) replace the former terms for quality filtering.
- Slightly updated filtering and bias correction as compared to v11.

3.3 OCO-2 Updates for Version 11r Full Physics Products

The version 11 of the OCO-2 L2 products includes several improvements and fixes when compared to previous versions. The most important updates in v11 include:

- Improvements in the LIB processing, including: gain degradation, dispersion trend, instrument line shape (ILS), noise model, footprint dependence
- Mitigation of previous issue with inadvertent flagging of majority of soundings over South Atlantic Anomaly

- Improvements to increase the throughput of the solar-induced chlorophyll fluorescence (SIF) retrievals
- Improvements to the IMAP-DOAS preprocessor, including updates to its spectroscopy to match that used by the L2 Full-Physics algorithm.
- Spectroscopy updates
- Updates to the absorption coefficient scaling factors used in the L2 retrievals that will help mitigate the overall X_{CO_2} bias and CO₂ profile shape issues
- Improvements to the ocean surface treatment that improve the linearity of retrievals over ocean
- Minor updates to land bidirectional reflectance distribution function (BRDF)
- New CO₂ *a priori* profiles
- Minor changes to the rules that govern sounding selection
- A fix for an issue with SIF availability for target mode observations (this will be seen in the L2 SIF lite files)

Users should note that the OCO-2 v11 level 2 standard and diagnostic data files (L2Std, L2Dia) will be smaller than in previous versions. This is due to new compression used in creating the files, as well as the removal of the albedo fields (Albedo folder in files).

4 What is New OCO-3 v10/v10.4

4.1 Radiometric errors

The radiometric calibration of v10 was significantly improved compared to vEarly. In contrast to vEarly, which contains a discontinuity at April 8, 2020, all lamp data across the entire mission is now processed with the same algorithms. The key improvement for v10 was to tie radiometric degradation to Lamp 1, which is used roughly once a week. Initially, Lamp 3 was being used with no correction for lamp aging. Additionally, v10 featured an updated stray light model which aims to account for spatial variability.

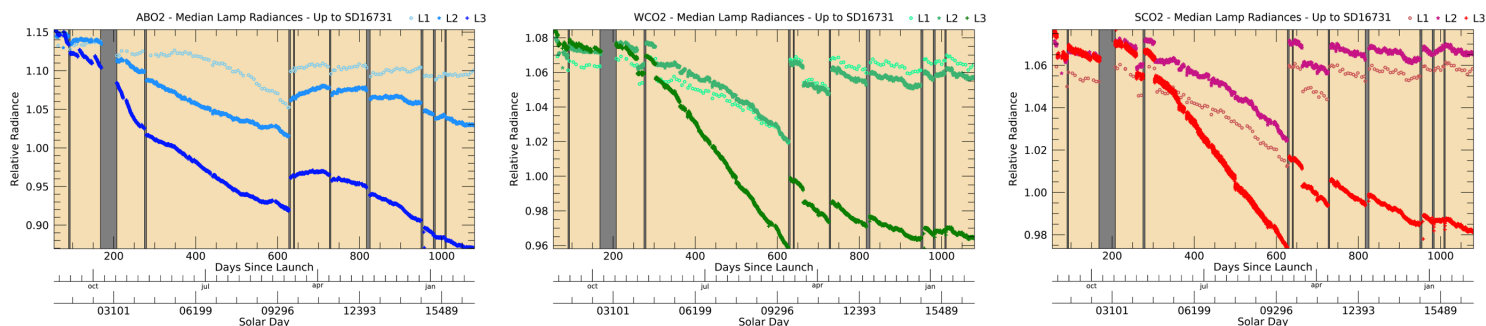


Figure 4-1: Lamp radiance trends relative to prelaunch over the course of the OCO-3 mission. The three panels are for the ABO2, WCO2, and SCO2 channels. Within each panel, different colors indicate different lamps. Lamp 3 is used roughly 12 times per day, Lamp 2 is used roughly 3 times per day, and Lamp 1 is used roughly 1 time per week.

Since the focal plane arrays are operated at cryogenic temperatures, ice accumulates over time, leading to increased stray light and decreased throughput. Several decontaminations have been performed to counteract this. The largest discontinuity in the gain degradation record (Figure 4-1) occurs following the decon from solar day 9720, which was nearly a year after the previous one.

A key indicator of calibration improvements was a reduction in time dependent and footprint dependent behavior in the L2 data in v10 compared to vEarly. The science team examined the behavior of dP , the difference between the retrieved and prior surface pressure, a parameter in the retrieval that is very sensitive to ABO2 radiometric calibration. We found that this parameter was more stable in v10 than in vEarly, although an increase in value correlated with detector icing remained. A clear increase is visible between June 2020 and Jan 2021. The dP test data record shown in Figure 4-2 ends in Dec 2020, just before a major decontamination event.

In addition to the time dependence, there is some variation in the dP values among footprints, which is consistent with our understanding that icing impacts are spatially nonuniform, but the magnitude in v10 is substantially reduced from vEarly. This is also seen in the throughput of data in L2 which worsened later in the vEarly record, especially for high numbered footprints. This pattern is not seen in v10.

Since the release of the OCO-3 v10 dataset, the team has continued to further characterize Level 1B calibration. The v10.4r Lite products incorporate an ad hoc correction to the Level 2 X_{CO_2} that aims to account for outstanding issues in the Level 1B calibration.

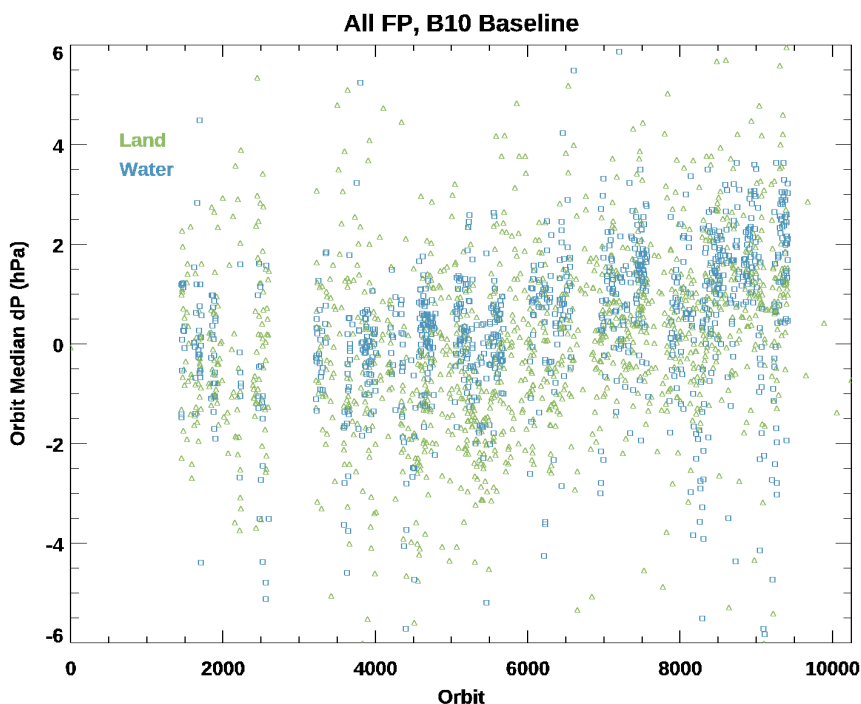


Figure 4-2: L2 dP values from OCO-3 v10 test data from Aug 2019 to Dec 2020.

4.2 Geolocation errors

Geolocation errors were substantially improved for v10 compared to vEarly in three general areas. First, calibration of the Pointing Mirror Assembly (PMA) was completed and integrated directly into the geolocation algorithm. Second, an offset between the science detectors and the PMA camera was characterized and removed. Third, the OCO-3 project obtained a supplemental attitude source, derived from the CALET instrument which is near OCO-3 on the JEM-EF, for periods when the OCO-3 Stellar Reference Unit (SRU) is not available. The supplemental attitude data reduces geolocation errors associated with flexure between the ISS center, where the primary ISS ephemeris is reported, and the OCO-3 location on the JEM-EF. For periods when the OCO-3 SRU is available, geolocation errors are typically less than 500 m. For periods where the SRU is not available and CALET-derived attitude is available, errors are typically less than 1 km. Finally, a small percentage of the data remains when neither of the two primary attitude sources are available, and for these periods the errors are typically less than 2 km, with a small “tail” with errors up to 3 km. Starting with v10, the OCO-3 L2 products contain a field called `/RetrievalGeometry/retrieval_att_data_source`. A value of 1 in this field represents the “no supplemental attitude” case, with the largest errors. Other values in the range 2-9, have good geolocation, with the errors listed above. The different numbers in the 2-9 range represent various permutations of SRU and CALET, accounting for nominal operations with the possibility of small gaps.

The improvements that rely on the CALET data are only available in the retrospective processing (v10r). In the forward stream processing, we rely solely on the OCO-3 SRU and ISS BAD data, so geolocation performance may be poorer than in the retrospective data. The attitude source information that is included in the product can help the user to differentiate these cases.

4.3 OCO-3 v10.4 Lite File Update

The v10.4r Lite file release addresses a problem with the v10r X_{CO_2} data. The new Lite file data version was necessary because it was noticed during routine validation of the v10r data product that a time dependent bias could be seen in the OCO-3 X_{CO_2} data compared to collocated OCO-2 observations (dX_{CO_2}). The magnitude of the bias is correlated with the amount of time between instrument decontamination cycles, and so is assumed to be associated with icing on the OCO-3 detectors. One proxy for the build-up of ice on the detectors is an instrument calibration metric called the zero-level-offset (ZLO). For OCO-3, ZLO is measured for both the weak CO_2 and the O_2 A-band, but the weak CO_2 band measurements of ZLO are less noisy, making them a more convenient metric than A-band ZLO. A bias correction term was calculated from a fit of dX_{CO_2} to the ZLO from the weak CO_2 band. Comparisons between the new bias corrected X_{CO_2} data and data from the Total Carbon Column Observation Network show that v10.4r Lite X_{CO_2} data is minimally affected by the time dependence related to build up of ice on the detectors. Comparisons of OCO-3 data to OCO-2 X_{CO_2} also show that the effects of the ice build up have been resolved by the updated bias correction. The impact and magnitude of the correction can be seen in Figure 1-1. We have also completed validation of the OCO-3 v10.4r Lite products against TCCON and multimodel median, showing over all good agreement with these truth proxies – more details on these are available in Section 3

The OCO-3 v10.4r Lite data product should be used instead of the previous v10r Lite. Note that the time-dependent X_{CO_2} correction for the v10.4r product comes in via the Level 2 bias correction. (Improvements between the previous OCO-3 v10r and vEarly data products were achieved via updates to the Level 1b radiometric calibration and geolocation.)

Users should be aware that the geolocation of the retrospective product in some cases will be superior to the forward stream of the data.

The L2 algorithms used to create the OCO-3 data are the same as those that are used for the current OCO-2 v10 L2 data release, to aid in the use of the two datasets together.

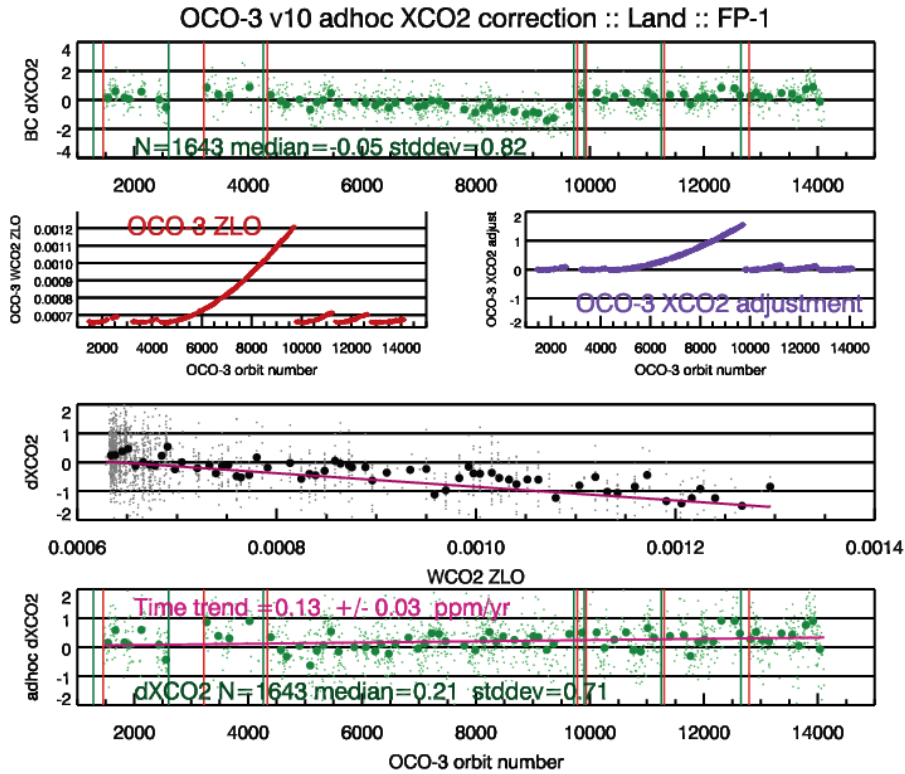


Figure 4-3: Showing the updated bias correction and the improvement in dxco2. Compare the value of dxco2 at the top of the figure (prior to the new bias correction) to that at the bottom (corrected). The middle of the figure shows the OCO-3 ZLO and the adjustment in X_{CO2} with time (orbit number).

5 OCO-2 v11.2/v11.1 Lite Files: Description, Data Filtering and Bias Correction

In order to develop both the screening criteria and bias correction parameters, a set of “truth proxies” are defined:

- TCCON (compared to OCO-2 data acquired in nadir, glint and target modes)
- The “Small Area Analysis”, in which X_{CO_2} is assumed to be constant for OCO-2 observations taken over distances $< \sim 100$ km within the same orbit.
- A multi-model mean of 4 models (CarbonTracker CT2022+NRT2023-1, University of Edinburgh v5.1, CAMS v21r1, and the GMAO GEOS5 CO₂ product dubbed LoFI, version m2ccv1sim) that have all assimilated in-situ data, and only using soundings for which all the model values agree with each other to within a specified tolerance.

The process for using the truth proxies to develop screening and bias correction criteria and the full screening/bias correction process is available in O'Dell et al., (2018) with specifics for v11.1 provided below.

Note that the changes made for OCO-2 v11.2 do not affect the bias correction process that was performed for v11.1. The bias correction terms and analysis are the same for both versions.

5.1 Quality Filtering

Users of OCO-2 L2Std data can do a rough quality filtering of the soundings using the `outcome_flag` variable, which is set to “1” or “2” for retrievals completed successfully.

When using the data contained in the Lite files, filtering can be done with `xco2_quality_flag` (“0” is good). This filter has been derived by comparing retrieved X_{CO_2} for a subset of the data to the various truth proxies, and identifying thresholds for different variables that correlate with poor data quality. It applies quality filters based on a number of retrieved or auxiliary variables that correlate with excessive X_{CO_2} scatter or bias (described below).

5.2 Bias Correction

The bias correction (BC) maps the original X_{CO_2} retrievals of the OCO-2 L2 algorithm to our best estimate of X_{CO_2} . We used v11 data spanning November of 2014 through 2022. The BC approach implemented in the Lite files uses regional analysis to identify, within the OCO-2 X_{CO_2} data records themselves, which terms best predict bias (or Unexplained Variance (%UV)) in the retrievals. Our definition of %UV always uses a null-hypothesis denominator for ease of comparison. The full bias correction procedure was similar to that used in version V8, described in detail in O'Dell et al. (2018).

We have constructed several training datasets for our bias correction, such that the set provides an approximation of the X_{CO_2} truth against which the retrievals are evaluated while attempting to ensure that real X_{CO_2} atmospheric gradients are not removed by in the BC. The model-based training data set was the largest, with ~ 9 million soundings, and includes data over Greenland and Antarctica (new starting in v10). The TCCON-based data set was also large, with ~ 7 million soundings. Note that we used TCCON ggg2020 for the v11.2/v11.1 bias correction, as ggg2014 has been retired and replaced with this new version. A new small area dataset was created with 7.1M soundings (more than double v11). Figure 5-1 shows the spatial distribution of these training data sets. We used v11 data spanning February 2015 through the end of 2022

for all cases, so roughly 7 years of OCO-2 data are included in the training data for filtering and bias correction.

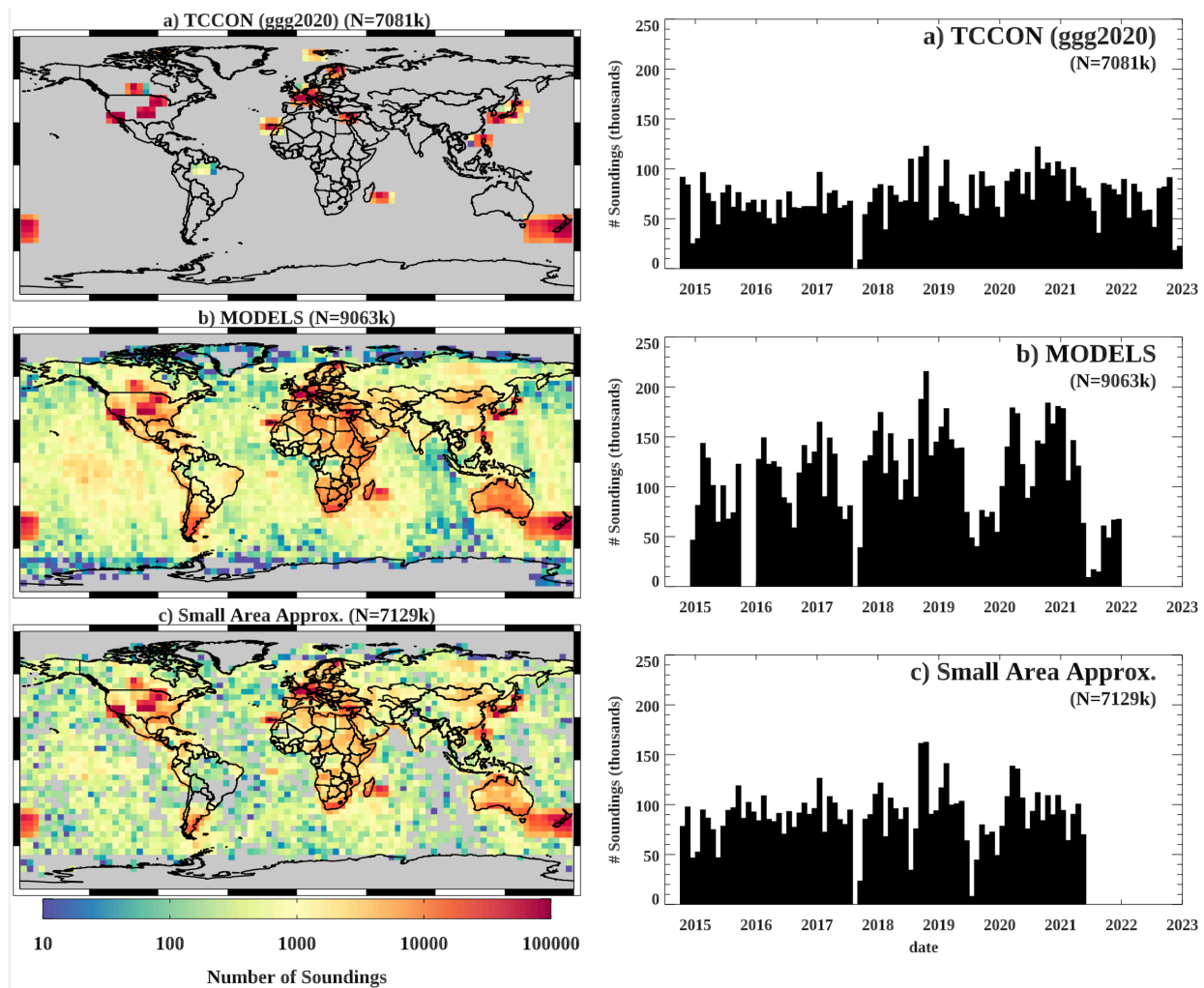


Figure 5-1: Sounding density maps and time series of soundings for the three v11 training data sets.

The three steps to finalize the terms in the BC equation are as follows:

$$XCO_2 \text{ Corrected} = \frac{XCO_2 \text{ Raw} - \text{FOOT}[fp, mode] - \text{FEATS}[mode]}{\text{TCCON_ADJUST}[mode]}$$

5.2.1 Step 1 – Removing Footprint Bias (term FOOT)

OCO-2 obtains 8 side-by-side, simultaneous, nearly-collocated measurement scenes called footprints. Although the XCO_2 retrievals made from these soundings should, on average, be identical, there are small and highly statistically significant differences. These undoubtedly arise from imprecision in the L1 calibration.

For the v11 data set, we examined highly filtered data grouped into small areas. For each mode, the data set contained millions of soundings, so they were further filtered to only include the best data. Data were selected for the analysis when all 8 footprints in one sounding frame (ID) converged. We computed the median X_{CO_2} as the “ground truth” value, and subtracted this from the observed X_{CO_2} to calculate the deviations for each footprint. The reported values are the average of the differences across all soundings per footprint. The footprint offsets are listed in Figure 5-2 under the term FOOT and shown in Table 5-1. One set of biases was obtained for land, and a different set for ocean glint. Land nadir, glint, and target observations had statistically indistinguishable biases and hence were set to the same values. Once obtained, these biases are subtracted from all sounding X_{CO_2} in preparation for the next steps of BC.

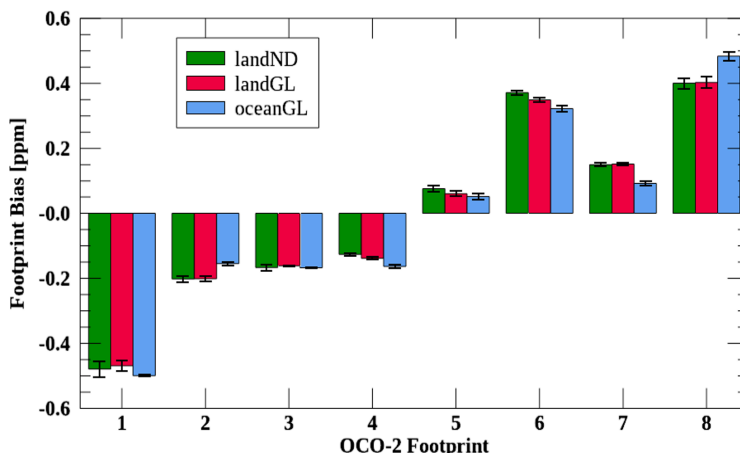


Figure 5-2: Footprint Bias per viewing mode. The land nadir and glint biases were set to be the same in the end, as they were statistically indistinguishable, but the ocean glint footprint biases were statistically different and hence set to their own values.

5.2.2 Step 2 – Remove X_{CO_2} Errors Correlated with Specific Variables (FEAT)

In this second step, we identify variables retrieved simultaneously with X_{CO_2} that are correlated with unphysical X_{CO_2} variability using a multivariate linear regression. This is the procedure followed by nearly all ACOS/GOSAT and OCO-2 X_{CO_2} bias corrections to date (e.g., Wunch et al. 2011, Guerlet et al. 2013). The procedure followed was very similar to that described in O’Dell et al. (2018).

Table 5-1: Features used in the OCO-2 v11.2/v11.1 Land Nadir (ND) + Glint (GL) bias correction, with reduction in unexplained variance in parentheses. Note SAA in this table is “Small Area Analysis”. Coefficient uncertainties are 1σ .

| | N | Stddev (ppm) | dPfrac | Co2_grad_del | logDWS | aod_fine | aod_ice | Albedo_quad_wco2*1e6 |
|--------------------|-------|--------------|--------------|---------------|--------------|------------|------------|----------------------|
| TCCON: ggg2020 | 1638K | 1.75 → 1.18 | -0.82 (25%) | -0.0322 (27%) | -0.22 (2%) | 5.6 (0.3%) | -29 (0.9%) | 0.77 (0.5%) |
| Models: | 3004K | 1.64 → 1.09 | -0.81 (26%) | -0.0317 (26%) | -0.20 (2%) | 8.4 (0.8%) | -27 (0.9%) | 0.61 (0.4%) |
| SAA: | 2516K | 1.50 → 0.75 | -0.825 (34%) | -0.0330 (33%) | -0.28 (5%) | 7.6 (0.8%) | -37 (2.1%) | 0.58 (0.4%) |
| v11.2/v11.1 | | | -0.82 | -0.032 | -0.25 | 7.2 | -31 | 0.60 |
| v11.0 | | | -0.83 | -0.033 | -0.27 | 6.7 | -33 | 0.48 |

| | N | Stddev (ppm) | dPfrac | Co2_grad_del | logDWS | aod_fine | aod_ice | Albedo_quality_wco2*1e6 |
|-----|---|--------------|--------|--------------|--------|----------|---------|-------------------------|
| v10 | - | - | -0.855 | -0.0335 | -0.335 | 5.2 | 0 | |

The different analysis regions and modes have minor differences in the order of features chosen, but overall, the features selected and their slopes are remarkably consistent. Table 5-2 shows the bias correction parameters for Land Target soundings for the different training datasets, and Table 5-3 shows the same for Ocean Glint. Each table shows the reduction in unexplained variance (UV in %) as features are added to the bias correction fit. Note that in each table, the X_{CO_2} quality flag has been applied.

Table 5-2: Features used in the OCO-2 v11.2/v11.1 Land Target (TG) bias correction, with reduction in unexplained variance in parentheses. Coefficient uncertainties are 1σ .

| | N | Stddev (ppm) | dPfrac | Co2_grad_del | logDWS | aod_fine | aod_ice | Albedo_quality_wco2*1e6 |
|--------------------|-------|--------------|--------------|---------------|--------------|----------|---------|-------------------------|
| TCCON: ggg2020 | 1368K | 1.50 → 1.18 | -0.75 (19%) | -0.0217 (15%) | -0.35 (3%) | - | - | - |
| Models | 854K | 1.41 → 1.10 | -0.74 (20%) | -0.0216 (17%) | -0.25 (2%) | - | - | - |
| SAA | 772K | 1.20 → 0.70 | -0.83 (33%) | -0.0245 (31%) | -0.25 (3%) | | | |
| v11.2/v11.1 | | | -0.77 | -0.024 | -0.30 | - | - | - |
| v11.0 | | | -0.77 | -0.025 | -0.25 | - | - | - |
| v10 | - | - | -0.855 | -0.0335 | -0.335 | 5.2 | - | - |

These terms are the differences between the retrieved and the *a priori* surface pressure evaluated at the geographic location of the strong CO band (dP_{sco2}), the retrieved abundance of coarse aerosol (e.g., dust, sea salt, or water clouds), and (very large and unphysical) variation in the retrieved vertical profile of CO₂ (parameter $co2_grad_del$) from that assumed in the prior. Also, note that over land, we have created a new quantity called “dPfrac”. This term is similar to dP, but also takes into account that higher elevation surfaces have a smaller dry air column above them, and therefore over these locations, the dP correction must be proportionally stronger. A full derivation of this term is given in the appendix of Kiel et al. (2019). Here, we simply give the definition of dPfrac, which is:

$$dPfrac = X_{CO_2,raw} (1 - P_{ap,sco2}/P_{ret})$$

where $P_{ap,sco2}$ is the prior surface pressure at the location of the strong CO₂ band, and P_{ret} is the surface pressure retrieved by the L2 algorithm. There are several additional terms in the land bias correction:

- $\logDWS : \max(\log(aod_dust + aod_water + aod_seasalt), -5)$
- $aod_fine : aod_oc + aod_sulfate$ (where “oc”=organic carbon)

- `albedo_quad_wco2 * 1e6`: This is the quadratic component of the retrieved amplitude of the surface BRDF in the weak CO₂ band. As it is naturally of order 1e-6, we scale it up by a factor of 1e6 for ease of use.

Table 5-3: Features used in the OCO-2 v11.2/v11.1 Ocean Glint (GL) bias correction, with reduction in unexplained variance in parentheses. Note SAA in this table is “Small Area Analysis”. Coefficient uncertainties are 1σ .

| | N | Stddev (ppm) | dP_sco2 | Sqrt(Albedo_wco2) | Co2_grad_del | Max_Declocking_wco2 | AOD_Water | XCO2_uncertainty |
|--------------------|-------|--------------|--------------|-------------------|----------------|---------------------|------------|------------------|
| TCCON: ggg2020 | 1606K | 1.11 → 0.79 | -0.260 (34%) | 7.6 (9%) | -0.018 (4%) | -2.0 (0.9%) | -8 (0.4%) | 1.9 (1.7%) |
| Models: | 2216K | 1.05 → 0.70 | -0.255 (37%) | 7.9 (9%) | -0.019 (5%) | -2.1 (1.3%) | -12 (0.9%) | 2.4 (2.9%) |
| SAA: | 1861K | 0.90 → 0.46 | -0.240 (47%) | 8.3 (16%) | -0.019 (6%) | -1.6 (0.9%) | -12 (1.1%) | 2.0 (3.1%) |
| v11.2/v11.1 | | | -0.25 | 8.0 | -0.0185 | -2.0 | -12 | 2.0 |
| v11 | | | -0.25 | 8.0 | -0.0175 | -2.0 | -14 | 2.0 |
| v10 | - | - | -0.213 | - | 0.087 | - | - | - |

Because the ocean surface parameterization changed significantly in B11, this led to a large change in the bias correction for ocean glint. Instead of two terms in the parametric part of the bias correction. We now use six:

- $dP_sco2 = (P_{ret} - P_{ap,sco2})$ as discussed above, in units of hPa
- $\sqrt{\text{albedo_wco2}}$ is the square root of the retrieved effective reflectivity (or surface albedo) in the weak CO_2 band.
- $Co2_grad_del$: As always, the retrieved CO_2 at the surface minus the same at pressure level 13 (~ 700 hPa), minus the a priori of the same, given in a priori.
- $Max_Declocking_wco2$: The term “max_declocking_wco2” is related to the subsense radiance variability in the weak CO_2 band as measured from the color slices. The original term in the L2Std files varies about unity. We therefore subtract off unity and take the absolute value, and multiply by 100 to express in %, to obtain the value used in the Lite files, as well as in the filtering and bias correction.
- AOD_water is of course the retrieved optical depth of water cloud at 755 microns wavelength.
- $xco2_uncertainty$ is the retrieval posterior uncertainty of X_{CO2} , in ppm.

Figure 5-3, Figure 5-4 and Figure 5-5 shows the bias correction plots for version 11 land Nadir+Glint, land Target, and Ocean Glint, respectively, all relative to TCCON (ggg2014).

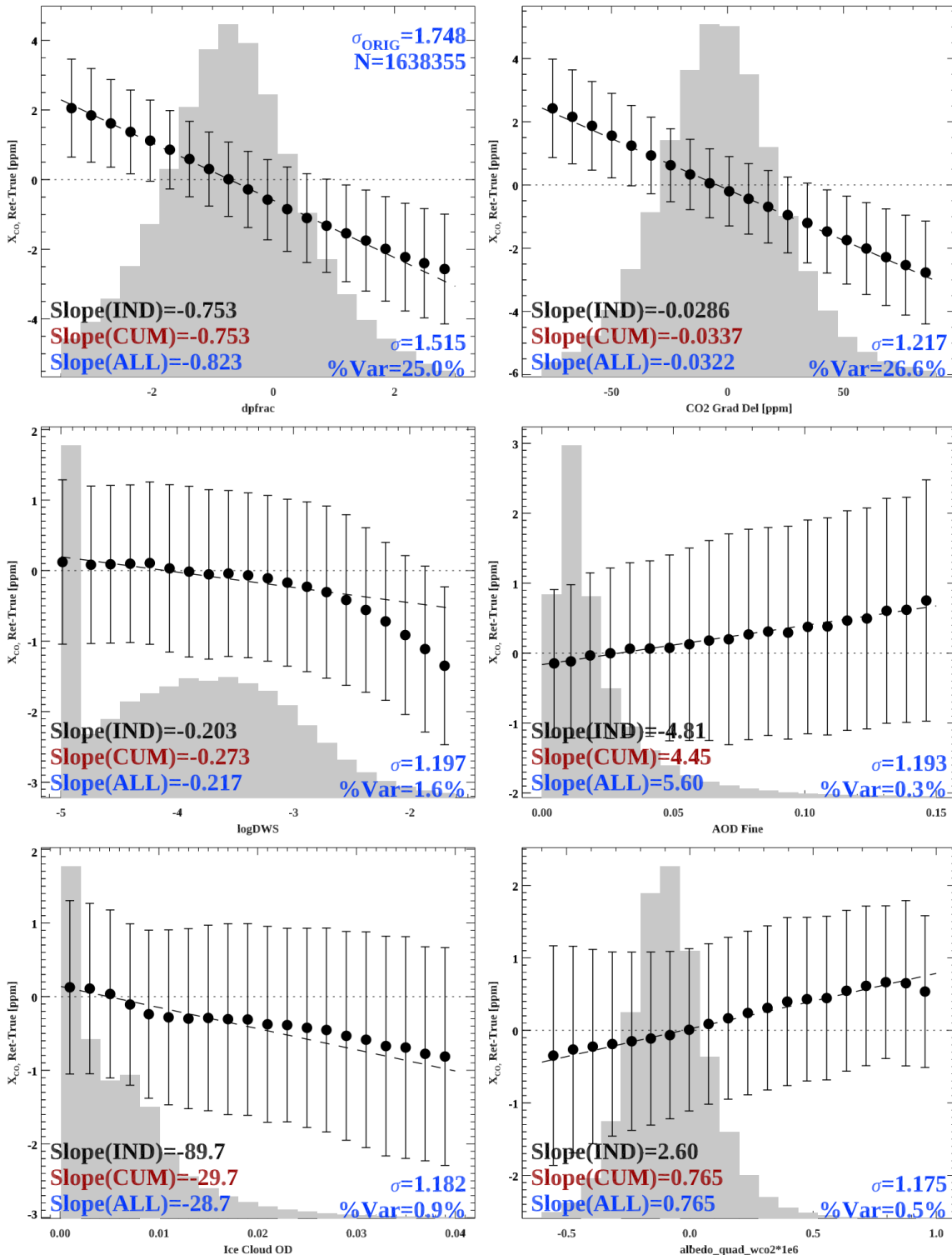


Figure 5-3: Plot of X_{CO_2} errors relative to TCCON (ggg2020) for v11.1 land nadir & glint observations. The regression coefficients for a simultaneous fit of all terms are given in blue ("ALL"), bottom left of each panel.

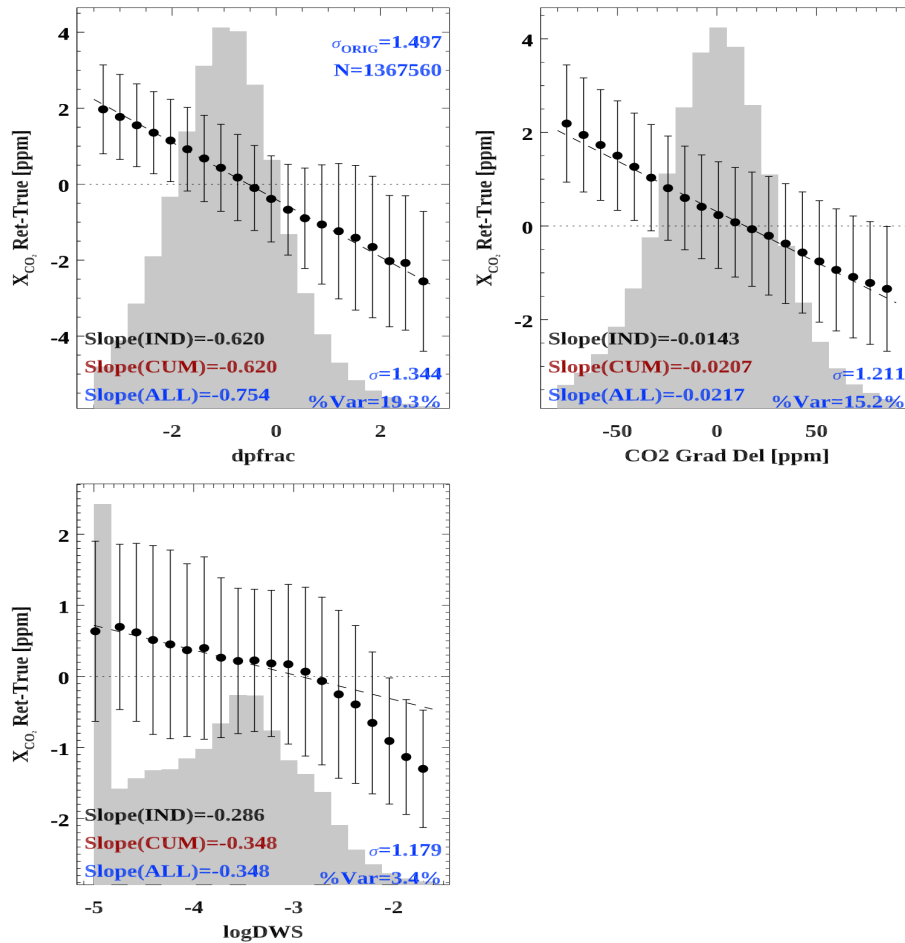


Figure 5-4: Same as Figure 4-3 but for Land Target Observations.

5.2.3 Step 3 – Determine global offset from TCCON (TCCON_Adjust)

The analyses described in Steps 1 and 2 provide no estimate of the overall global bias in X_{CO_2} . To determine the offset over land, we used nadir, glint, and target mode observations obtained over the TCCON sites. The final numbers only used the recent ggg2020 data. A linear regression between TCCON X_{CO_2} and the bias-corrected OCO-2 target mode X_{CO_2} was performed, with the intercept forced to zero. Table 5-4 shows the process for TCCON target observations. Overall, this analysis scales the OCO-2 land nadir, glint, and target data to TCCON: $OCO-2 = (0.9997 \pm 0.003) TCCON$. While the fit to individual modes have lower uncertainties, the fit across different modes and multiple time periods lead us to conclude that the real uncertainty is greater, on the order of 0.003.

To determine the global divisor for Ocean Glint, we exclusively used coastline crossings as discussed in O'Dell et al. (2018). The final global divisor adopted for ocean data was 0.9997 ± 0.003 , identical to that of land soundings.

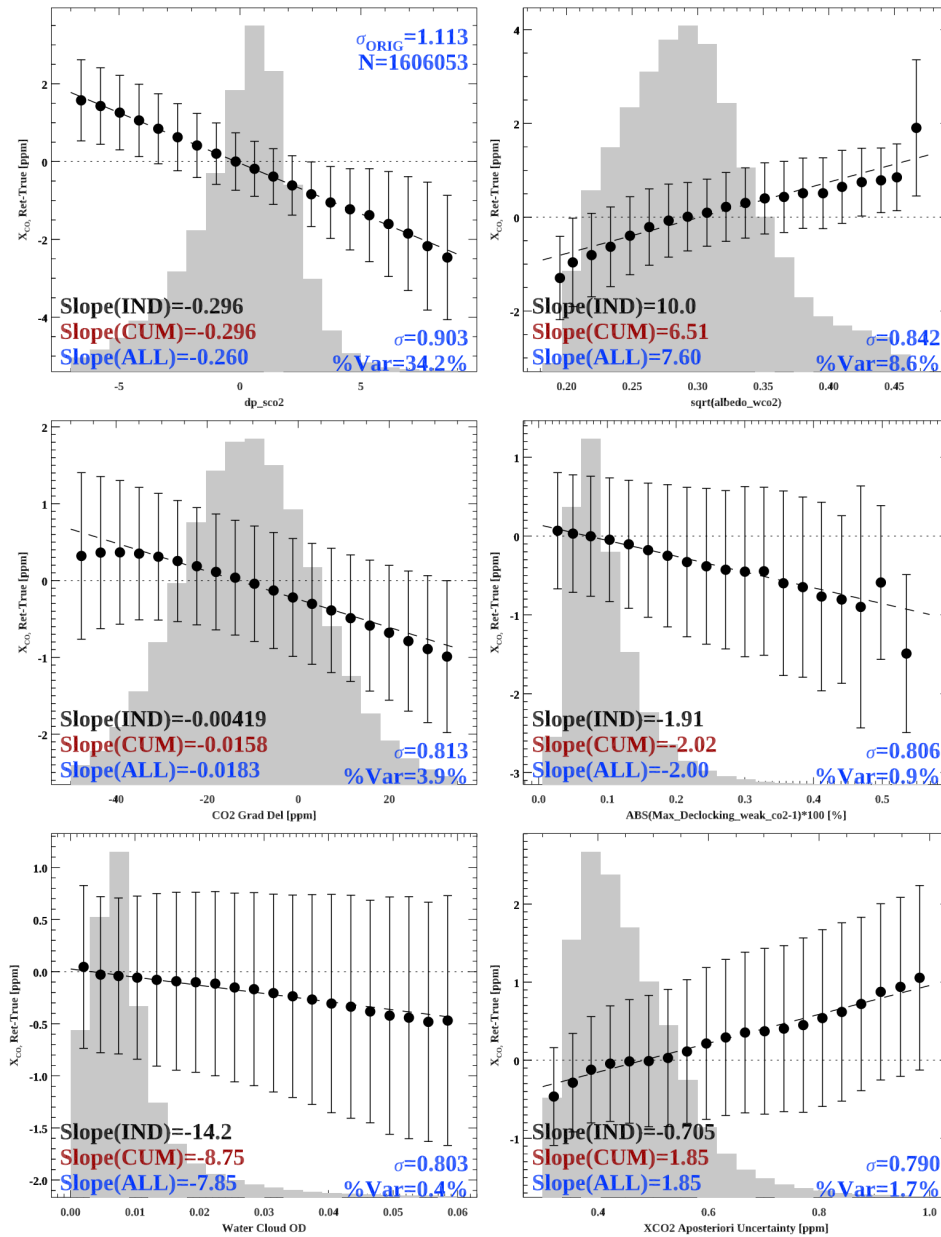


Figure 5-5: Same as Figure 5-4 but for Ocean Glint Observations.

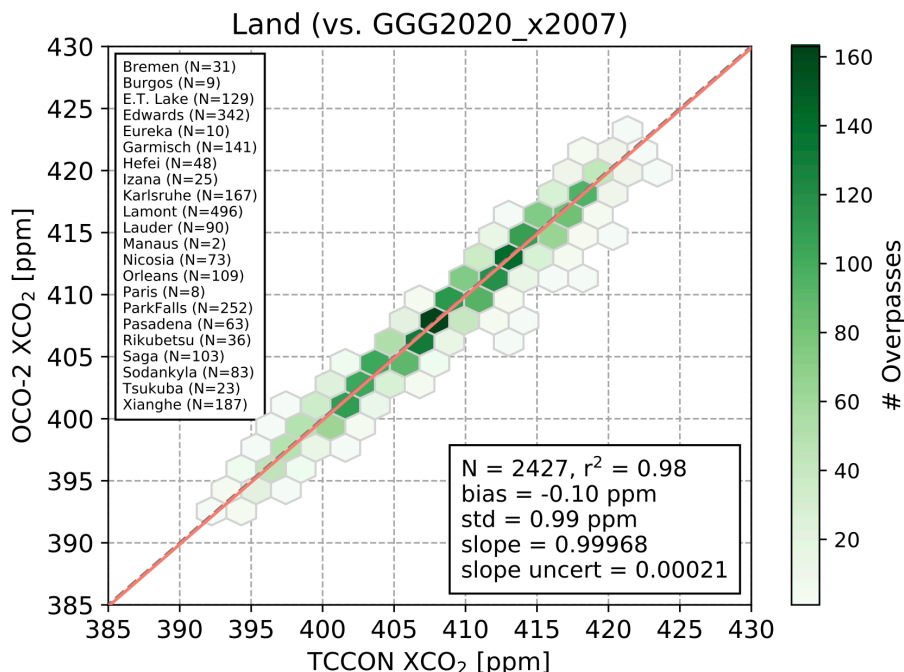


Figure 5-6: Linear Fit of OCO-2 v10 to TCCON X_{CO2} for a subset of land (ND+GL) mode overpasses of TCCON sites. Both Quality Filtering as well as the feature and footprint biases have been applied.

Table 5-4: Bias Correction formulation for OCO-2 v11.2/v11.1

| FOOTPRINT BIAS (FOOT) (ppm) | | | | | | | | |
|--|---|--------|--------|---|-------|-------|-------|-------|
| Footprint (fp) | 1 | 2 | 3 | 4 | 5 | 6 | 7 | 8 |
| Land | -0.510 | -0.220 | -0.160 | -0.120 | 0.090 | 0.370 | 0.150 | 0.400 |
| Ocean | -0.500 | -0.160 | -0.160 | -0.160 | 0.060 | 0.330 | 0.100 | 0.490 |
| FEATURE BIAS (FEATS) (ppm) | | | | | | | | |
| LAND (ND, GL) | $-0.82*(dPfrac) - 0.032*(co2_grad_del - 5) - 0.25*(max(logDWS, -5) + 5.3) + 7.2*(aod_fine - 0.03) - 31*(aod_ice - 0.006) + 0.60*(albedo_quad_wco2*1e6 + 0.06)$ | | | | | | | |
| LAND (TG) | $-0.77*(dPfrac + 0.3) - 0.024*(co2_grad_del) - 0.30*(max(logDWS, -5) + 4.2)$ | | | | | | | |
| OCEAN (GL) | $-0.25*(dP_{sco2}) + 8.0*(sqrt(albedo_wco2) - 0.28) - 0.0185*(co2_grad_del + 14) - 2.0*(max_declocking_wco2) - 12*(aod_water - 0.011) + 2.0*(xco2_uncertainty - 0.46)$ | | | | | | | |
| OVERALL DIVISOR (TCCON_ADJUST) | | | | Method | | | | |
| LAND GL LAND ND LAND TG | 0.9997 | | | Comparison to TCCON ggg2020 (average of ND, GL, and TG modes) | | | | |
| OCEAN GL | 0.9997 | | | Coastline Crossings such that ocean glint matches land | | | | |

| | Variable definitions using full/HDF5/path for Lite files |
|----------------------------|--|
| co2_grad_del | Retrieval/co2_grad_del |
| dP_{sco2} | Retrieval/psurf – Meteorology/psurf_apriori_sco2 |
| logDWS | Max(ln(aod_dust + aod_water + aod_seasalt), -5) |
| aod_fine | Retrieval/aod_sulfate + Retrieval/aod_oc |
| aod_ice | Retrieval/aod_ice |
| max_declocking_wco2 | Preprocessors/max_declocking_wco2 |
| xco2_uncertainty | xco2_uncertainty |
| Albedo_quad_wco2 | Retrieval/abedo_quad_wco2 |

5.2.4 v11.2/v11.1 Quality Flagging

After bias correction, additional outlier filtering is developed and applied. The `xco2_quality_flag` is set to “0” for good quality data and set to “1” for lower quality data. This allows users to remove the effects of one or more tests if they so choose.

Table 5-4 lists the details on the parameters that define the data quality flag. Table 5-5 illustrates these parameters as applied to land data.

Because this is a simple binary flag, we have created two additional bit-flag variables that give the user information as to which tests failed that leads to soundings marked as “bad” quality (`xco2_quality_flag = 1`). There is variable `xco2_qf_bitflag` which currently uses all 32 bits of a long integer to report the result of each individual test. A bit value of 0 means passed, and 1 means failed. If they all pass, the value of this variable will be 0, just as for the normal quality flag variable. The individual bits are given in Table 5-5. Furthermore, a new “simple bitflag”, `xco2_qf_simple_bitflag`, has also been created. This 8-bit integer divides the tests into seven categories currently; each of the individual tests falls into exactly one of these categories. For instance, aerosol-related, surface-albedo related, etc. Table 5-6 gives the bit definitions for these variables.

For those unused to bit-flags, let us suppose a given sounding has a bitflag value of X . To get the value of bit b , which we call will B , simply do

$$\begin{aligned} \text{IDL: } B &= (X \text{ AND } 2^b) \text{ EQ } 2^b \\ \text{Python: } B &= (X \text{ and } 2^b) == 2^b \\ \text{Fortran: } b2 &= 2^{**}b \\ B &= (X \text{ .AND. } b2) == b2 \end{aligned}$$

Table 5-5: OCO-2 v11.2/v11.1 Quality Filter Thresholds and bit numbers for the associated bit-flags. Range denotes allowed ranges for each variable. All variables must pass for a given sounding to be considered “good” (xco2_quality_flag = 0).

| Bit | Simple Bit | Field | Units | Land Range | Ocean Glint Range |
|-----|------------|---|--------------------|-------------------|-------------------|
| 0 | 2 | Preprocessors/co2_ratio_bc | | 0.987, 1.012 | 0.99, 1.008 |
| 1 | 2 | Preprocessors/h2o_ratio_bc | | 0.73, 1.038 | 0.85, 1.04 |
| 2 | 0 | Sounding/altitude_stddev | m | 0, 120 (0, 50) | |
| 3 | 2 | Preprocessors/max_declocking_wco2 | % | 0, 1.5 | |
| 4 | 6 | Retrieval/dp_o2a | hPa | -9, 6 | |
| 5 | 6 | Retrieval/dpfrac | ppm | -3.5, 3.0 | |
| 6 | 6 | Retrieval/co2_grad_del | ppm | -80, 90 | -50, 35 |
| 7 | 3 | Retrieval/albedo_slope_sco2 | 1/cm ⁻¹ | -15e-5, 100e-5 | 4e-6, 4e-5 |
| 8 | 4 | Retrieval/aod_total | | 0, 0.25 | |
| 9 | 4 | Retrieval/aod_ice | | 8e-5, 0.04 | 0, 0.035 |
| 10 | 3 | Retrieval/albedo_sco2 | | 0.03, 0.60 | |
| 11 | 3 | Retrieval/albedo_quad_wco2 | 1/cm ⁻² | -0.6e-6, 1e-6 | |
| 12 | 3 | Retrieval/albedo_quad_sco2 | 1/cm ⁻² | -3.5e-6, 4e-6 | |
| 13 | 5 | Retrieval/rms_rel_wco2 | % | 0, 0.35 | |
| 14 | 5 | Retrieval/rms_rel_sco2 | % | 0, 0.80 | |
| 15 | 5 | Retrieval/chi2_sco2 | | 0, 2.7 (0, 3.0) | 0, 1.65 |
| 16 | 6 | Retrieval/deltaT | K | -0.8, 1.5 | |
| 17 | 4 | Retrieval/aod_sulfate+Retrieval/aod_oc | | 0, 0.15 | |
| 18 | 4 | Retrieval/aod_water | | 0.0006, 0.07 | 0, 0.06 |
| 19 | 4 | Retrieval/dust_height | | 0.85, 2.0 | |
| 20 | 4 | Retrieval/aod_strataer | | 1e-4, 0.03 | |
| 21 | 4 | Retrieval/aod_seasalt | | 0, 0.12 | |
| 22 | 6 | Retrieval/fs_rel | | -0.025, 0.03 | |
| 23 | 4 | Retrieval/dws | | 0, 0.20 | 0, 0.30 |
| 24 | 2 | Preprocessors/dp_abp | hPa | -15, 12 (-15, 50) | -10, 10 |
| 25 | 2 | Preprocessors/h_continuum_wco2 | | 0, 50 | |
| 26 | 0 | Retrieval/snow_flag | | 0, 0 | |
| 27 | 3 | Retrieval/brdf_weight_slope_sco2 | | | 0, 4e-4 |
| 28 | 6 | Retrieval/dp_sco2 | hPa | | -7, 9 |
| 29 | 5 | Retrieval/chi2_wco2 | | | 0, 1.6 |
| 30 | 2 | Preprocessors/max_declocking_sco2 | % | | 0, 0.40 |
| 31 | 3 | Retrieval/albedo_o2a – Retrieval/albedo_sco2 | | | 0.002, 0.027 |
| 32 | 3 | Retrieval/brdf_weight_slope_wco2 | | | -8.5e-5, 4.1e-5 |
| 33 | 3 | Retrieval/albedo_o2a | | | 0.04, 0.20 |
| 34 | 1 | xco2_uncertainty | Ppm | | 0.3, 1.0 |
| 35 | 6 | Abs(Retrieval/eof3_1_rel) | | | 0, 0.45 |
| 36 | 4 | Retrieval/ice_height | | | -0.5, 0.5 |
| 37 | 2 | Preprocessors/ color_slice_noise_ratio_wco2 | | | 0, 6 |
| 38 | 0 | Sounding/airmass | | | 2, 4.2 |

Note: Numbers in (red) are used for target-mode soundings.

“Bit” denotes the bit number in xco2_qf_bitflag, a 32-bit integer in the v1 Lite files. (0=pass, 1=fail)

“Simple Bit” denotes the bit number in xco2_qf_simple_bitflag, an 8-bit integer in the v1 Lite files.

Table 5-6: Bit definitions in xco2_qf_simple_bitflag.

| Bit | Category | Notes |
|-----|--------------------------------|---|
| 0 | Direct Exclusion | Directly excluded due to snow, uncharacterized modes (ocean non-glint obs, etc), topography features |
| 1 | Signal | Signal-related features (SNR or signal ratios out of bounds, posterior uncertainty too high) |
| 2 | Preprocessors | Failed one or more preprocessor-related quality flags (co2_ratio, h2o_ratio, max_declocking, dp_abp) |
| 3 | Retrieved Surface Reflectivity | Failed a surface-reflectivity related quality flag (surface albedo, surface albedo slope, retrieved wind speed) |
| 4 | Retrieved Aerosols | Failed a retrieved aerosol related quality flag (aerosol AOD or aerosol heights) |
| 5 | Retrieval Fit Quality | L2FP fit quality too poor (in terms of rms_rel or chi^2) |
| 6 | Other Retrieval Quantities | Failed other L2FP retrieval flags (SIF, dp quantities, etc) |
| 7 | Unused | Currently unused |

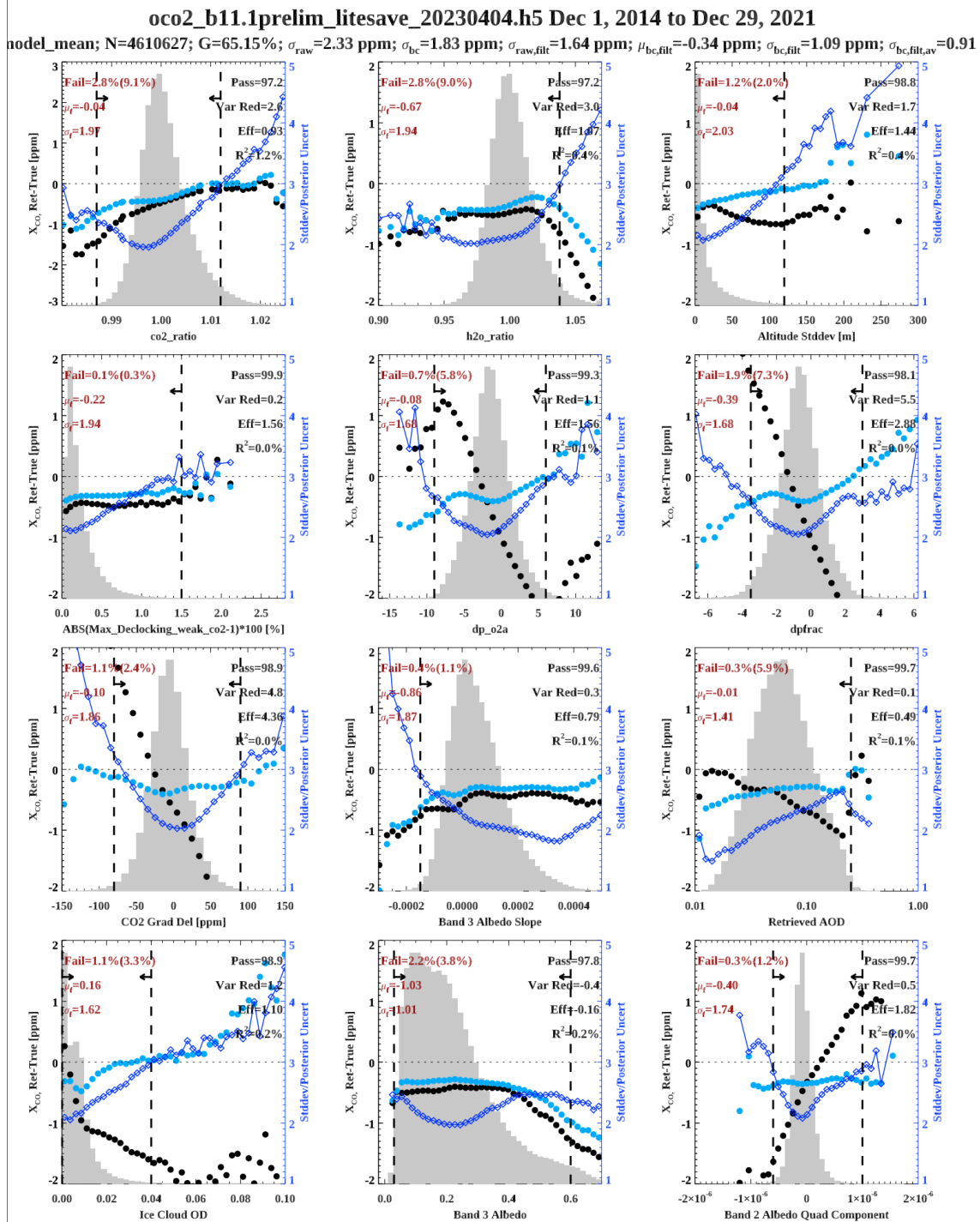


Figure 5-7: Bias & Stddev of error as a function of selected outlier filtering variables for land observations. Here, the error is derived using the model comparison.

5.2.5 Definition of Key Data Parameters

Some of the parameters used in the data screening or bias correction of the L2 data have different names in the L2Std and Lite files. There are also a few parameters which are calculated from terms in the L2Std or Lite files. The subsections below give the parameter names within the Lite file structure, their names in the L2Std files and a description. Note “Parent field refers to the field name in the L2Std file. The full listing of the OCO-2 and OCO-3 Lite file data fields are in the tables in Section 9.

5.2.6 Assessment of potential spurious X_{CO_2} drift with time

Given that the OCO-2 data record is now ~ 9 years long, there is always the possibility that there could be a small drift, related to priors or calibration, in our retrieved X_{CO_2} . Therefore, for the truth datasets, we performed simple time-sensitivity analyses vs. TCCON and the model median. Specifically, we perform a linear least-squares fit of monthly mean of the X_{CO_2} difference of OCO2 – Truth, accounting for averaging kernel effects. Only good quality soundings are included. To assign an uncertainty, each monthly mean X_{CO_2} difference is assigned the same uncertainty, required to yield a fit reduced χ^2 value of unity. A sample time series and fit is shown in Figure 5-8, which shows the time series of OCO-2 minus TCCON X_{CO_2} . The results for each fit are given in Table 5-7. Of the five slopes calculated, two (land ND+GL vs Models, and ocean Glint vs. TCCON) have drifts that are significant at 95% confidence; however, these drifts are of opposite sign. The first, landNG vs Models, -0.035 ± 0.010 , may easily be related to the models themselves, which seem inconsistent with TCCON in terms of growth rate at a level of about 0.04 ppm/yr. The other is oceanG vs. TCCON, at a level of 0.052 ± 0.024 ppm/yr, or about 0.5 ppm/decade. To put this in context, these potentially spurious trend represents less than about 2% of the mean secular increase of 2.5 ppm/yr due to anthropogenic CO_2 emissions. Further, our errors are purely empirical as described above, and do not take into account the possible errors in TCCON or models in terms of drifts, which very well could be significant at this level. As the OCO-2 data record lengthens, spurious time trends should become easier to see (and remove). At this time, no time-dependent term is included in our bias correction.

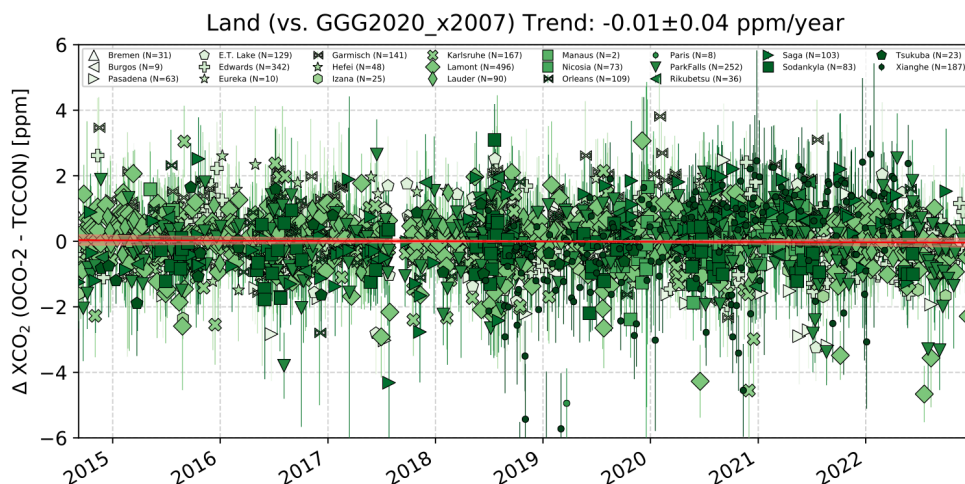


Figure 5-8 Sample linear Fit of OCO-2 v11.1 Land ND+GL minus TCCON(ggg2020) vs. time, binned monthly, to determine possible spurious time trend. Bias-corrected X_{CO_2} differences are shown in (Blue); raw X_{CO_2} differences are shown in (Red). In this case, there is an apparent negative trend, but it is only significant at 2.4σ . Comparisons vs models and other viewing modes yield a range of results.

Table 5-7: Time Drifts vs. Models & TCCON

| Observation Mode | Truth Source | Drift $\pm 1\sigma$ uncertainty |
|--------------------|-----------------|---------------------------------|
| Land (Nadir+Glint) | TCCON (ggg2020) | -0.01 ± 0.04 ppm/yr |
| Land (Nadir+Glint) | Model Median | -0.01 ± 0.02 ppm/yr |
| Ocean Glint | TCCON (ggg2020) | 0.04 ± 0.04 ppm/yr |
| Ocean Glint | Model Median | 0.02 ± 0.02 ppm/yr |
| Land Target | TCCON (ggg2020) | 0.055 ± 0.022 ppm/yr |

5.3 CO₂ scale change

Atmospheric CO₂ measurements are ultimately tied back to primary standards maintained by the NOAA Global Monitoring Laboratory. [Hall et al. \(2021\)](#) recently published a revision to the WMO CO₂ calibration scale that increases CO₂ mixing ratios by on the order of 0.2 ppm at 400 ppm. In situ CO₂ measurements have been undergoing recalibration to the new CO₂ scale, identified as WMO-CO₂-X2019 (here referred to as X2019), since it was finalized.

The initial OCO-2 v11.1 release and the OCO-3 v10 releases remain tied to the X2007 CO₂ scale. This is because OCO-2 and -3 data are tied to the WMO CO₂ scale vicariously, using TCCON as a transfer standard, with TCCON scaled to match in situ measurements by comparing TCCON data with aircraft or balloon CO₂ profiles taken over TCCON sites (e.g. [Wunch et al. 2010](#)). The process of updating the TCCON scaling from the previous X2007 CO₂ scale to the new X2019 CO₂ scale has now been finalized, and the updated TCCON (ggg2020) files now contain X_{CO_2} on both scales. Therefore, for OCO-2 v11.1, we now include an additional variable “XCO2_X2019”, which is simply the OCO-2 estimate of X_{CO_2} on the X2019 scale. This was obtained by re-fitting the global divisor (“TCCON_ADJUST” value, see section 5.2.3). In this case, a value of 0.9995 was obtained (as opposed to 0.9997 for the x2007 scale). This implies that the x2019 X_{CO_2} value is roughly 0.08 ppm higher than that of x2007.

Future releases of v11 data may formally update the X_{CO_2} data to tie to the X2019 scale. This will be indicated by the “comment” attribute of the “xco2” variable in the lite files. It is highly recommended that users check this attribute when downloading new versions of the lite files to verify which scale the X_{CO_2} data is reported on.

6 OCO-3 v10: Description, Data Filtering and Bias Correction

6.1 Quality Filtering and Bias Correction

Similar to X_{CO_2} derived from OCO-2 measurements, for OCO-3 we apply a quality filtering procedure to remove soundings that show larger than expected scatter differences in X_{CO_2} compared to a “truth” metric (O’Dell et al., 2018). Further, a large fraction of the error in X_{CO_2} correlates with retrieved components of the state vector in the retrieval algorithm. It was shown that a linear correction demonstrably reduces such errors in X_{CO_2} estimates from space-based measurements (Wunch et al., 2011a, Wunch et al., 2017, O’Dell et al., 2018, Kiel et al., 2019). In order to derive quality filters and bias correction terms for OCO-3, the same approach is followed as for OCO-2 (O’Dell et al., 2018). The retrieved X_{CO_2} values are compared to independent estimates, so-called truth proxies. For OCO-3 v10, we use three different truth proxy training data sets: TCCON, a small area approximation (SAA), and a truth proxy based on results from global carbon flux inverse models (“multi-model median”).

6.1.1 Truth Proxy Training Data Sets

The TCCON truth proxy includes data from 19 TCCON stations. We use the GGG2014 data set covering the time period between August 2019 and December 2020 and spanning from 55°N to 45°S in latitude. We use similar coincidence criteria as O’Dell et al. (2018) to match airmasses observed by TCCON and OCO-3. In total, we count ~101K coincident soundings between ground based TCCON measurements and OCO-3 in nadir mode over land, ~91K coincident soundings in SAM/target mode over land, and 18K soundings in glint mode over water.

The SAA truth proxy (for more details see O’Dell et al., 2018) makes use of the low spatial variability of X_{CO_2} over small regions (up to 100 km) and short time spans (~10s). Here we define continuous segments of soundings that were collected along-track within ~10s as small areas. Between August 2019 and December 2020, the SAA truth proxy consists of ~656K soundings in nadir mode over land, ~219K sounding in SAM/target mode over land, and ~ 869K soundings in glint mode over water.

For the multi-model median truth proxy, a suite of four models sampled at the OCO-3 sounding locations and times was used (for more details see O’Dell et al., 2018). The models generally differ in their prior flux assumptions, prior flux uncertainty, transport model, initial conditions, spatial resolution, and inverse method. Each model assimilates either in-situ CO_2 concentration data, GOSAT X_{CO_2} data, OCO-2 X_{CO_2} data, or a combination of the above. Between August 2019 and December 2020, the multi-model median truth proxy consists of ~1358K soundings in nadir mode over land, ~797K soundings in SAM/target mode over land, and ~ 1500K soundings in glint mode over water.

An overview of the different truth proxies is given in Table 6-1.

Table 6-1: Overview of the truth proxy training datasets for OCO-3 v10.

| Name | Observation Mode | Number of Obs (x10 ³) | Details |
|-------|------------------|--------------------------------------|---------|
| TCCON | Nadir over land | ~110 | GGG2014 |
| TCCON | Target/SAM | ~91 | GGG2014 |
| TCCON | Glint over water | ~18 | GGG2014 |

| Name | Observation Mode | Number of Obs (x10 ³) | Details |
|--------------------|------------------|--------------------------------------|-------------------------------|
| SAA | Nadir over land | ~656 | Areas < 100 km along track |
| SAA | Target/SAM | ~219 | Areas < 100 km along track |
| SAA | Glint over water | ~869 | Areas < 100 km along track |
| Multi Model Median | Nadir over land | ~1358 | |
| Multi Model Median | Target/SAM | ~797 | |
| Multi Model Median | Glint over water | ~1500 | |

6.1.2 Filter Variables and Limits

Soundings that show errors in X_{CO_2} when compared to a truth proxy that are too large to provide reliable constraints on CO₂ fluxes are removed by threshold-based filters for multiple retrieval parameters. For v10, we apply two different sets of filter variables and limits for observations over land and water. The selection of filter variables and limits is based on Mandrake et al. (2015), Eldering et al. (2017) and O'Dell et al. (2018). The v10 quality filters are based on a number of retrieved or auxiliary variables that correlate with excessive X_{CO_2} scatter or bias.

The selection of the variables was done sequentially by identifying individual variables responsible for the largest fraction of the variance in δx_{CO_2} (defined as the retrieved – true X_{CO_2}). We then created a simple threshold-based filter for these variables. The selection of thresholds for particular filter variables followed the following procedure: both, scatter and bias, were considered with the latter being considered as more important. Variables were typically selected as filters if they were correlated with bias greater than ~0.5 ppm, or significant scatter (greater than 2 ppm). The filtering variables and thresholds were derived separately for land (nadir, Target/SAM) and ocean (glint) soundings. Filtering variables selected and their thresholds were the same or similar, regardless of the particular truth proxy used. On average, ~65% of all soundings in the truth proxy datasets pass the v10 quality filters over land (nadir, Target/SAM) and ~60% over water (glint).

Similar to the OCO-2 Lite Files, filtering can be done with `xco2_quality_flag` variable in the OCO-3 Lite Files (“0” is good). Table 6-2 lists the details on the parameters that define the data quality flag. In addition, we use the same bitflag convention as for OCO-2 to provide information as to which tests failed that leads to soundings marked as “bad” quality (see Table 5-5). For more details, see Section 5.1 and Section 5.2.4.

Table 6-2: Filter variables and limits for the X_{CO_2} quality flag definition in OCO-3 v10. For the definitions of the individual variables see Section 9 or O'Dell et al. (2018), Kiel et al. (2019).

| Bit | Simple Bit | Field | Units | Land Range | Ocean Glint Range |
|-----|------------|-------------------------|-------|--------------|-------------------|
| 0 | 2 | Preprocessors/co2 ratio | | 0.998, 1.035 | 0.998, 1.035 |
| 1 | 2 | Preprocessors/h2o ratio | | 0.850, 1.035 | 0.850, 1.030 |
| 2 | 6 | Retrieval/dp_o2a | hPa | -7, 7 | |
| 3 | 6 | Retrieval/dpfrac | ppm | -3.0, 2.8 | |
| 4 | 5 | Retrieval/rms_rel_o2a | % | 0, 0.35 | 0, 1.0 |
| 5 | 5 | Retrieval/chi2_wco2 | | 0, 1.40 | 0, 1.25 |
| 6 | 3 | Retrieval/albedo_wco2 | | 0.12, 2.0 | 0, 0.02 |

| Bit | Simple Bit | Field | Units | Land Range | Ocean Glint Range |
|-----|------------|--|--------------------|---------------|-------------------|
| 7 | 3 | Retrieval/albedo slope o2a | 1/cm ⁻¹ | -1e-4, 1e-4 | |
| 8 | 3 | Retrieval/albedo slope sco2 | 1/cm ⁻¹ | -2e-4, 5e-4 | -5e-5, 7e-5 |
| 9 | 6 | Retrieval/co2 grad del | ppm | -60, 85 | -22, 5 |
| 10 | 0 | Sounding/altitude stddev | m | 0, 120 | |
| 11 | 4 | Retrieval/dust height | | 0.7, 10 | |
| 12 | 4 | Retrieval/ice height | | -0.15, 0.6 | -10, 0.5 |
| 13 | 6 | Retrieval/eof2 2 rel | | -1.2, 1.2 | |
| 14 | 4 | Retrieval/aod sulfate + Retrieval/aod oc | | 0, 0.20 | |
| 15 | 4 | Retrieval/aod ice | | 8e-5, 0.035 | 0, 0.045 |
| 16 | 4 | Retrieval/dws | | 0, 0.20 | |
| 17 | 5 | Retrieval/ndiv | | 0, 1 | 0, 0 |
| 18 | 1 | Retrieval/xco2 uncert | ppm | 0, 1.25 | 0, 1.0 |
| 19 | 1 | Retrieval/dof co2 | | 1.5, 2.2 | |
| 20 | 6 | Retrieval/Fs rel | | -0.020, 0.035 | |
| 21 | 5 | Retrieval/rms rel sco2 | % | 0, 0.70 | |
| 22 | 6 | Retrieval/dp | hPa | | -4, 10 |
| 23 | 2 | Preprocessors/dp abp | hPa | | -17, 10 |
| 24 | 3 | Retrieval/windspeed | m/s | | 2, 25 |
| 25 | 1 | Sounding/snr o2a | | | 200, 550 |
| 26 | 3 | Retrieval/albedo slope wco2 | 1/cm ⁻¹ | | -2e-5, 2e-5 |
| 27 | 4 | Retrieval/aod total | | | 0, 0.4 |
| 28 | 2 | Preprocessor/l1b csstd ratio wco2 | | | 0, 6 |
| 29 | 1 | Sounding/s31 | | | 0.15, 0.25 |

"Bit" denotes the bit number in `xco2_qf_bitflag`, a 32-bit integer in the `Xco2` Lite files. (0=pass, 1=fail)

"Simple Bit" denotes the bit number in `xco2_qf_simple_bitflag`, an 8-bit integer in the `Xco2` Lite files.

6.1.3 Footprint Bias Correction

OCO-3 obtains eight side-by-side, simultaneous, nearly-located measurement scenes called footprints. Similar to OCO-2, there are small and highly statistically significant differences between these eight footprints which likely arise from imprecision in the L1 calibration. To derive the v10 footprint biases for OCO-3, we follow the same procedure as for OCO-2 v10 (for more details see Section 3.2.1). For that, we used the SAA truth proxy. Data were selected for the analysis when all 8 footprints in one sounding frame (ID) converged. We computed the median X_{CO_2} as the "ground truth" value, and subtracted this from the observed X_{CO_2} to calculate the deviations for each footprint. The reported values are the average of the differences across all soundings per footprint. The footprint offsets are listed in Table 6-3 under the term FOOT. One set of biases was obtained for land (nadir, Target/SAM), and a different set for ocean glint. These biases are subtracted from all sounding X_{CO_2} in preparation for the next steps of the bias correction. For both, land and water soundings, the largest bias is estimated for footprint seven (-0.35 ppm over land, -0.18 ppm over water) which is consistent with the pre-flight tests.

Table 6-3: Bias Correction Parameters for OCO-3 v10.

| Footprint (fp) | FOOTPRINT BIAS (FOOT) (ppm) | | | | | | | |
|----------------|-----------------------------|------|-------|-------|------|------|-------|------|
| | 1 | 2 | 3 | 4 | 5 | 6 | 7 | 8 |
| Land | -0.09 | 0.13 | -0.04 | -0.33 | 0.33 | 0.19 | -0.35 | 0.16 |

| | | | | | | | | |
|---|---|------|-------|-------|---|------|-------|------|
| Ocean Glint | 0.00 | 0.09 | -0.03 | -0.16 | 0.12 | 0.10 | -0.18 | 0.06 |
| | FEATURE BIAS (FEATS) (ppm) | | | | | | | |
| LAND (ALL) | $-0.62*(dPfrac) - 0.30*(\max(\log DWS, -5) + 5) - 0.011*(co2_grad_del - 5) - 2.5*(albedo_wco2 - 0.25)$ | | | | | | | |
| OCEAN GLINT | $-0.16*\max(dP, 0) + 0.13*(co2_grad_del + 6.0)$ | | | | | | | |
| | OVERALL DIVISOR (TCCON_ADJUST) | | | | Method | | | |
| LAND GLINT LAND NADIR LAND TARGET LAND SAM | 0.9963 | | | | Direct Comparison to TCCON (using Target & Nadir observations only) | | | |
| OCEAN GLINT | 0.9961 | | | | Coastline bootstrap & bootstrap | | | |
| | Variable definitions using full/HDF5/path for Lite files | | | | | | | |
| co2_grad_del | Retrieval/co2_grad_del | | | | | | | |
| dP | Retrieval/dp | | | | | | | |
| dPfrac | Retrieval/dpfrac | | | | | | | |
| logDWS | MAX(ln(Retrieval/dws), -5) | | | | | | | |
| albedo_wco2 | Retrieval/albedo_wco2 | | | | | | | |

6.1.4 Parametric Bias Correction

The procedure to derive the Parametric Bias Correction is very similar to that described in O'Dell et al. (2018) and Section 3.2.2 above. This is the procedure followed by nearly all ACOS/GOSAT and OCO-2 X_{CO_2} bias corrections to date (e.g., Wunch et al. 2011, Guerlet et al. 2013). As previous versions of the OCO-2 data product, the OCO-3 v10 analysis found that over land, the different viewing modes (nadir, target, SAM) all had similar biases. The different analysis regions and modes have minor differences in the order of features chosen, but overall the features selected and their slopes are consistent with the exception of the SAA truth proxy. By definition, the SAA truth proxy is not able to provide information about spurious variations in X_{CO_2} on large (>500km) scales (e.g. changing surface albedo over land). Therefore, coefficients derived from the SAA over land were not considered in the derivation of the final parametric bias correction coefficients. Table 6-4 shows the bias correction parameters for land soundings for the different training datasets, and Table 6-5 shows the same for glint observations over water. Each table shows the reduction in unexplained variance as features are added to the bias correction fit. Note that in each table, the X_{CO_2} quality flag has been applied.

Table 6-4: Features used in land bias correction, with reduction in unexplained variance in parentheses. Coefficient uncertainties are 1σ .

| | N | Stddev (ppm) | dPfrac | Co2_grad_del | logDWS | albedo_wco2 |
|---------------|-----|--------------|--------------|----------------|---------------|--------------|
| TCCON (nadir) | 77K | 1.53 → 1.33 | -0.646 (16%) | -0.0094 (2.1%) | -0.325 (2.8%) | -3.66 (3.7%) |

| | N | Stddev (ppm) | dPfrac | Co2_grad_del | logDWS | albedo_wco2 |
|--------------------------|------|--------------|---------------------|-----------------------|---------------------|-------------------|
| TCCON (TG/SAM) | 61K | 1.50 → 1.31 | -0.629 (20%) | -0.0077 (1.7%) | -0.248 (1.2%) | -1.79 (1.0%) |
| Models (nadir) | 673K | 1.51 → 1.23 | -0.627 (18%) | -0.0165 (6%) | -0.348 (6%) | -2.48 (3.9%) |
| Models (TG/SAM) | 518K | 1.46 → 1.22 | -0.595 (19%) | -0.0121 (4%) | -0.244 (3%) | -2.88 (4.0%) |
| SAA (nadir) | 414K | 1.07 → 0.81 | -0.516 (27%) | -0.0107 (6%) | -0.373 (9%) | -0.14 (0%) |
| SAA (TG/SAM) | 151K | 1.16 → 0.95 | -0.542 (25%) | -0.0081 (2.7%) | -0.264 (3.4%) | -1.03 (0.8%) |
| B10 (adapted, all modes) | - | - | -0.62 ± 0.02 | -0.011 ± 0.004 | -0.29 ± 0.05 | -2.7 ± 0.8 |

Table 6-5: Same as Table 6-4 but for glint measurements over water.

| | N | Stddev (ppm) | dP_sco2 > 0 | co2_grad_del |
|---------------|------|--------------|----------------------|----------------------|
| TCCON | 10K | 1.18 → 0.98 | -0.202 (15%) | 0.098 (16%) |
| Models | 795K | 1.21 → 0.77 | -0.190 (23%) | 0.145 (37%) |
| SAA | 621K | 0.97 → 0.37 | -0.090 (22%) | 0.158 (63%) |
| B10 (adapted) | - | - | 0.161 ± 0.061 | 0.134 ± 0.032 |

For v10 observations over land in nadir and Target/SAM mode, four different parameters account for the largest fraction of the variability in X_{CO_2} : dPfrac, co2_grad_del, logDWS, and albedo_wco2. The definition of these variables is given in Section 9 and 11. The reduction in unexplained variance due to dPfrac and co2_grad_del is smaller for OCO-3 v10 than for all previous OCO-2 data versions. It appears that due to the more complex viewing geometry of the OCO-3 instrument, the unexplained variance is distributed across multiple retrieval variables, with each variable accounting for a small fraction of the variance. This is in contrast to the OCO-2 v10 parametric bias correction, where a large part of the unexplained variance can be explained by two variables (dPfrac and co2_grad_del).

For measurements over water in glint mode, the v10 parametric bias correction includes two variables: dP_sco2 and co2_grad_del. Here, the dP_sco2 term accounts for roughly ~20% of the unexplained variance and is only applied where dP_sco2 > 0 hPa. The co2_grad_del term, on average, accounts for ~40% of the unexplained variance. The contribution of each parametric bias correction term to the raw X_{CO_2} is shown in Figure 4-2 for land observations and in Figure 4-3 for observations over water.

6.1.5 Global Scaling Factor

The global scaling factor corrects for an overall bias in X_{CO_2} and ties it to the WMO trace gas standard scale. TCCON serves as a link between the WMO trace gas standard scale and satellite measurements. Over land, this factor is derived by comparing OCO-3 nadir and target mode observations to ground-based TCCON measurements over several sites globally. We use similar coincidence criteria as O'Dell et al. (2018). A linear regression between TCCON X_{CO_2} and the bias-corrected OCO-3 X_{CO_2} was performed, with the intercept forced to zero. For v10, we use the TCCON GGG2014 dataset to derive the global scaling factor. Overall, this analysis scales the OCO-3 land data to TCCON in the following way: OCO-3 = (0.9963 ± 0.003) TCCON.

7 Overview of OCO-2 v11 and OCO-3 v10 Data Products

With the exception of the Lite files, all OCO-2 and OCO-3 product files are in Hierarchical Data Format-5 (HDF), developed at the National Center for Supercomputing Applications (<http://www.hdfgroup.org>). This format facilitates the creation of logical data structures by organizing the data product into folders and subfolders. Each file corresponds to one orbit contiguous mode set of data. Spectral radiances are contained in the SoundingMeasurements folder of the L1BSc product; retrieved X_{CO2} values are contained in the RetrievalResults folder of the L2Std product. Official data products are stored at the NASA GES DISC <https://disc.gsfc.nasa.gov/datasets?keywords=oco2&page=1>.

The OCO-2 and OCO-3 L2 data files are consistent in format to the degree possible, the primary differences having to do with how each instruments points and differences in the orbits of OCO-2 and the ISS.

OCO-2 provides multiple L2Std data files per day, generally one per orbit. However, OCO-2 data will be further separated into separate files for nadir, glint and target. As a result, for orbits with a target observation, there could be a file for the target data and another for the nadir/glint data. OCO-3 also breaks the data into separate files per orbit, but because OCO-3 could possible observe in different modes in a single orbit, the data is not further separated by observation mode.

As with past releases, the OCO-2 team has produced lite files for both X_{CO2} and the Solar Induced Fluorescence (SIF) product. The OCO-3 team has done this as well.

The OCO-2 L2 Lite files contain a subset of the information in the standard OCO-2 L2 product. They are meant to be significantly smaller but still contain all necessary information for typical science analyses. In addition, they have some value added:

- Only contain L2 soundings that converged
- They include a nominal recommended filtering flag (`xco2_quality_flag`)
- They include the recommended bias correction already applied to X_{CO2} (the X_{CO2} without bias correction is also contained in the Lite files)

There is one file per day, for each day that had at least one retrieved sounding.

The OCO-2 Lite files are in the NetCDF-4 format. Because NetCDF -4 is a subset of HDF-5, the files may be read with both NetCDF and HDF software.

7.1 File Naming Conventions

The OCO-3 data follow the OCO-2 file naming convention with one difference. The data from all modes in combined into one file for OCO-3, and the Mode element is specified as 'SC in the file name. Otherwise, the convention noted below applies.

- The OCO-2 L1BSc files follow this convention:
`oco2_L1bSc[Mode]_[Orbit][ModeCounter]_[AcquisitionDate]_[ShortBuildId]_[Production DateTime][Source].h5`
- The OCO-2 L2Std files follow this convention:
`oco2_L2Std[Mode]_[Orbit][ModeCounter]_[AcquisitionDate]_[ShortBuildId]_[Production DateTime] [Source].h5`
- The OCO-2 L2Dia files follow this convention:

oco2_L2Dia[Mode]_[Orbit][ModeCounter]_[AcquisitionDate]_[ShortBuildId]_[ProductionDateTime]_[Source].h5

- The OCO-2 L2IDP files follow this convention:

oco2_L2IDP[Mode]_[Orbit][ModeCounter]_[AcquisitionDate]_[ShortBuildId]_[ProductionDateTime][Source].h5

- The OCO-2 LtCO2 files follow this convention (note that these are NetCDF, not HDF):

oco2_LtCO2_[AcquisitionDate]_[ShortBuildId]_[ProductionDateTime][Source].nc4

There is no Orbit or Mode, as one day of data is aggregated.

Similarly,

- The OCO-2 LtSIF files follow this convention (note that these are NetCDF, not HDF):

oco2_LtSIF_[AcquisitionDate]_[ShortBuildId]_[ProductionDateTime][Source].nc4

For all files, the fields are defined as below.

- [Mode] is the acquisition mode as a two-character string:
 - GL—Sample Glint
 - ND—Sample Nadir
 - TG—Sample Target
 - DS—Sample Dark Calibration
 - LS—Sample Lamp Calibration
 - SS—Sample Solar Calibration
 - BS—Sample Limb Calibration
 - NP—Single-Pixel Nadir
 - GP—Single-Pixel Glint
 - TP—Single-Pixel Target
 - DP—Single-Pixel Dark Calibration
 - LP—Single-Pixel Lamp Calibration
 - SP—Single-Pixel Solar Calibration
 - BP—Single-Pixel Limb Calibration
 - XS—Sample Transition
 - XP—Single-Pixel Transition
 - MS—Sample Lunar Calibration
 - MP—Single-Pixel Lunar Calibration
- [Orbit] is the five-digit orbit number
- [ModeCounter] is a letter (a, b, c, d) denoting the times an acquisition mode occurred in an orbit. If a mode occurs only once, ModeCounter is set to “a”
- [AcquisitionDate] is the UTC date (yymmdd) the data were acquired
- [ShortBuildId] identifies the L1B build version used (Bn.m.uu) where n is the major version, m is subversion number, and the uu is the incremental/patch number
- [ProductionDateTime] is the date and time the file was produced (yymmddhhmmss)

- [Source] (if present) identifies production sources different from the standard operations pipeline. This field will be missing from normal pipeline data

A note regarding the short build ID. All data with the same build version can be used together for science, regardless of the subversion and patch number.

For both OCO-2 and OCO-3 there is the retrospective processing (10r), which we recommend for science. The forward processing stream (10), has predicted calibration, and 10r has interpolated calibration. In addition, the forward stream has only 6% of the data, the 10r collection has all data that was deemed to be cloud free enough for processing.

Example filenames for both L2Std and Lite files can be found in Table 7-1.

Table 7-1: Example L2 filenames for OCO-2 and OCO-3

| Filename | Instrument | Type | Orbit | Date | Mode |
|--|------------|-------------|-------|-------------------------|-------------|
| oco2_L2StdND_30114a_200229_B10007r_200404203338.h5 | OCO-2 | L2 Standard | 30114 | Feb 29, 2020 (200229) | Nadir (ND) |
| oco2_L2StdGL_30113a_200229_B10007r_200404181241.h5 | OCO-2 | L2 Standard | 30113 | 200229 | Glint (GL) |
| oco2_L2StdTG_30113a_200229_B10007r_200404201105.h5 | OCO-2 | L2 Standard | 30113 | 200229 | Target (TG) |
| oco3_L2StdSC_05416a_200417_B10200_200419001142.h5 | OCO-3 | L2 Standard | 5416 | April 17, 2020 (200417) | All |
| oco2_LtCO2_191018_B10_v0.nc4 | OCO-2 | L2 Lite | N/A | Oct 18, 2019 (191018) | All |
| oco3_LtCO2_200219_B10_yearly.nc4 | OCO-3 | L2 Lite | N/A | 200219 | All |

7.1.1 File Format and Structure

The OCO-2 product files contain data structures indexed by sounding (1 to N soundings/file) and are associated by the sounding_id variable in all products.

Variables are combined into groups by type (e.g., SoundingGeometry). Within each type, a variable has one or more values per sounding. Variables may be single-valued (e.g., sounding_altitude) or multi-valued (e.g., co2_profile).

The metadata of each variable describes the variable's attributes, such as dimensions, data representation, and units.

Note that many variables in the L2 products use _fph to denote full physics algorithm, _idp for IMAP-DOAS, and _abp for the O₂ A band preprocessor. For example, surface pressure is calculated in each of the algorithms, so it is reported with a tag on the variable to differentiate them.

7.1.2 Data Definition

The OCO-2 data products contain many variables with a variety of dimensions. The following list describes only the most important of the dimensions. Dimensions and data shapes are fully described within the HDF files.

- Retrieval—the number of retrievals reported (those soundings for which retrievals converged or were converging when the maximum number of iterations was reached)
- Band—the three bands of OCO-2 are O₂ A, weak CO₂, and strong CO₂.
- Footprint—the eight footprints across the swatch are identified as 1 to 8.
- Sample—the spectral element. Each band has 1016 spectral elements, although some are masked out in the L2 retrieval.
- Sounding—one set of measurements (one footprint across three bands) that is the primary unit for retrievals.

7.1.3 Global Attributes

In addition to variables and arrays of variables, global metadata is stored in the files. The granule-level metadata is described in Table 12-2. ECHO metadata and other metadata related to HDF version and production location can be found in the HDF file but are not discussed here.

7.2 Data Files Content

7.2.1 L2Std

Geolocated retrieved CO₂ column-averaged dry air mole fraction - physical model. This file contains the retrieved values for the state vector as well as geolocation information. A number of fields from the iterative maximum *a posteriori* differential optical absorption spectroscopy (IMAP-DOAS) and O₂ A-band (ABO2) cloud preprocessors are brought forward to the L2 products.

7.2.2 L2Dia

This file has the data that is in the L2Std, as well as averaging kernels, *a priori* covariance matrices, posterior covariance matrices, and measured and model radiances.

7.2.3 L2IDP

There are the results from the IMAP-DOAS process. The IMAP-DOAS process is used in cloud screening, but also provides solar induced fluorescence (SIF) measurements for a much larger set of data than contained in L2.

7.2.4 L1BSc

These are the radiance spectra that are the input to the L2 retrievals.

8 OCO-2 and OCO-3 L2 Standard Data Products

8.1 Data Description and User Alerts

The primary data products for both missions are the L2 Standard files. Figure 8-1 shows the folders in a L2Std folder of OCO-2. The folders are the same for the OCO-3 folders. A complete list of all the variables in each of the folders are contained in the tables in Section 11.

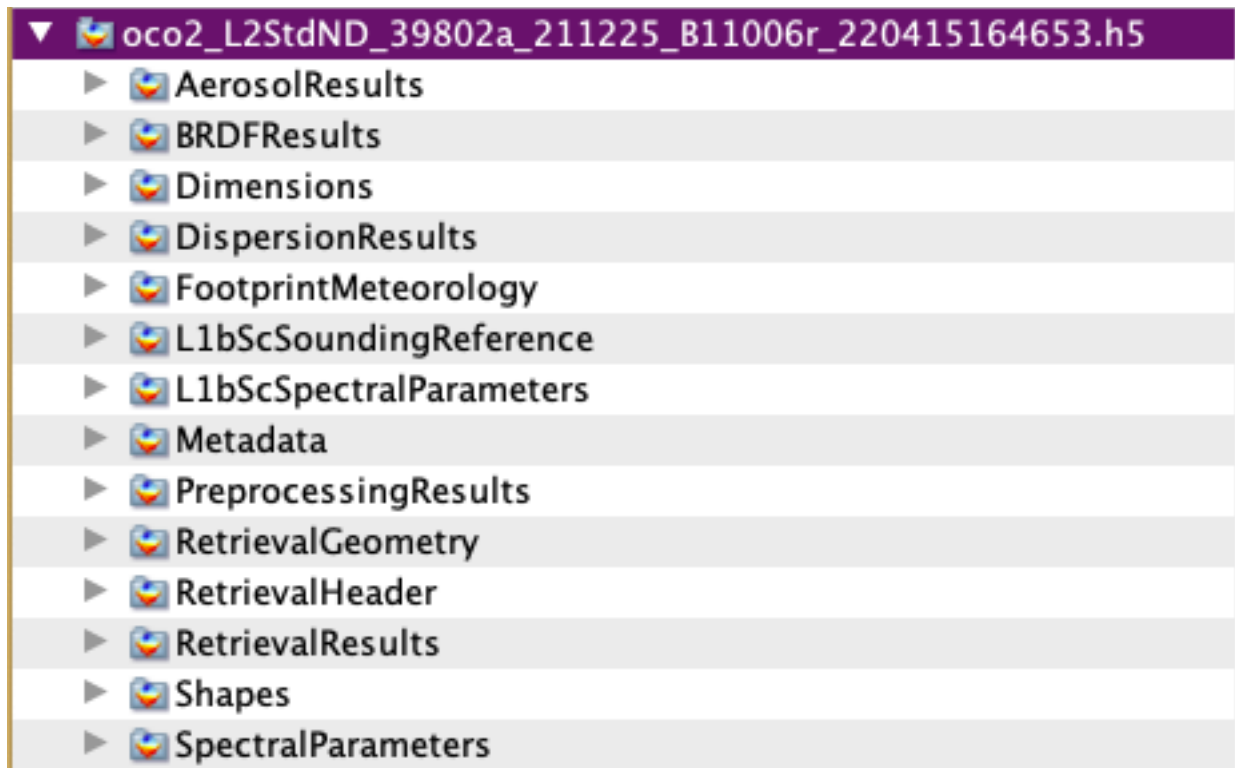


Figure 8-1: Data folders in the L2Std file.

8.2 The RetrievalHeader Folder

Figure 8-2 shows the variables contained in the RetrievalHeader folder for an OCO-2 L2Std file. The list of variables is identical for the OCO-3 RetrievalHeader folder.

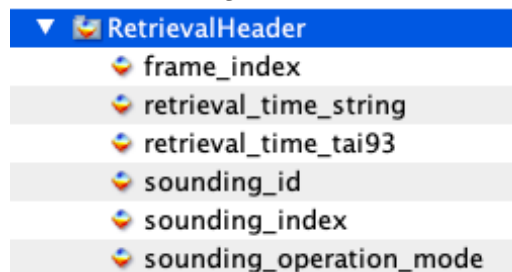


Figure 8-2: Variables in the Retrieval Header folder.

- ***Sounding_ID*** – This is the label for the sounding that will let you link the data across all of the product files. The `sounding_id` is the primary identification number for soundings Figure 8-3Figure 8-3acquired and the footprint number (f) in the form `yyyymmddhhmmsssf`.
- ***Retrieval_time_string*** – This is the time as a string. An example of this field is `2010-09-23T18:36:04.334Z`.
- ***Retrieval_time_tai93*** – This field is the time of the measurement, in seconds since Jan. 1, 1993. The TAI time corresponding to the example above is `559.420571E6`.

8.3 RetrievalGeometry Folder

Figure 8-3 shows the variables contained in the RetrievalGeometry folder for an OCO-2 file and Figure 8-4 shows the variables for an OCO-3 folder. The OCO-3 files have additional variables related to the PMA and PCS.

- `Retrieval_latitude` – This is the latitude of the sounding. These values range from -90 to $+90$.
- `Retrieval_longitude` – This is the longitude. We use the convention of -180 to $+180$ longitude, with fractional degrees.
- `Retrieval_zenith` - The satellite zenith angle (in degrees) at the target.
- `Retrieval_altitude` - Altitude of the sounding based on Earth topography.
- `Retrieval_pma_azimuth` – The OCO-3 Pointing Mirror Assembly azimuth rotation angle in science reference.
- `Retrieval_pma_elevation` – The OCO-3 PMA elevation rotation angle in science reference.



The image shows a screenshot of a file explorer window. The top bar is purple and contains a downward arrow and a folder icon followed by the text "RetrievalGeometry". Below this, a list of variables is displayed, each preceded by a small globe icon. The variables are listed in a single column, alternating between white and light gray background rows. The variables are: retrieval_altitude, retrieval_altitude_per_band, retrieval_altitude_uncert, retrieval_aspect, retrieval_azimuth, retrieval_center_offset_o2_weak_co2, retrieval_center_offset_strong_co2_o2, retrieval_center_offset_weak_co2_strong_co2, retrieval_land_fraction, retrieval_land_water_indicator, retrieval_latitude, retrieval_latitude_geoid, retrieval_longitude, retrieval_longitude_geoid, retrieval_los_surface_bidirectional_angle, retrieval_num_topo_points, retrieval_overlap, retrieval_overlap_o2_weak_co2, retrieval_overlap_strong_co2_o2, retrieval_overlap_weak_co2_strong_co2, retrieval_plane_fit_quality, retrieval_polarization_angle, retrieval_relative_velocity, retrieval_slant_path_diff_o2_weak_co2, retrieval_slant_path_diff_strong_co2_o2, retrieval_slant_path_diff_weak_co2_strong_co2, retrieval_slope, retrieval_solar_azimuth, retrieval_solar_distance, retrieval_solar_relative_velocity, retrieval_solar_surface_bidirectional_angle, retrieval_solar_zenith, retrieval_surface_roughness, retrieval_vertex_latitude, retrieval_vertex_longitude, and retrieval_zenith.

| Variable Name |
|---|
| retrieval_altitude |
| retrieval_altitude_per_band |
| retrieval_altitude_uncert |
| retrieval_aspect |
| retrieval_azimuth |
| retrieval_center_offset_o2_weak_co2 |
| retrieval_center_offset_strong_co2_o2 |
| retrieval_center_offset_weak_co2_strong_co2 |
| retrieval_land_fraction |
| retrieval_land_water_indicator |
| retrieval_latitude |
| retrieval_latitude_geoid |
| retrieval_longitude |
| retrieval_longitude_geoid |
| retrieval_los_surface_bidirectional_angle |
| retrieval_num_topo_points |
| retrieval_overlap |
| retrieval_overlap_o2_weak_co2 |
| retrieval_overlap_strong_co2_o2 |
| retrieval_overlap_weak_co2_strong_co2 |
| retrieval_plane_fit_quality |
| retrieval_polarization_angle |
| retrieval_relative_velocity |
| retrieval_slant_path_diff_o2_weak_co2 |
| retrieval_slant_path_diff_strong_co2_o2 |
| retrieval_slant_path_diff_weak_co2_strong_co2 |
| retrieval_slope |
| retrieval_solar_azimuth |
| retrieval_solar_distance |
| retrieval_solar_relative_velocity |
| retrieval_solar_surface_bidirectional_angle |
| retrieval_solar_zenith |
| retrieval_surface_roughness |
| retrieval_vertex_latitude |
| retrieval_vertex_longitude |
| retrieval_zenith |

Figure 8-3: Variables in the Retrieval Geometry folder for an OCO-2 file.



Figure 8-4: Variables in the Retrieval Geometry folder for an OCO-3 file.

8.4 RetrievalResults

The retrieval results folder contains all of the elements of the state vector in the L2 full physics retrieval. The list of fields in this folder is the same for both OCO-2 and OCO-3.

- `xco2` – This variable expresses the column-averaged CO₂ dry air mole fraction for a sounding. Those soundings that did not converge will not be present. These values have units of mol/mol. This can easily be converted to ppm by multiplying by 10⁶.
- `xco2_uncert` – This is an estimate of the uncertainty on the reported X_{CO_2} . These values have units of mol/mol.
- `xco2_apriori` – This is the initial guess for the X_{CO_2} , in mol/mol.
- `xco2_avg_kernel` – This is the averaging kernel. Note that the normalized averaging kernel (`RetrievalResults/xco2_avg_kernel_norm`) for a given pressure level is equal to the non-normalized value (`retrieval-results/xco2_avg_kernel`) divided by the pressure weighting function at that level. Note that levels are “layer boundaries” and have no thickness. See Appendix A of O’Dell et al. [2012] for details on how these quantities are defined.

| RetrievalResults | | |
|-------------------------------------|--|----------------------------------|
| apriori_o2_column | fluorescence_at_reference | xco2 |
| co2_profile | fluorescence_at_reference_apriori | xco2_apriori |
| co2_profile_apriori | fluorescence_at_reference_uncert | xco2_avg_kernel |
| co2_profile_averaging_kernel_matrix | fluorescence_slope | xco2_avg_kernel_norm |
| co2_profile_covariance_matrix | fluorescence_slope_apriori | xco2_pressure_weighting_function |
| co2_profile_uncert | fluorescence_slope_uncert | xco2_uncert |
| co2_vertical_gradient_delta | h2o_scale_factor | xco2_uncert_interf |
| diverging_steps | h2o_scale_factor_apriori | xco2_uncert_noise |
| dof_co2_profile | h2o_scale_factor_uncert | xco2_uncert_smooth |
| dof_full_vector | iterations | |
| eof_1_scale_apriori_o2 | last_step_levenberg_marquardt_parameter | |
| eof_1_scale_apriori_strong_co2 | num_active_levels | |
| eof_1_scale_apriori_weak_co2 | outcome_flag | |
| eof_1_scale_o2 | retrieved_co2_column | |
| eof_1_scale_strong_co2 | retrieved_dry_air_column_layer_thickness | |
| eof_1_scale_uncert_o2 | retrieved_h2o_column | |
| eof_1_scale_uncert_strong_co2 | retrieved_h2o_column_layer_thickness | |
| eof_1_scale_uncert_weak_co2 | retrieved_o2_column | |
| eof_1_scale_weak_co2 | retrieved_wet_air_column_layer_thickness | |
| eof_2_scale_apriori_o2 | specific_humidity_profile_met | |
| eof_2_scale_apriori_strong_co2 | surface_pressure_apriori_fph | |
| eof_2_scale_apriori_weak_co2 | surface_pressure_fph | |
| eof_2_scale_o2 | surface_pressure_uncert_fph | |
| eof_2_scale_strong_co2 | surface_type | |
| eof_2_scale_uncert_o2 | temperature_offset_apriori_fph | |
| eof_2_scale_uncert_strong_co2 | temperature_offset_fph | |
| eof_2_scale_uncert_weak_co2 | temperature_offset_uncert_fph | |
| eof_2_scale_weak_co2 | temperature_profile_met | |
| eof_3_scale_apriori_o2 | tropopause_altitude | |
| eof_3_scale_apriori_strong_co2 | tropopause_pressure | |
| eof_3_scale_apriori_weak_co2 | vector_altitude_levels | |
| eof_3_scale_o2 | vector_altitude_levels_apriori | |
| eof_3_scale_strong_co2 | vector_pressure_levels | |
| eof_3_scale_uncert_o2 | vector_pressure_levels_apriori | |
| eof_3_scale_uncert_strong_co2 | vector_pressure_levels_met | |
| eof_3_scale_uncert_weak_co2 | wind_speed | |
| eof_3_scale_weak_co2 | wind_speed_apriori | |
| | wind_speed_u_met | |
| | wind_speed_uncert | |
| | wind_speed_v_met | |

Figure 8-5: Variable in the Retrieval Results folder of the L2Std file.

8.5 Aerosols

The aerosol retrieval for uses eight aerosol types. These are the same types used in previous data releases. The L2 ATBD contains a complete description of the aerosols. For any particular sounding, 5 types are included. Ice clouds, water clouds, and a stratospheric aerosol are included in all soundings, and the other two types change, depending on the dominant aerosols in the GMAO *a priori* fields.

To simplify the use of data and identification of the types used, we store the aerosol results in arrays that are at least number of soundings by 8 (the total number of aerosol types).

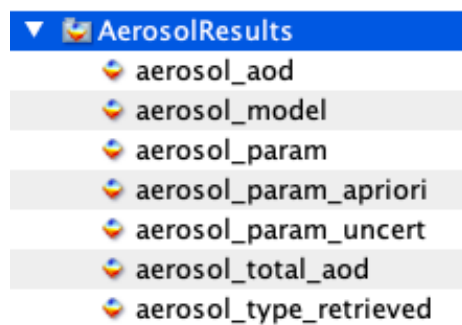


Figure 8-6: Variables in the AerosolResults folder.

The fields and brief descriptions:

- `aerosol_aod`- This field is N soundings x 8 x 4. This contains retrieved column-integrated aerosol optical depth for column segment: [Total, Low, Med, High]. The data are fill values where that aerosol type was not retrieved, and contains a value where it was included.
- `aerosol_model` – This string field is N soundings x 8, and contains the aerosol model used, if retrieved. The options are [profile_linear, profile_log, linear_aod, gaussian_linear, gaussian_log]. For v10, all retrievals are in gaussian log.
- `aerosol_param` – This N sounding by 8 by 3 field contains the retrieved aerosol parameter values. For the Gaussian log set up, these parameters are the natural log of total aod, center pressure/surf-pressure, pressure sigma/surf-pressure. If a fill value is present (-999999.0), the aerosol type was not included for that retrieval. There are similar fields for the apriori and the uncertainty.
- `aerosol_total_aod` – This field in a vector with N sounding elements and contains the retrieved total column-integrated aerosol optical depth for all aerosol types. It can be useful for data screening.
- `aerosol_type_retrieved` – This N soundings x 8 field is a flag that indicates whether aerosol type was retrieved or not (1 yes, 0 no). You can multiply the `aerosol_aod` field by this to get the data you are interested.
- Note that Metadata/AllAerosolTypes contains the list of the 8 aerosol types. They are DU, SS, BC, OC, SO, Ice, water, and ST. This stands for dust, sea salt, black carbon, organic carbon, sulfate, ice, water, and stratospheric aerosol.

8.6 L1B Spectral Parameters

This folder contains selected L1B parameters that could be useful in L2 data analysis. In particular there are variables related to the declocking algorithm that has been implemented to correct for the slight misalignment of the focal plane arrays (FPAs) (for more information see the L1B ATBD). The algorithm uses spatial information from selected color slices to estimate a correction factor by which L1B spectra are multiplied to eliminate discontinuities. The selected color slices are first aggregated into “groups” for statistical purposes. For each group an estimate is made of a correction factor needed at each clocking boundary. Then, a correction function is determined from averages of these estimates, weighted by a column's distance to a group. A much more detailed description can be found in the Level 1B Algorithm Theoretical Basis Document (L1B ATBD).

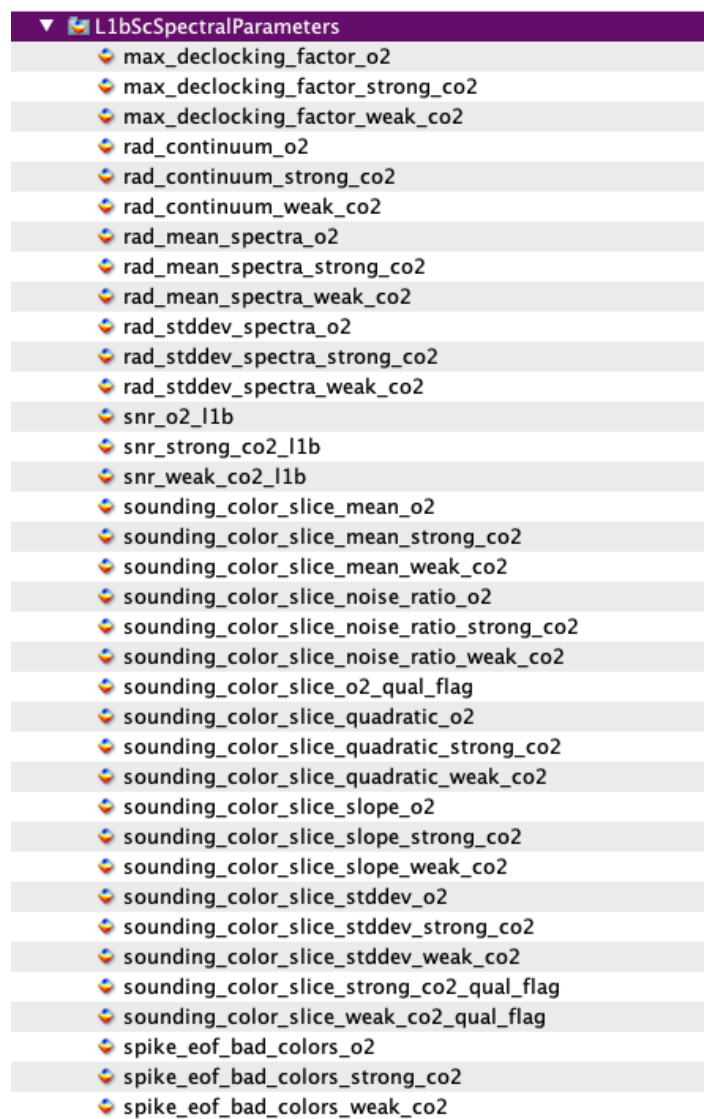


Figure 8-7: Variables in the L1BSCSpectralParameters folder.

9 ABO2 Preprocessor

The O₂-A band cloud screening algorithm was developed at Colorado State University (CSU) under the ACOS program. It employs a fast Bayesian retrieval to estimate surface pressure and surface albedo, assuming clear-sky conditions with only molecular Rayleigh scattering, from high-resolution spectra of the O₂-A band near 765 nm. The estimated surface pressure, surface albedo and the chi-squared goodness-of-fit statistic are used to flag scenes as cloudy, clear, or indeterminate [Taylor et al., 2012].

The basic method is that, absent clouds or aerosols, the surface pressure of a clear scene can be determined to within 2 – 5 hPa accuracy using the O₂-A band spectrum of reflected sunlight. This is because of the strong oxygen absorption features that are present in this band. When surface pressure is higher, the absorption features are deeper for a given observation geometry. When clouds or aerosols are present, they change the path lengths for most photons, either via shortening or lengthening, such that the retrieved surface pressure can be very different from the expected value based on a meteorological forecast, and also the O₂-A spectrum itself cannot be well-fit with a clear-sky assumption.

9.1 Prescreening of OCO-2 Soundings for Cloud and Aerosol

The primary objective of the ABO2 algorithm is to remove from the OCO-2 operational processing streams the soundings that are deemed too contaminated by clouds and /or aerosol for reliable X_{CO_2} retrieval in the computationally expensive L2 algorithm. The key screening parameters are interpreted internally via thresholds to provide a simple cloud flag. Furthermore, the key screening parameters can be used as inputs to a genetic algorithm used for individual sounding selection [Mandrake et al., 2013]. Details of the technique will be described in the Level 2 Algorithm Theoretical Basis Document (L2 ATBD) as well as an upcoming publication [Taylor et al., 2016]. As this is used as a preprocessor, the primary objective is to flag as cloudy scenes that are obviously cloudy or aerosol-contaminated. Therefore, thresholds are set rather loosely so scenes that have some cloud or aerosol contamination will sometimes pass the filter. This is by design. These scenes are sometimes useful for science, or may be rejected by additional pre- or postprocessor flags. The prescreening also checks for observations are impacted by cosmic rays. Starting with V8, soundings that might have been affected by the South Atlantic Anomaly are screened by the ABO2 preprocessor. New for b10, the ABO2 preprocessor contains in the state vector a zero level offset to the calculated top of the atmosphere radiances to account for uncalibrated instrument stray light and SIF. ABP b10 also uses gas absorption cross-section tables (ABSCO) v5.1, consistent with those used by the b10 L2FP.

9.2 Key ABO2 Preprocessor Data Fields in Preprocessing Results Folder

The ABO2 data fields can be found in the standard L2 product (L2Std) PreprocessingResults folder, labeled with the `_abp` data field designation.

Figure 9-1 shows a screenshot of an example OCO-2 L2Sc product file as viewed by HDFView. The ABO2 data fields within the PreprocessingResults folder are highlighted and will be described in detail below.

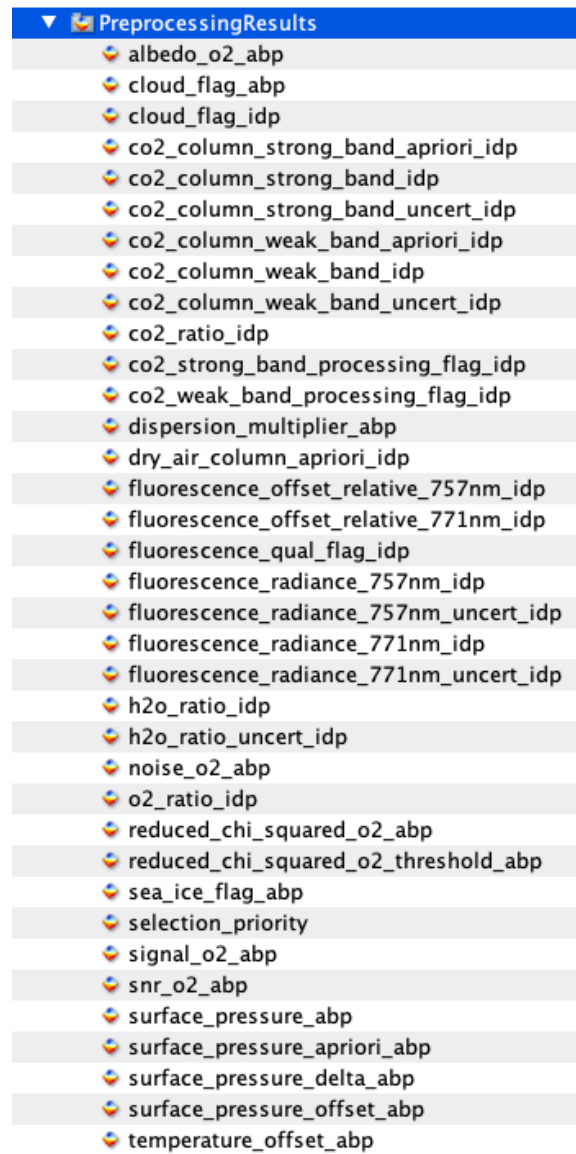


Figure 9-1: Screenshot of an HDFView look at the ABO2 preprocessor file.

- `surface_pressure_delta_abp` - The delta surface pressure is calculated as meteorological forecast surface pressure – retrieved pressure – offset:

$$surface_pressure_apriori_abp - surface_pressure_abp - surface_pressure_offset_abp$$
 in SI units (Pascals). This is the primary screening criterion for the ABO2 preprocessor, and represents the difference between the retrieved and meteorologically estimated surface pressure in the target field of view. Because the algorithm uses imperfect spectroscopy to retrieve surface pressure, there is a path length dependent offset term that is determined by analyzing clear scenes and subtracted from the retrieved value. This yields an unbiased estimate of the retrieved surface pressure. A threshold value can be set independently for nadir, glint, and target viewing modes. At the time of this writing, scenes with a difference greater than 25 hPa (2500 Pa) are flagged as cloudy, for all OCO-2 viewing modes.

- `albedo_o2_abp` – The retrieved surface albedo at 0.755 μm and 0.785 μm . Note that the retrieval assumes a perfect Lambertian surface albedo that varies linearly with wavelength. This assumption is currently made for all viewing modes; in glint mode, this means that the retrieved surface albedo can sometimes exceed unity. Over a dark ocean surface, the retrieved surface albedo is a good way to tell the presence of cloud: if the retrieved surface albedo is too large, a cloud or reflective aerosol layer is likely present. This test is not useful in glint mode or over land, and therefore is generally not used for OCO-2 prescreening.
- `reduced_chi_squared_o2_abp` – The reduced χ^2 value of the spectral fit of the fast retrieval. Values greater than a specified threshold value are also indicative of clouds or aerosols present; as they are not accounted for in the retrieval, spectra containing them cannot be well fit. The threshold χ^2 value is a parameterized function of SNR, as there are persistent spectral features (due to imperfect spectroscopy or instrument calibration) that scale with the signal level.
- `dispersion_multiplier_abp` – This parameter is also fit in the retrieval, and accounts for wavelength shifts in the spectra due primarily to the Earth-instrument Doppler shift. This is typically a maximum of ± 7 km/sec, which corresponds roughly to shifts of ± 0.3 cm⁻¹ or ± 0.018 nm (at maximum). This Doppler shift is easily fit for in the retrieval. Because the Doppler shift is formally a wavelength scaling, the ABO2 algorithm fits it as a scaling rather than a simple shift, though because of the narrowness of the fitted spectral region, it amounts to roughly the same thing.
- `noise_o2_abp` – The determined radiance noise value in the continuum based on the preflight calibration.
- `reduced_chi_squared_o2_threshold_abp` – The threshold reduced χ^2 as described above. The logarithm of the reduced χ^2 in clear scenes is assumed to be a piecewise linear function of SNR. This relationship is determined from clear scenes separately for nadir and glint modes.
- `signal_o2_abp` – The determined radiance mean value in the continuum.
- `snr_o2_abp` – The ratio of `signal_o2_abp` to `noise_o2_abp`.
- `surface_pressure_abp` – The retrieved value of surface pressure by the ABO2 algorithm, in units of Pa.
- `surface_pressure_apriori_abp` – The prior estimate of surface pressure in the target field of view, as determined from short-term meteorological forecasts, and adjusted based on the mean elevation in the target field of view.
- `surface_pressure_offset_abp` – The empirically determined offset of the retrieved surface pressure for clear sky scenes. This offset is determined as a piecewise linear function of solar zenith angle, separately for nadir and glint modes, and is based on soundings that are determined to be approximately clear based on other methods (which include output from the IMAV-DOAS preprocessor as well as soundings collocated with the MODIS sensor aboard Aqua).
- `temperature_offset_abp` – The retrieved temperature offset, a simple additive offset to the meteorological estimate of the temperature profile. At the time of this writing this parameter is included in the state vector, but may be taken out to increase processing speed.
- `cloud_flag_abp` – The result of the surface pressure, χ^2 , and albedo tests to determine if a scene is likely cloudy (or heavily aerosol-laden). If a single test is failed, the cloud flag is set equal to 1, indicating the likely presence of cloud and/or aerosol. If all threshold

checks are successfully passed, then the cloud flag is assigned a value of 0, indicating a sufficiently clear-sky scene. The cloud flag can also be set to 2 for “undetermined” cases. These are chiefly caused by solar zenith angle out of bounds or when viewing water surfaces in nadir observation mode (insufficient SNR).

10 IMAP-DOAS Preprocessor

The iterative maximum a posteriori differential optical absorption spectroscopy preprocessor is a non-scattering fast retrieval algorithm for optically thick absorbers [Frankenberg et al., 2005]. The preprocessor now serves two purposes for OCO 2: (1) retrieve vertical columns of trace gases in all bands individually for advanced cloud and aerosol screening and (2) retrieve solar induced chlorophyll fluorescence (SIF) using an algorithm described in Frankenberg et al. [2011]. The IMAP-DOAS Preprocessor code is essentially unchanged for the b10 software build.

The SIF data from IMAP is also available in the SIF lite files. These are described in more detail in a separate SIF Lite File User's Guide.

10.1 Advanced Cloud and Aerosol Screening

For OCO-2, it is being used to derive vertical column densities of H₂O and CO₂ independently in both CO₂ bands (1.6 and 2.0 μm) with the assumption of a non-scattering atmosphere. Given that Rayleigh scattering is very low in the near-infrared, this assumption holds true if neither aerosols nor clouds are present. In this case, both bands should yield an accurate and consistent result, i.e., the ratio of retrieved quantities in both CO₂ bands is approaching unity in clear sky conditions.

We found that the ratio of both CO₂ and H₂O vertical column densities is deviating significantly from unity in the presence of aerosols and clouds [e.g., Mandrake et al., 2013]. The details of this technique will be described in the algorithm theoretical basis document as well as an upcoming publication.

10.2 Retrievals of Solar-Induced Chlorophyll Fluorescence

The possibility of retrieving solar induced chlorophyll fluorescence from high-resolution spectra in the vicinity of the O₂-A band have been shown in Frankenberg et al. [2011] and Joiner et al. [2011]. Here, we apply the retrieval algorithm described in Frankenberg et al. [2011], embedded in the IMAP-DOAS retrieval code. It is important to note that this is the dedicated fluorescence retrieval, as opposed to the fluorescence retrieval within the full-physics L2 code. Interference with scattering properties in this retrieval is thus minimized [e.g., Frankenberg et al., 2012].

10.3 Key Science Data Fields

The Preprocessing folder (

Figure 9-1) includes many of the key IDP variables from the preprocessing step.

- `co2_column_strong_band_apriori_idp` – *A priori* vertical column density of CO₂ in the strong (2.0 μm) band in molecules/m². Note that a constant volume mixing ratio (VMR) is assumed across the globe in this IMAP-DOAS version and that the *a priori* thus mostly depends on surface pressure.
- `co2_column_weak_band_apriori_idp` – See above but for weak band (both are identical).
- `co2_column_strong_band_idp` - Retrieved vertical column density of CO₂ in the strong (2.0 μm) band in molecules/m². Note that this is different from the FP L2 CO₂ vertical column as this variable here is only retrieved in one band and ignores scattering.
- `co2_column_weak_band_idp` - See above but for the weak band.

- `co2_column_strong_band_uncert_idp` – Uncertainty in retrieved vertical column density of CO₂ in the strong (2.0 μm) band in molecules/m².
- `co2_column_weak_band_uncert_idp` – See above but for weak band.
- `co2_column_strong_band_processing_flag_idp` – Processing flag for the strong CO₂ band retrieval. Every sounding will have a value: 0 (successfully processed), 1 (not converged) or 2 (not processed).
- `co2_column_weak_band_processing_flag_idp` – See above but for weak band.
- `dry_air_column_apriori_idp` – *A priori* total dry air column (mol/m²) of the respective sounding (based purely on meteorological input data and topography).
- `cloud_flag_idp` - Tentative cloud flag based purely used on the IMAP preprocessor. Values can be:
 - 2 = unusable (not processed)
 - 1 = not all retrievals converged
 - 0 = clearly cloudy
 - 1 = probably cloudy
 - 2 = probably clear
 - 3 = very clear

The values are based on simple threshold criteria and based on the ratios defined in the same folder. This flag is *not* being used as input for FP L2 sounding selection and is also not being validated.
- `co2_ratio_idp` – Ratio of retrieved CO₂ vertical column density (VCD) in weak and strong band ($VCD_{1.6\mu m}/VCD_{2.0\mu m}$). Please note that there might be a footprint dependence of this ratio, i.e., each OCO-2 footprint may have a different optimal ratio value. Eventually, we will document these subtleties but the users of early mission data should be aware of this fact, which applies to all variables discussed here.
- `h2o_ratio_idp` – Ratio of retrieved H₂O vertical columns in weak and strong band ($VCD_{1.6\mu m}/VCD_{2.0\mu m}$).
- `h2o_ratio_uncert_idp` - 1-sigma uncertainty of the ratio of retrieved H₂O vertical columns in weak and strong band ($VCD_{1.6\mu m}/VCD_{2.0\mu m}$).
- `o2_ratio_idp` – Ratio of retrieved vs. expected O₂ column density based on the fluorescence 771 nm retrieval window, which includes some weak O₂ line used to derive an O₂ column. Values substantially lower than 1 indicated the presence of clouds.
- `fluorescence_offset_relative_757nm_idp` – Fraction of continuum level radiance explained by an additive offset term in the 757 nm spectral window (unitless). In the absence of instrumental errors, this will be only caused by fluorescence. Rotational Raman scattering should be negligible over typical vegetated surface and moderate solar zenith angles (<65 degrees).
- `fluorescence_offset_relative_771nm_idp` – Same as above but for the 771 nm window.
- `fluorescence_radiance_757nm_idp` – Fluorescence term expressed in absolute radiance units (ph/s/m²/sr/μm) in the 757 nm fit window. This is a derived quantity based on the fit of the relative contribution multiplied with the overall continuum level radiance.
- `fluorescence_radiance_771nm_idp` – Same as above but for the 771 nm window.
- `fluorescence_radiance_757nm_uncert_idp` – Estimated uncertainty (1-sigma) of the fluorescence term expressed in absolute radiance units (ph/s/m²/sr/μm) in the 757 nm fit window.

- `fluorescence_radiance_771nm_uncert_idp` – Same as above but for the 771 nm window.
- `fluorescence_qual_flag_idp` – Quality flag for the fluorescence retrieval (0 = ok, 1 = did not pass quality filter or unprocessed).

11 Format Specification for OCO-2 v11 and OCO-3 v10 Lite Files

11.1 Overview

The OCO-2 and OCO-3 L2 Lite files contain a subset of the information in the standard OCO-2 L2 product. They are meant to be significantly smaller but still contain all necessary information for typical science analyses. In addition, they have some value added:

- Only contain L2 soundings that converged
- They include a nominal recommended filtering flag (`xco2_quality_flag`)
- For this release, they do NOT contain warn levels. This is a difference from previous releases such as V8.
- They include the recommended bias correction already applied to X_{CO_2} (the X_{CO_2} without bias correction is also contained in the Lite files)

There is one file per day, for each day that had at least one retrieved sounding.

The OCO-2 Lite files are in the NetCDF-4 format (http://www.unidata.ucar.edu/software/netcdf/docs/netcdf/NetCDF_002d4-Format.html).

Because NetCDF-4 is a subset of HDF-5, the files may be read with both NetCDF and HDF software.

Generally speaking, each field in the file is described in the Attributes of that field within the file itself. Descriptions for selected fields are given below, but please be sure to read the Attributes of each used field within the actual Lite file. A few fields are present in OCO-2 files but not OCO-3, and vice versa, as indicated.

11.2 File Structure & Fields

The primary variables that most users will need exist at the main level. In addition, there are some additional variables that certain users might want, contained in three groups within the file: Preprocessors, Retrieval, and Sounding. Some NetCDF readers may not see these groups; if this happens, please update your NetCDF reader or use an HDF-5 reader.

11.2.1 Main Level Variables

- ***latitude*** The latitude at the center of the sounding field-of-view.
Parent Field: L2Std/RetrievalGeometry/retrieval_latitude
- ***longitude*** The longitude at the center of the sounding field-of-view.
Parent Field: L2Std/RetrievalGeometry/retrieval_longitude
- ***vertex_latitude*** The latitude at each of the corners of the parallelogram that defines the field-of-view.
Parent Field: L2Std/RetrievalGeometry/retrieval_vertex_latitude
- ***vertex_longitude*** The longitude at each of the corners of the parallelogram that defines the field-of-view.
Parent Field: L2Std/RetrievalGeometry/retrieval_vertex_longitude
- ***time*** The time of the sounding in seconds since 1970-01-01 00:00:00 UTC.
Parent Field: None (computed from RetrievalHeader/retrieval_time_string)

- ***date*** The full date and time of the sounding in UTC, organized as [year,month,day,hour,minute,second,milliseconds]. This information is redundant with that from the *time* variable.
Parent Field: None (computed from RetrievalHeader/retrieval_time_string)
- ***solar_zenith_angle*** The solar zenith angle (in degrees) at the target.
Parent Field: L2Std/RetrievalGeometry/retrieval_solar_zenith
- ***sensor_zenith_angle*** The satellite zenith angle (in degrees) at the target.
Parent Field: L2Std/RetrievalGeometry/retrieval_zenith
- ***xco2*** The bias-corrected X_{CO_2} (in units of ppm), on the original X2007 CO₂ scale. This *should be used for science analysis*. The bias correction formulae are contained in the metadata of the file.
Parent Field: None (derived using bias-correction formula)
- ***xco2_x2019*** The bias-corrected X_{CO_2} (in units of ppm), on the X2019 CO₂ scale. This *should be used for science analysis*.
Parent Field: None
- ***xco2_apriori*** The prior X_{CO_2} assumed by the L2 retrieval, in ppm.
*Parent Field: L2Std/RetrievalResults/xco2_apriori * 1e6*
- ***xco2_uncertainty*** The posterior uncertainty in X_{CO_2} calculated by the L2 algorithm, in ppm. This is generally 30-50% smaller than the true retrieval uncertainty.
*Parent Field: L2Std/RetrievalResults/xco2_uncert * 1e6*
- ***xco2_quality_flag*** A simple quality flag denoting science quality data. 0=higher quality, 1=lower quality.
Parent Field: None
[Note, the "warn_level" field has been removed from version 10].
- ***xco2_qf_bitflag*** Similar to *xco2_quality_flag*, but each bit is meaningful. The different bits of this 32 (or 64)-bit integer tells whether a given threshold test passed (0) or failed (1). See Section 5.2.4 and Table 5-5 in the quality flagging section for detail. The attribute "qf_variables" of the field give the names of the threshold variables.
Parent Field: None
- ***xco2_qf_simple_bitflag*** An 8-bit version of *xco2_qf_bitflag*, but the various quality flag tests are grouped into eight simpler test categories, as described Table 5-6. OCO-2 only.
Parent Field: None
- ***co2_profile_apriori*** The prior profile of CO₂ in ppm.
*Parent Group: L2Std/RetrievalResults/co2_profile_apriori * 1e6*
- ***xco2_averaging_kernel*** The normalized column averaging kernel for the retrieved X_{CO_2} (dimensionless).
Parent Group: L2Std/RetrievalResults/xco2_avg_kernel
- ***pressure_levels*** The retrieval pressure level grid for each sounding in hPa. Note that is simply equal to SigmaB multiplied by the surface pressure.
*Parent Group: L2Std/RetrievalResults/vector_pressure_levels * 0.01*

- ***pressure_weight*** The pressure weighting function *on levels* used in the retrieval. It has the same dimensions as both “pressure levels” and “co2_profile_apriori”.
Parent Group: L2Std/RetrievalResults/pressure_weighting_function
- ***sounding_id*** The sounding_id of the sounding. For GOSAT, this is a 14-digit number defined as YYYYMMDDhhmmss. {YYYY=year, MM=month 1-12, DD=day 1-31, hh=hour 0-23, mm=minute 0-59, ss=seconds 0-59, m=hundreds of milliseconds 0-9, f=footprint number 1-8}. For OCO, it is a 16-digit number defined as YYYYMMDDhhmmssmf. {YYYY=year, MM=month 1-12, DD=day 1-31, hh=hour 0-23, mm=minute 0-59, ss=seconds 0-59, m=hundreds of milliseconds 0-9, f=footprint number 1-8}.
Parent Field: L2Std/RetrievalHeader/sounding_id
- ***source_files*** The L2Std files used to generate this file.
Parent Group: None
- ***file_index*** The 1-based index used to identify which source file each sounding was drawn from. I.e., file_index=2 for a particular sounding means that sounding was drawn from the 2nd element of *source_files*.
Parent Group: None

Main-Level Dimension Variables

(these variables are part of the netcdf-4 definition and will not be needed by most users)

- ***bands***: The three OCO-2 bands.
- ***levels***: The twenty vertical levels in the OCO-2 level-2 full-physics retrieval.
- ***epoch_dimension***: Variable used for dimensioning the 7-integer *date* variable.
- ***vertices***: The 4 vertex indices for vertex_latitude and vertex_longitude.
- ***footprints***: The 8 footprint indices for footprint-dimensioned variables such as *Preprocessors/co2_ratio_offset_per_footprint*.

11.2.2 Preprocessors Group

This group contains information for the two OCO-2 preprocessor algorithms: The A-Band Preprocessor (ABP) and the IMAP-DOAS Preprocessor (IDP).

- ***co2_ratio***: Contains the ratio of the retrieved CO₂ column from the weak CO₂ band relative to that from the strong CO₂ band. This ratio should be near unity. Significant departure from unity is currently used as a way to flag bad soundings (usually cloud or aerosol-contaminated). This value has also been footprint corrected using *co2_ratio_offset_per_footprint*, and further it has been bias corrected to remove a small feature-dependent bias.
Parent Field: L2Std/PreprocessingResults/co2_ratio_idp (and then footprint-corrected).
- ***co2_ratio_offset_per_footprint***: Contains the approximate offset in *co2_ratio* from the mean value across all footprints, used in the construction of *co2_ratio*. OCO-2 only.
Parent Field: none.
- ***co2_ratio_bc***: Contains the ratio of the retrieved CO₂ column from the weak CO₂ band relative to that from the strong CO₂ band. This ratio should be near unity. Significant

departure from unity is currently used as a way to flag bad soundings (usually cloud or aerosol-contaminated). This value been bias corrected to remove a small feature- and footprint-dependent bias.

Parent Field: L2Std/PreprocessingResults/co2_ratio_idp (and then bias-corrected).

- **h2o_ratio**: Contains the ratio of the retrieved H₂O column from the weak CO₂ band relative to that from the strong CO₂ band. This ratio should be near unity. Significant departure from unity is currently used as a way to flag bad soundings (usually cloud or aerosol-contaminated). This value has also been footprint corrected using *h2o_ratio_offset_per_footprint*.
Parent Field: L2Std/PreprocessingResults/h2o_ratio_idp (and then footprint-corrected).
- **h2o_ratio_offset_per_footprint**: Contains the approximate offset in *h2o_ratio* from the mean value across all footprints, used in the construction of *h2o_ratio*. OCO-2 only.
Parent Field: none.
- **h2o_ratio_bc**: Contains the ratio of the retrieved H₂O column from the weak CO₂ band relative to that from the strong CO₂ band. This ratio should be near unity. Significant departure from unity is currently used as a way to flag bad soundings (usually cloud or aerosol-contaminated). This value been bias corrected to remove a small feature- and footprint-dependent bias, and re-scaled to deal with scatter when the amount of water vapor in the atmosphere is low.
Parent Field: L2Std/PreprocessingResults/h2o_ratio_idp (and then bias-corrected).
- **dp_abp**: This is the retrieved surface pressure minus the “best-guess” surface pressure from the meteorological forecast model. This has been adjusted for a clear-sky bias as well as the local surface elevation of the observed footprint. A value of this greater than about 50 hPa absolute value typically indicates cloud or aerosol contamination. Note: for v11.1, this value was recalculated using the Copernicus DEM elevation, which modifies the prior surface pressure.
*Parent Field: L2Std/PreprocessingResults/surface_pressure_delta_abp * 1e-2*
- **xco2_strong_idp**: Estimate of X_{CO_2} using only the IMAP-DOAS strong CO₂ band retrieval at 2.06 μm. The dry air column is taken from the prior. It is constructed as the ratio of the co2 column from the strong CO₂ band, divided by the dry air column. Units are ppm.
Parent Fields: L2Std/PreprocessingResults/co2_column_strong_band_idp, L2Std/PreprocessingResults/dry_air_column_apriori_idp
- **xco2_weak_idp**: Estimate of X_{CO_2} using only the IMAP-DOAS weak CO₂ band retrieval at 1.61 μm. The dry air column is taken from the prior. It is constructed as the ratio of the CO₂ column from the weak CO₂ band, divided by the dry air column. Units are ppm.
Parent Fields: L2Std/PreprocessingResults/co2_column_weak_band_idp, L2Std/PreprocessingResults/dry_air_column_apriori_idp
- **max_declocking_{o2a,wco2,sco2}**: An estimate of the absolute value of the clocking error in the O₂-A, Weak CO₂, and Strong CO₂ bands (used in the clocking correction algorithm that attempts to correct the L1b radiances for clocking errors). Expressed in percent. Typical values range from 0 to 10%.
*Parent Field: abs(L2Std/L1bSpectralParameters/max_declocking_factor_{o2,weak_co2,strong_co2}-1)*100*

- ***color_slice_noise_ratio_{o2a,wco2,sco2}***: An estimate of the sub-FOV variability in continuum radiance as estimated from the color slices for each of the three spectral bands. This is a calculation done only for the Lite Files, but it uses information from `L1bScSpectralParameters/sounding_color_slice_noise_ratio_{o2,weak_co2,strong_co2}`.
- ***h_continuum_{o2a,wco2,sco2}***: This is the standard deviation of the continuum for all soundings in the the frame in which a desired sounding is located, divided by the continuum of that sounding. This is a calculation only done for the lite files. It uses `L1bScSpectralPararameters/radiance_continuum_{o2,weak_co2,strong_co2}` as input. This is a measure of the fov-scale variability of the continuum radiance in each band.

11.2.3 Retrieval Group

This group contains information from the OCO-2 level-2 retrieval algorithm. It contains many fields that will only briefly be summarized here. These are other fields that may be useful to users. Some were used for quality filtering, some for bias correction, and others for neither.

- ***xco2_raw*** is the “raw” X_{CO_2} retrieved by the L2 code *without bias correction*. It should not be used for science analysis.
*Parent Field: L2Std/RetrievalResults/xco2*1e6*
- ***surface_type*** Surface type used in the retrieval: 0=ocean and corresponds to a Cox-Munk+Lambertian surface; 1=land and corresponds to a non-Lambertian surface with a fixed BRDF shape (this is applied to land surfaces). The BRDF is described in the L2 ATBD.
Parent Group: L2Std/RetrievalResults/surface_type (changing Coxmunk,Lambertian->0, Non-Lambertian->1)
- ***snow_flag*** Flag to denote the presence of snow on the ground. For snow to be indicated, this requires `albedo_o2a >= 0.55 AND albedo_sco2 <= 0.35`. Land soundings only. OCO-2 only.
Parent Group: None.
- ***psurf*** Retrieved surface pressure (in hPa) from the L2 algorithm. Note: this can be multiplied with the variable *SigmaB* to determine the profile of pressures for any sounding.
Parent Group: L2Std/RetrievalResults/surface_pressure_fph
- ***psurf_apriori*** A priori surface pressure (in hPa) assumed by the L2 algorithm, taken originally from GEOS5-FP-IT analysis. Calculated from the band-averaged pointing location on the ground. Note: this should be used in conjunction with the variable *SigmaB_Coefficient* to determine the a priori profile of pressures.
Parent Group: L2Std/RetrievalResults/surface_pressure_apriori_fph
- ***dp_o2a*** The difference `psurf - psurf_apriori_o2a`, in hPa. Note: for OCO-2 v11.1, this value was recalculated using the Copernicus DEM elevation which modifies the prior surface pressure.
Parent Group: None.
- ***dp_sco2*** The difference `psurf - psurf_apriori_sco2`, in hPa. This variable is used in the X_{CO_2} bias correction over both land and water surfaces. Note: for OCO-2 v11.1, this value was recalculated using the Copernicus DEM elevation which modifies the prior surface

pressure.

Parent Group: None.

- ***dpfrac*** A quantity used in the X_{CO_2} bias correction. It is essentially the change in X_{CO_2} that results from a change in surface pressure, all other things being equal. It has units of ppm. Formally, $dpfrac = X_{CO_2_raw} * (1 - psurf_apriori_sco2 / psurf)$. For details, see Kiel et al. (2019). Note: for OCO-2 v11.1, this value was recalculated using the Copernicus DEM elevation which modifies the prior surface pressure.
Parent Group: None.
- ***tcwv*** Retrieved Total Column Water Vapor (TCWV) in units of $kg\ m^{-2}$.
*Parent Group: L2Std/RetrievalResults/retrieved_h2o_column * (0.0180153/6.0221415e23).* The latter is required to convert from molecules of H_2O per m^2 to $kg\ H_2O$ per m^2 .
- ***tcwv_apriori*** A priori value of the TCWV derived from the prior H_2O profile in units of $kg\ m^{-2}$. Obtained by dividing the retrieved *tcwv* by the retrieved *h2o_scale* factor.
Parent Group: RetrievalResults/h2o_scale_factor (along with tcwv).
- ***tcwv_uncertainty*** Noise-driven uncertainty on the retrieved TCWV in $kg\ m^{-2}$. Obtained from the product of *tcwv_apriori* times the posterior uncertainty on the *h2o_scale* factor.
Parent Group: RetrievalResults/h2o_scale_factor_uncert
- ***albedo_o2a*** Over-land retrievals: Surface reflectance at a reference wavelength in band 1 ($0.77\ \mu m$) in the primary scattering geometry (sun->ground->sensor) derived from the retrieved BRDF. Over-water retrievals: Retrieved Lambertian albedo at the band 1 reference wavelength.
Parent Group: L2Std/AlbedoResults/albedo_o2_fph (b10: water), L2Std/BRDFResults/brdf_reflectance_o2 (land).
- ***albedo_wco2*** Over-land retrievals: Surface reflectance at a reference wavelength in band 2 ($1.615\ \mu m$) in the primary scattering geometry (sun->ground->sensor) derived from the retrieved BRDF. Over-water retrievals: Retrieved Lambertian albedo at the band 2 reference wavelength.
Parent Group: L2Std/AlbedoResults/albedo_weak_co2_fph (b10: water), L2Std/BRDFResults/brdf_reflectance_weak_co2 (land).
- ***albedo_sco2*** Over-land retrievals: Surface reflectance at a reference wavelength in band 3 ($2.06\ \mu m$) in the primary scattering geometry (sun->ground->sensor) derived from the retrieved BRDF. Over-water retrievals: Retrieved Lambertian albedo at the band 3 reference wavelength.
Parent Group: L2Std/AlbedoResults/albedo_strong_co2_fph (b10: water), L2Std/BRDFResults/brdf_reflectance_strong_co2 (land).
- ***albedo_slope_o2a*** Slope of the *albedo_o2a* term with respect to wavenumber.
Parent Group: L2Std/AlbedoResults/albedo_slope_o2_fph (b10: water), L2Std/BRDFResults/brdf_reflectance_slope_o2 (land).
- ***albedo_slope_wco2*** Slope of the *albedo_wco2* term with respect to wavenumber.
Parent Group: L2Std/AlbedoResults/albedo_slope_weak_co2_fph (b10: water), L2Std/BRDFResults/brdf_reflectance_slope_weak_co2 (land).

- ***albedo_slope_sco2*** Slope of the albedo_sco2 term with respect to wavenumber.
Parent Group: L2Std/AlbedoResults/albedo_slope_strong_co2_fph (b10: water), L2Std/BRDFResults/brdf_reflectance_slope_strong_co2 (land).
- ***albedo_quad_o2a*** Quadratic coefficient of the albedo_o2a term with respect to wavenumber (land only).
Parent Group: L2Std/BRDFResults/brdf_reflectance_quadratic_o2 (land).
- ***albedo_quad_wco2*** Quadratic coefficient of the albedo_wco2 term with respect to wavenumber (land only).
Parent Group: L2Std/BRDFResults/brdf_reflectance_quadratic_weak_co2.
- ***albedo_quad_sco2*** Quadratic coefficient of the albedo_sco2 term with respect to wavenumber (land only).
Parent Group: L2Std/BRDFResults/brdf_reflectance_quadratic_strong_co2 (land).
- ***aod_ice*** Retrieved Extinction Optical Depth of cloud ice at 0.755 μm .
Parent Group: L2Std/AerosolResults/aerosol_aod[,6,1] (1-based counting)*
- ***aod_water*** Retrieved Extinction Optical Depth of cloud water at 0.755 μm .
Parent Group: L2Std/AerosolResults/aerosol_aod[,7,1] (1-based counting)*
- ***aod_dust*** Retrieved Extinction Optical Depth of dust aerosol at 0.755 μm .
Parent Group: L2Std/AerosolResults/aerosol_aod[,1,1] (1-based counting)*
- ***aod_fine_apriori*** A priori Extinction Optical Depth of sulfate+organic carbon aerosol at 0.755 μm .
Parent Group: L2Std/AerosolResults/aerosol_param_apriori
- ***aod_seasalt*** Retrieved Extinction Optical Depth of sea salt aerosol at 0.755 μm .
Parent Group: L2Std/AerosolResults/aerosol_aod[,2,1] (1-based counting)*
- ***aod_bc*** Retrieved Extinction Optical Depth of black carbon at 0.755 μm .
Parent Group: L2Std/AerosolResults/aerosol_aod[,3,1] (1-based counting)*
- ***aod_oc*** Retrieved Extinction Optical Depth of organic carbon at 0.755 μm .
Parent Group: L2Std/AerosolResults/aerosol_aod[,4,1] (1-based counting)*
- ***aod_strataer*** Retrieved Extinction Optical Depth of stratospheric aerosol at 0.755 μm .
Parent Group: L2Std/AerosolResults/aerosol_aod[,8,1] (1-based counting)*
- ***aod_sulfate*** Retrieved Extinction Optical Depth of sulfate aerosol at 0.755 μm .
Parent Group: L2Std/AerosolResults/aerosol_aod[,5,1] (1-based counting)*
- ***aod_total*** Retrieved Extinction Optical Depth of cloud+aerosol at 0.755 μm .
Parent Group: L2Std/AerosolResults/aerosol_total_aod
- ***aod_total_apriori*** A priori value Extinction Optical Depth of cloud+aerosol at 0.755 μm .
Parent Group: L2Std/AerosolResults/aerosol_param_apriori
- ***brdf_weight_slope_{wco2,sco2}*** Retrieved slope across the band of the weight of the parent BRDF function (soil over land, Cox-Munk over ocean) in the weak & strong CO₂ band. *L2Std/BRDFResults/brdf_weight_slope_{weak,strong}_co2*

- ***dws*** Retrieved aod's of the large aerosols, given by $aod_dust + aod_water + aod_seasalt$. This is used in the X_{CO_2} bias correction for soundings over land.
Parent Group: none
- ***dust_height*** Retrieved central pressure of the dust aerosol layer, relative to the retrieved surface pressure. OCO-2 only.
Parent Group: L2Std/AerosolResults/aerosol_param[1,]*
- ***ice_height*** Retrieved central pressure of the cloud ice layer, relative to the retrieved surface pressure.
Parent Group: L2Std/AerosolResults/aerosol_param[1,]*
- ***water_height*** Retrieved central pressure of the cloud water layer, relative to the retrieved surface pressure. OCO-2 only.
Parent Group: L2Std/AerosolResults/aerosol_param[1,]*
- ***deltaT*** Retrieved offset (in Kelvin) to a priori temperature profile.
Parent Group: L2Std/RetrievalResults/temperature_offset_fph
- ***h2o_scale*** Retrieved water vapor scale factor.
Parent Group: L2Std/RetrievalResults/h2o_scale_factor
- ***co2_grad_del*** Change (between the retrieved profile and the prior profile) of the CO₂ dry air mole fraction difference from the surface minus that at level 13, measured in ppm. Level 13 is at a pressure $P = 0.631579$ P_{surf}. This variable is used in the X_{CO_2} bias correction over both land and water surfaces.
Derived from L2Std/RetrievalResults/co2_profile and co2_profile_apriori.
If $c=co2_profile$ and $a=co2_profile_apriori$, then
$$\Delta_{grad_co2} = (c[20]-c[13])*1e6 - (a[20]-a[13])*1e6$$
- ***fs*** Retrieved fluorescence in units of $W\ m^{-2}\ \mu m^{-1}\ sr^{-1}$ at 757 nm.
Derived from: L2Std/RetrievalResults/fluorescence_at_reference.
- ***fs_rel*** Retrieved fluorescence relative to Band 1 continuum signal. OCO-2 only.
Derived from: L2Std/RetrievalResults/fluorescence_at_reference.
- ***chi2_o2a*** Reduced chi-squared value of the L2 fit residuals for band 1.
Parent Group: L2Std/SpectralParameters/reduced_chi_squared_o2_fph
- ***chi2_wco2*** Reduced chi-squared value of the L2 fit residuals for band 2.
Parent Group: L2Std/SpectralParameters/reduced_chi_squared_weak_co2_fph
- ***chi2_sco2*** Reduced chi-squared value of the L2 fit residuals for band 3.
Parent Group: L2Std/SpectralParameters/reduced_chi_squared_strong_co2_fph
- ***rms_rel_o2a*** RMS of the L2 fit residuals for band 1, relative to the continuum signal, in percent.
*Parent Group: L2Std/SpectralParameters/relative_residual_mean_square_o2*100*
- ***rms_rel_wco2*** RMS of the L2 fit residuals for band 2, relative to the continuum signal, in percent.
Parent Group:
*L2Std/SpectralParameters/relative_residual_mean_square_weak_co2*100*

- **rms_rel_sco2** RMS of the L2 fit residuals for band 3, relative to the continuum signal, in percent.
*Parent Group: L2Std/SpectralParameters/relative_residual_mean_square_strong_co2*100*
- **windspeed** Retrieved surface wind speed (in m/s) from the L2 algorithm, over water surfaces only.
Parent Group: L2Std/RetrievalResults/wind_speed
- **windspeed_apriori** Prior surface wind speed (in m/s) used in the L2 algorithm, over water surfaces only. Taken from the GEOS5-FP-IT analysis.
Parent Group: L2Std/RetrievalResults/wind_speed_apriori
- **t700** The estimated temperature at 700 hPa for each sounding, taken from the GEOS5-FP-IT forecast and estimated using linear interpolation. Invalid for soundings in which the surface pressure is lower than 700 hPa.
Parent Group: None.
- **s31** Ratio of continuum signal in the strong CO₂ band to that of the o2a band.
Derived from: L2Std/SpectralParameters/signal_strong_co2_fph
(divided by)
L2Std/SpectralParameters/signal_o2_fph
- **s32** Ratio of continuum signal in the strong CO₂ band to that of the weak CO₂ band.
Derived from: L2Std/SpectralParameters/signal_strong_co2_fph
(divided by)
L2Std/SpectralParameters/signal_weak_co2_fph
- **iterations** Number of iterations taken by the retrieval.
Parent Group: L2Std/RetrievalResults/iterations
- **diverging_steps** Number of diverging steps taken by the retrieval.
Parent Group: L2Std/RetrievalResults/diverging_steps
- **eof3_1_rel** Relative amplitude of the 1st EOF in the strong CO₂ band. OCO-2 only.
*Parent Group: (L2Std/RetrievalResults/eof_3_scale_strong_co2) / (L2Std/SpectralParameters/signal_strong_co2_fph) * 1.7e19 * 100*
- **SigmaB** The coefficients by which to multiply *psurf* to determine the pressure at each vertical level in the profile. Note this is a single list of numbers, rather than repeated for each sounding (as all the other quantities are).

11.2.4 Sounding Group

Contains all the geolocation and time information for each sounding. For GOSAT, these contain the corrected geolocation information.

- **altitude** The mean surface elevation in the target field of view, in meters. Note: for OCO-2 v11.1, this was taken from the Copernicus DEM.
Parent Field: L2Std/RetrievalGeometry/retrieval_altitude
- **altitude_stddev** The standard deviation of the surface elevation in the target field of view, in meters. Note: for OCO-2 v11.1, this was taken from the Copernicus DEM.
Parent Field: L2Std/RetrievalGeometry/retrieval_surface_roughness

- ***orbit*** is the orbit number within the current repeat cycle.
Parent Field: L2Std/Metadata/StartOrbitNumber
- ***path*** The WRS path number of the current orbit. 1-233.
Parent Field: L2Std/Metadata/StartPathNumber
- ***footprint*** The footprint number of each sounding (1-8).
Parent Field: L2Std/RetrievalHeader/sounding_index
- ***land_water_indicator*** determines the land surface properties at the field of view. 0: land; 1: water; 2: inland water; 3: mixed.
Parent Field: L2Std/RetrievalGeometry/retrieval_land_water_indicator
- ***land_fraction*** The fraction of land contained in the field-of-view for each sounding.
Parent Field: L2Std/RetrievalGeometry/retrieval_land_fraction.
- ***11b_type*** gives the version number of the input level-1B data. (e.g., “5000”, which means B5.0.00)
Parent Field: Derived from parent file name.
- ***operation_mode*** Nadir (0), Glint (1), Target (2), Transition (3), or Snapshot Area Mode (4).
Parent Field: Derived from L2Std/RetrievalGeometry/retrieval_operation_mode
- ***solar_azimuth_angle*** The solar azimuth angle (in degrees) at the target, measured east of north from the point of view of an observer on the ground at the target.
Parent Field: L2Std/RetrievalGeometry/retrieval_solar_azimuth
- ***sensor_azimuth_angle*** The satellite azimuth angle (in degrees) at the target, measured east of north from the point of view of an observer on the ground at the target.
Parent Field: L2Std/RetrievalGeometry/retrieval_sensor_azimuth
- ***polarization_angle*** The angle (in degrees) between the polarization axis of the sensor and the local meridian plane (as defined by the plane made between the local normal at the target location and the ray from the satellite to the target).
Parent Field: L2Std/RetrievalGeometry/retrieval_polarization_angle
- ***glint_angle*** The angle (in degrees) between the local direction to the sensor, and the direction for pure glint observation (i.e., the outgoing direction from the surface for specularly reflected solar rays).
- ***airmass*** The relative airmass of the sounding, defined as $1/\cos(\text{solar_zenith_angle}) + 1/\cos(\text{sensor_zenith_angle})$.
- ***snr_o2a*** The estimated signal-to-noise ratio in the continuum of the O2A-band.
Parent Field: L2Std/L1bScSpectralParameters/snr_o2_11b
- ***snr_wco2*** The estimated signal-to-noise ratio in the continuum of the weak CO₂ band.
Parent Field: L2Std/L1bScSpectralParameters/snr_weak_co2_11b
- ***snr_sco2*** The estimated signal-to-noise ratio in the continuum of the strong CO₂ band.
Parent Field: L2Std/L1bScSpectralParameters/snr_strong_co2_11b

- ***pcs_data_source*** The data source used by PCS in determining sounding times. OCO-3 only.
Parent Field: L2Std/RetrievalGeometry/retrieval_pcs_data_source
- ***pma_zenith_angle*** The zenith angle of the pointing mechanism assembly, in degrees. OCO-3 only.
Parent Field: L2Std/RetrievalGeometry/retrieval_pma_zenith_angle
- ***pma_azimuth_angle*** The azimuth angle of the pointing mechanism assembly, in degrees. OCO-3 only.
Parent Field: L2Std/RetrievalGeometry/retrieval_pma_azimuth_angle
- ***target_id*** For target or SAM-mode data, the id of the target. OCO-3 only.
Parent Field: Derived from an offline file.
- ***target_name*** For target or SAM-mode data, the name of the target. OCO-3 only.
Parent Field: Derived from an offline file.

11.2.5 Meteorology Group

Contains updated meteorological information specific to version 9, using the updated GEOS5-FP-IT meteorological resampler code, as well as the updated pointing information. The resampler is run for both per-band pointing information, as well as the band-averaged location.

- ***psurf_apriori_o2a*** The estimated a priori surface pressure (hPa), for the O2A-band pointing location. Note: for OCO-2 v11.1, this value was recalculated using the Copernicus DEM elevation which modifies the prior surface pressure.
*Parent Field: Met/FootprintMeteorology/footprint_surface_pressure_met[0] * 0.01*
- ***psurf_apriori_wco2*** The estimated a priori surface pressure (hPa), for the WCO2-band pointing location. Note: for OCO-2 v11.1, this value was recalculated using the Copernicus DEM elevation which modifies the prior surface pressure.
*Parent Field: Met/FootprintMeteorology/footprint_surface_pressure_met[1] * 0.01*
- ***psurf_apriori_sco2*** The estimated a priori surface pressure (hPa), for the SCO2-band pointing location. Note: for OCO-2 v11.1, this value was recalculated using the Copernicus DEM elevation which modifies the prior surface pressure.
*Parent Field: Met/FootprintMeteorology/footprint_surface_pressure_met[2] * 0.01*
- ***windspeed_u_met*** Prior surface wind speed (in m/s) in the horizontal U (North-South) direction. Positive *u* means the N-S wind component is flowing to the north (is from the south). Taken from the GEOS5-FP-IT analysis. Can be used along with *windspeed_v_met* to calculate the prior wind direction.
Parent Group: Met/RetrievalResults/wind_speed_u_met
- ***windspeed_v_met*** Prior surface wind speed (in m/s) in the horizontal V (East-West) direction. Positive *v* means the E-W wind component is flowing to the east (is from the west). Taken from the GEOS5-FP-IT analysis. Can be used along with *windspeed_u_met* to calculate the prior wind direction.
Parent Group: Met/RetrievalResults/wind_speed_v_met

11.2.6 Auxiliary Group (OCO-2 v11.1 only)

Contains information specific to OCO-2 v11.1.

- ***altitude_b11*** The original altitude used for the v11 full-physics retrieval, taken from the original v11 DEM.
Parent Field: L2Std/RetrievalGeometry/retrieval_altitude
- ***altitude_stddev_b11*** The altitude stddev in the target field of view taken from the original v11 DEM.
Parent Field: L2Std/RetrievalGeometry/retrieval_surface_roughness

12 Full Data Tables for OCO-2 and OCO-3 Level 2 Standard Files (L2Std)

The tables below give a full listing of the variables in each folder/group and a short description including the data type. We suggest that users familiarize themselves with the data dimensions by browsing with HDFview or a similar tool.

The L2 data products in these tables are from the v10 L2Std and Lite files.

12.1 OCO-2 and OCO-3 L2Std Metadata Group

The Metadata group (see Table 12-1 below) contains detailed information about the metadata fields from the L2 retrievals. The values in the table apply to both OCO-2 and OCO-3 data products.

Table 12-1: Metadata in Level 2 Standard Data file (L2Std).

| Element | Storage | Comment |
|-------------------------------|-----------|--|
| AbscoCO2Scale | Float32 | Empirical scaling factors for CO ₂ ABSCO tables. Values should be different for the 1.6 micron and 2.06 micron bands and were chosen to provide agreement of retrieved X_{CO_2} with TCCON X_{CO_2} . |
| AbscoH2OScale | Float32 | Empirical scaling factor for H ₂ O ABSCO tables. Currently should be 1.0. |
| AbscoO2Scale | Float32 | Empirical scaling factor for O ₂ ABSCO tables. Values chosen to improve agreement between retrieved surface pressure and independent estimates from a numerical weather prediction model. |
| AcquisitionMode | VarLenStr | The instrument mode in which the data in the product were collected. Valid values are: '\Glint', '\Nadir', '\Target', '\Sample Dark Calibration', '\Sample Lamp Calibration', '\Sample Solar/limb Calibration', '\Single-Pixel Dark Calibration', '\Single-Pixel Lamp Calibration', '\Single-Pixel Solar/limb Calibration' |
| ActualFrames | Signed32 | Actual number of frames reported in this product |
| ActualGoodRetrievals | Signed32 | Number of retrievals with outcome flag that passed convergence/divergence criteria |
| ActualRetrievals | Signed32 | Actual number of retrievals reported in the product |
| AllAerosolTypes | VarLenStr | List of aerosol types available for use in retrieval"; |
| AncillaryDataDescriptors | VarLenStr | An array of file names that specifies all of the ancillary data files that were used to generate this output product. Ancillary data sets include all input except for the primary input files. |
| ARPAncillaryDatasetDescriptor | VarLenStr | The name of the Ancillary Radiometric Product file used to calibrate this file |

| Element | Storage | Comment |
|--|-----------|---|
| AscendingEquatorCrossingDate (OCO-2 Only) | FixLenStr | The date of the equator crossing of the spacecraft ground track in the ascending direction |
| AscendingEquatorCrossingLongitude (OCO-2 Only) | FixLenStr | The longitude of the equator crossing of the spacecraft ground track in the ascending direction |
| AscendingEquatorCrossingTime (OCO-2 Only) | FixLenStr | The time of the equator crossing of the spacecraft ground track in the ascending direction |
| BuildId | VarLenStr | The identifier of the build containing the software that created the product. |
| CollectionLabel | VarLenStr | Label associating files in a collection |
| ColorSlicePositionO2 | Signed16 | Absolute spectral position of each ABO2 color slice. |
| ColorSlicePositionStrongCO2 | Signed16 | Absolute spectral position of each SCO2 color slice. |
| ColorSlicePositionWeakCO2 | Signed16 | Absolute spectral position of each WCO2 color slice. |
| DataFormatType | FixLenStr | 'NCSA HDF' - A character string that describes the internal format of the data product. |
| EphemerisType (OCO-2 Only) | VarLenStr | The source of the spacecraft ephemeris data that were utilized to generate this data file |
| EquatorCrossingDate (OCO-2 Only) | FixLenStr | The date of the equator crossing of the spacecraft ground track in the descending direction |
| EquatorCrossingLongitude (OCO-2 Only) | Float32 | The longitude of the equator crossing of the spacecraft ground track in the descending direction |
| EquatorCrossingTime (OCO-2 Only) | FixLenStr | The time of the equator crossing of the spacecraft ground track in the descending direction |
| ExpectedFrames | Signed32 | Nominal number of frames in this product |
| FirstSoundingId | Signed64 | The ID of the first sounding in this file |
| GapStartTime | FixLenStr | The timestamp after which a nonexistent, unnecessary, spurious, questionable, or erroneous data segment begins |
| GapStopTime | FixLenStr | The timestamp before which a nonexistent, unnecessary, spurious, questionable, or erroneous data segment ends |
| GranulePointer | VarLenStr | The filename of this product |
| HDFVersionId | VarLenStr | '5.x\' - A character string that identifies the version of the HDF (Hierarchical Data Format) software that was used to generate this data file |
| InputPointer | VarLenStr | A pointer to one or more data granules that provide the major input that was used to generate this product. |
| InstrumentShortName | VarLenStr | "OCO-2\' - The name of the instrument that collected the telemetry data |

| Element | Storage | Comment |
|-------------------------------------|-----------|--|
| L2FullPhysicsAlgorithmDescriptor | VarLenStr | Identification of the algorithm and/or version used to generate this product |
| L2FullPhysicsDataVersion | VarLenStr | The source of the data used by the Full-physics algorithm: '\r01\' - initial processing; '\r02\'', '\r03\'', etc. - reprocessed data |
| L2FullPhysicsExeVersion | VarLenStr | The build version number of the Full-physics algorithm used to generate this product |
| L2FullPhysicsInputPointer | VarLenStr | Pointer to one or more data granules and auxilliary files that provide the major input that was used to generate this product |
| L2FullPhysicsProductionLocation | VarLenStr | Facility in which Full Physics code was run, typically: '\JPL\'', '\Pleiades\' |
| LastSoundingId | Int64 | he ID of the last sounding in this file |
| LongName | VarLenStr | A complete descriptive name for the data type of this product |
| ModeCounter | FixLenStr | The Nth occurrence of this particular mode for this orbit, indicated by letter ('\a\'', '\b\'', '\c\'', '\d\'', etc.) |
| OperationMode | FixLenStr | The two-letter abbreviation of the AcquisitionMode: GL, ND, TG, DS, LS, SS, BS, NP, GP, TP, DP, LP, SP, BP, XS, XP, MS, MP, SB |
| OrbitEccentricity (OCO-2 Only) | Float32 | The eccentricity of the spacecraft orbital path |
| OrbitInclination (OCO-2 Only) | Float32 | The angle between the plane of the spacecraft orbital path and the Earth equatorial plane |
| OrbitParametersPointer (OCO-2 Only) | VarLenStr | The data files that provided the orbit parameters used to generate this product |
| OrbitPeriod (OCO-2 Only) | Float32 | The time span between two consecutive descending node crossings |
| OrbitSemiMajorAxis (OCO-2 Only) | Float32 | The length of the semimajor axis of the spacecraft orbit |
| OrbitStartDate (OCO-2 Only) | FixLenStr | The date of the equator crossing of the spacecraft nadir track in the descending direction |
| OrbitStartLongitude (OCO-2 Only) | Float32 | The longitude of the equator crossing of the spacecraft ground track in the descending direction |
| OrbitStartTime (OCO-2 Only) | FixLenStr | The time of the equator crossing of the spacecraft ground track in the descending direction |
| PlatformLongName | VarLenStr | 'Orbiting Carbon Observatory 2' |
| PlatformShortName | VarLenStr | 'OCO-2' |
| PlatformType | VarLenStr | 'spacecraft' - The type of platform associated with the instrument which acquires the accompanying data |
| ProcessingLevel | VarLenStr | Indicates data level (Level 0, Level 1A, Level 1B, Level 2) in this product |

| Element | Storage | Comment |
|-------------------------------|-----------|---|
| ProducerAgency | VarLenStr | 'NASA' - Identification of the agency that provides the project funding |
| ProducerInstitution | VarLenStr | 'JPL' - Identification of the institution that provides project management. |
| ProductionDateTime | VarLenStr | The date and time at which the product was created (yyyy-mm-ddThh:mm:ss.mmmZ) |
| ProductionLocation | VarLenStr | Facility in which this file was produced, typically:'Operations Pipeline', 'Operations Pipeline 2', 'Science Computing Facility', 'Test Pipeline', Test Pipeline 2' |
| ProductionLocationCode | VarLenStr | One-letter code indicating the ProductionLocation, typically: ' ' - Operations Pipelines (1) or 2, 's' - Science Computing Facility, 't' - Test Pipelines (1) or 2 |
| ProjectId | VarLenStr | 'OCO-2' - The project identification string |
| QAGranulePointer | VarLenStr | A pointer to the quality assessment product that was generated with this product |
| RadianceConversionFactor | Float32 | Multiplicative factor used to convert $W m^{-2} sr^{-1} um^{-1}$ to $Ph sec^{-1} m^{-2} sr^{-1} um^{-1}$ at 760 nm (38.228×10^{17}) |
| RangeBeginningDate | FixLenStr | The date on which the earliest data contained in the product were acquired (yyyy-mm-dd) |
| RangeBeginningTime | FixLenStr | The time at which the earliest data contained in the product were acquired (hh:mm:ss.mmmZ) |
| RangeEndingDate | FixLenStr | The date on which the latest data contained in the product were acquired (yyyy-mm-dd) |
| RangeEndingTime | FixLenStr | The time at which the latest data contained in the product were acquired (hh:mm:ss.mmmZ) |
| ReportedSoundings | Signed8 | Indicates the inclusion of each footprint in the data: 0 - not included, 1 - included |
| RetrievalIterationLimit | String | Maximum number of iterations allowed before the algorithm gives up and sets the outcome_flag to 3 |
| ShortName | VarLenStr | The short name identifying the data type of this product |
| SISName | VarLenStr | The name of the document describing the contents of the product |
| SISVersion | VarLenStr | The version of the document describing the contents of the product |
| SizeMBECSDDataGranule | Float32 | The size of this data granule in Megabytes |
| SpectralChannel | String | A description of the spectral channels used for the measurements |
| StartOrbitNumber (OCO-2 Only) | Signed32 | The first orbit on which data contained in the product were acquired |
| StartPathNumber (OCO-2 Only) | Signed32 | The first WRS path on which data contained in the product was collected |

| Element | Storage | Comment |
|-----------------------------------|----------|---|
| StopOrbitNumber (OCO-2 Only) | Signed32 | The last orbit on which data contained in the product were acquired |
| StopPathNumber (OCO-2 Only) | Signed32 | The last WRS path on which data contained in the product was collected |
| StartMissionSolarDay (OCO-3 Only) | Signed32 | The first local solar day of the mission on which data contained in the product were acquired |
| StopMissionSolarDay(OCO-3 Only) | Signed32 | The last local solar day of the mission on which data contained in the product were acquired |
| VMRO2 | Float32 | The volume mixing ratio of atmospheric O2 |

12.2 Aerosol Results Group

The AerosolResults group (see Table 12-2 below) contains detailed information about the data fields from the L2 retrievals. The values in the table apply to both OCO-2 and OCO-3 data products.

Table 12-2: Aerosol Results data in Level 2 Standard Data file (L2Std).

| Data Element | Type | Comments |
|------------------------|-----------|--|
| aerosol_aod | Float32 | Retrieved column-integrated aerosol optical depth for column segment: [Total, Low, Med, High] |
| aerosol_model | FixLenStr | Aerosol model used, if retrieved, one of: [profile_linear, profile_log, linear_aod, gaussian_linear, gaussian_log] |
| aerosol_param | Float32 | Retrieved aerosol parameter value |
| aerosol_param_apriori | Float32 | A priori of retrieved aerosol parameter |
| aerosol_param_uncert | Float32 | Uncertainty of retrieved aerosol parameter |
| aerosol_total_aod | Float32 | Retrieved total column-integrated aerosol optical depth for all aerosol types |
| aerosol_type_retrieved | Signed8 | Flag that indicates whether aerosol type was retrieved or not (1 yes, 0 no) |

12.3 Albedo Results Group

The AlbedoResults group (see Table 12-3 below) contains detailed information about the albedo properties in the L2 retrievals. The values in the table apply only to OCO-3 v10 data products. These tables have been removed from the OCO-2 v11 data products.

Table 12-3: Albedo Results data in Level 2 Standard Data file (L2Std).

| Data Element | Type | Comments |
|-------------------------------|---------|--|
| albedo_apriori_o2_fph | Float32 | <i>a priori</i> of retrieved Lambertian component of albedo at 0.77 microns |
| albedo_apriori_strong_co2_fph | Float32 | <i>a priori</i> of retrieved Lambertian component of albedo at 2.06 microns |
| albedo_apriori_weak_co2_fph | Float32 | <i>a priori</i> of retrieved Lambertian component of albedo at 1.615 microns |

| Data Element | Type | Comments |
|---------------------------------|---------|---|
| albedo_o2_fph | Float32 | Retrieved Lambertian component of albedo at 0.77 microns |
| albedo_slope_apriori_o2 | Float32 | <i>a priori</i> of retrieved spectral dependence of Lambertian component of albedo within ABO2 band |
| albedo_slope_apriori_strong_co2 | Float32 | <i>a priori</i> of spectral dependence of Lambertian component of albedo within SCO2 band |
| albedo_slope_apriori_weak_co2 | Float32 | <i>a priori</i> of retrieved spectral dependence of Lambertian component of albedo within WCO2 band |
| albedo_slope_o2 | Float32 | Retrieved spectral dependence of Lambertian component of albedo within ABO2 band |
| albedo_slope_strong_co2 | Float32 | Retrieved spectral dependence of Lambertian component of albedo within SCO2 band |
| albedo_slope_uncert_o2 | Float32 | Uncertainty of retrieved spectral dependence of Lambertian component of albedo within ABO2 band |
| albedo_slope_uncert_strong_co2 | Float32 | Uncertainty of spectral dependence of Lambertian component of albedo within SCO2 band |
| albedo_slope_uncert_weak_co2 | Float32 | Uncertainty of retrieved spectral dependence of Lambertian component of albedo within WCO2 band |
| albedo_slope_weak_co2 | Float32 | Retrieved spectral dependence of Lambertian component of albedo within WCO2 band |
| albedo_strong_co2_fph | Float32 | Retrieved Lambertian component of albedo at 2.06 microns |
| albedo_uncert_o2_fph | Float32 | Uncertainty of retrieved Lambertian component of albedo 0.77 microns |
| albedo_uncert_strong_co2_fph | Float32 | Uncertainty of retrieved Lambertian component of albedo at 2.06 microns |
| albedo_uncert_weak_co2_fph | Float32 | Uncertainty of retrieved Lambertian component of albedo at 1.615 microns |
| albedo_weak_co2_fph | Float32 | Retrieved Lambertian component of albedo at 1.615 microns |

12.4 BRDF Results

The BRDFResults group (see Table 12-4 below) contains detailed information about the Bidirectional reflectance distribution function in L2 retrievals.

Table 12-4: BRDF Results data in Level 2 Standard Data file (L2Std) and Diagnostic file (L2Dia).

| Data Element | Type | Comments |
|------------------------------|---------|---|
| brdf_anisotropy_parameter_o2 | Float32 | RPV kernel anisotropy parameter for ABO2 band (set to 0.75) |

| Data Element | Type | Comments |
|---|---------|---|
| brdf_anisotropy_parameter_strong_co2 | Float32 | RPV kernel anisotropy parameter for SCO2 band (set to 0.75) |
| brdf_anisotropy_parameter_weak_co2 | Float32 | RPV kernel anisotropy parameter for WCO2 band (set to 0.75) |
| brdf_asymmetry_parameter_o2 | Float32 | RPV kernel asymmetry parameter for ABO2 band (set to -0.1) |
| brdf_asymmetry_parameter_strong_co2 | Float32 | RPV kernel asymmetry parameter for SCO2 band (set to -0.1) |
| brdf_asymmetry_parameter_weak_co2 | Float32 | RPV kernel asymmetry parameter for WCO2 band (set to -0.1) |
| brdf_breon_factor_o2 | Float32 | Amplitude factor applied for Breon part of BRDF for ABO2 band (set to 1e-20) |
| brdf_breon_factor_strong_co2 | Float32 | Amplitude factor applied for Breon part of BRDF for SCO2 band (set to 1e-20) |
| brdf_breon_factor_weak_co2 | Float32 | Amplitude factor applied for Breon part of BRDF for WCO2 band (set to 1e-20) |
| brdf_hotspot_parameter_o2 | Float32 | RPV kernel hotspot parameter for ABO2 band (set to 0.05) |
| brdf_hotspot_parameter_strong_co2 | Float32 | RPV kernel hotspot parameter for SCO2 band (set to 0.05) |
| brdf_hotspot_parameter_weak_co2 | Float32 | RPV kernel hotspot parameter for WCO2 band (set to 0.05) |
| brdf_rahman_factor_o2 | Float32 | Amplitude factor for Rahman (RPV) part of BRDF for ABO2 band (set to 1.0) |
| brdf_rahman_factor_strong_co2 | Float32 | Amplitude factor for Rahman (RPV) part of BRDF for SCO2 band (set to 1.0) |
| brdf_rahman_factor_weak_co2 | Float32 | Amplitude factor for Rahman (RPV) part of BRDF for WCO2 band (set to 1.0) |
| brdf_reflectance_apriori_o2 | Float32 | A priori of retrieved reflectance, computed from BRDF evaluated at the observation geometry, at 0.77 micron wavelength |
| brdf_reflectance_apriori_strong_co2 | Float32 | A priori of retrieved reflectance, computed from BRDF evaluated at the observation geometry, at 2.06 micron wavelength |
| brdf_reflectance_apriori_weak_co2 | Float32 | A priori of retrieved reflectance, computed from BRDF evaluated at the observation geometry, at 1.615 micron wavelength |
| brdf_reflectance_o2 | Float32 | Retrieved reflectance, computed from BRDF evaluated at the observation geometry, at 0.77 micron wavelength |
| brdf_reflectance_quadratic_apriori_o2 | Float32 | A priori of retrieved quadratic spectral dependence of reflectance in ABO2 band |
| brdf_reflectance_quadratic_apriori_strong_co2 | Float32 | A priori of retrieved quadratic spectral dependence of reflectance in SCO2 band |
| brdf_reflectance_quadratic_apriori_weak_co2 | Float32 | A priori of retrieved quadratic spectral dependence of reflectance in WCO2 band |

| Data Element | Type | Comments |
|--|-------------|--|
| brdf_reflectance_quadratic_o2 | Float32 | Retrieved quadratic spectral dependence of reflectance in ABO2 band |
| brdf_reflectance_quadratic_strong_co2 | Float32 | Retrieved quadratic spectral dependence of reflectance in SCO2 band |
| brdf_reflectance_quadratic_uncert_o2 | Float32 | Uncertainty of retrieved quadratic spectral dependence of reflectance in ABO2 band |
| brdf_reflectance_quadratic_uncert_strong_co2 | Float32 | Uncertainty of retrieved quadratic spectral dependence of reflectance in SCO2 band |
| brdf_reflectance_quadratic_uncert_weak_co2 | Float32 | Uncertainty of retrieved quadratic spectral dependence of reflectance in WCO2 band |
| brdf_reflectance_quadratic_weak_co2 | Float32 | Retrieved quadratic spectral dependence of reflectance in WCO2 band |
| brdf_reflectance_slope_apriori_o2 | Float32 | A priori of retrieved linear spectral dependence of reflectance in ABO2 band |
| brdf_reflectance_slope_apriori_strong_co2 | Float32 | A priori of retrieved linear spectral dependence of reflectance in SCO2 band |
| brdf_reflectance_slope_apriori_weak_co2 | Float32 | A priori of retrieved linear spectral dependence of reflectance in WCO2 band |
| brdf_reflectance_slope_o2 | Float32 | Retrieved linear spectral dependence of reflectance in ABO2 band |
| brdf_reflectance_slope_strong_co2 | Float32 | Retrieved linear spectral dependence of reflectance in SCO2 band |
| brdf_reflectance_slope_uncert_o2 | Float32 | Uncertainty of retrieved linear spectral dependence of reflectance in ABO2 band |
| brdf_reflectance_slope_uncert_strong_co2 | Float32 | Uncertainty of retrieved linear spectral dependence of reflectance in SCO2 band |
| brdf_reflectance_slope_uncert_weak_co2 | Float32 | Uncertainty of retrieved linear spectral dependence of reflectance in WCO2 band |
| brdf_reflectance_slope_weak_co2 | Float32 | Retrieved linear spectral dependence of reflectance in WCO2 band |
| brdf_reflectance_strong_co2 | Float32 | Retrieved reflectance, computed from BRDF evaluated at the observation geometry, at 2.06 micron wavelength |
| brdf_reflectance_uncert_o2 | Float32 | Uncertainty of retrieved reflectance, computed from BRDF evaluated at the observation geometry, at 0.77 micron wavelength |
| brdf_reflectance_uncert_strong_co2 | Float32 | Uncertainty of retrieved reflectance, computed from BRDF evaluated at the observation geometry, at 2.06 micron wavelength |
| brdf_reflectance_uncert_weak_co2 | Float32 | Uncertainty of retrieved reflectance, computed from BRDF evaluated at the observation geometry, at 1.615 micron wavelength |
| brdf_reflectance_weak_co2 | Float32 | Retrieved reflectance, computed from BRDF evaluated at the observation geometry, at 1.615 micron wavelength |

| Data Element | Type | Comments |
|--|-------------|---|
| brdf_weight_apriori_o2 | Float32 | A priori of overall retrieved weight for the composite BRDF, at reference wavelength, for ABO2 band |
| brdf_weight_apriori_strong_co2 | Float32 | A priori of overall retrieved weight for the composite BRDF, at reference wavelength, for SCO2 band |
| brdf_weight_apriori_weak_co2 | Float32 | A priori of overall retrieved weight for the composite BRDF, at reference wavelength, for WCO2 band |
| brdf_weight_o2 | Float32 | Overall retrieved weight for the composite BRDF, at reference wavelength, for ABO2 band |
| brdf_weight_quadratic_apriori_o2 | Float32 | A priori of overall retrieved in-band quadratic of the weight for the composite BRDF for ABO2 band |
| brdf_weight_quadratic_apriori_strong_co2 | Float32 | A priori of overall retrieved in-band quadratic of the weight for the composite BRDF for SCO2 band |
| brdf_weight_quadratic_apriori_weak_co2 | Float32 | A priori of overall retrieved in-band quadratic of the weight for the composite BRDF for WCO2 band |
| brdf_weight_quadratic_o2 | Float32 | Overall retrieved in-band quadratic of the weight for the composite BRDF for ABO2 band |
| brdf_weight_quadratic_strong_co2 | Float32 | Overall retrieved in-band quadratic of the weight for the composite BRDF for SCO2 band |
| brdf_weight_quadratic_uncert_o2 | Float32 | Uncertainty of overall retrieved in-band quadratic of the weight for the composite BRDF for ABO2 band |
| brdf_weight_quadratic_uncert_strong_co2 | Float32 | Uncertainty of overall retrieved in-band quadratic of the weight for the composite BRDF for SCO2 band |
| brdf_weight_quadratic_uncert_weak_co2 | Float32 | Uncertainty of overall retrieved in-band quadratic of the weight for the composite BRDF for WCO2 band |
| brdf_weight_quadratic_weak_co2 | Float32 | Overall retrieved in-band quadratic of the weight for the composite BRDF for WCO2 band |
| brdf_weight_slope_apriori_o2 | Float32 | A priori of overall retrieved in-band slope of the weight for the composite BRDF for ABO2 band |
| brdf_weight_slope_apriori_strong_co2 | Float32 | A priori of overall retrieved in-band slope of the weight for the composite BRDF for SCO2 band |
| brdf_weight_slope_apriori_weak_co2 | Float32 | A priori of overall retrieved in-band slope of the weight for the composite BRDF for WCO2 band |
| brdf_weight_slope_o2 | Float32 | Overall retrieved in-band slope of the weight for the composite BRDF for ABO2 band |
| brdf_weight_slope_strong_co2 | Float32 | Overall retrieved in-band slope of the weight for the composite BRDF for SCO2 band |

| Data Element | Type | Comments |
|-------------------------------------|---------|--|
| brdf_weight_slope_uncert_o2 | Float32 | Uncertainty of overall retrieved in-band slope of the weight for the composite BRDF for ABO2 band |
| brdf_weight_slope_uncert_strong_co2 | Float32 | Uncertainty of overall retrieved in-band slope of the weight for the composite BRDF for SCO2 band |
| brdf_weight_slope_uncert_weak_co2 | Float32 | Uncertainty of overall retrieved in-band slope of the weight for the composite BRDF for WCO2 band |
| brdf_weight_slope_weak_co2 | Float32 | Overall retrieved in-band slope of the weight for the composite BRDF for WCO2 band |
| brdf_weight_strong_co2 | Float32 | Overall retrieved weight for the composite BRDF, at reference wavelength, for SCO2 band |
| brdf_weight_uncert_o2 | Float32 | Uncertainty of overall retrieved weight for the composite BRDF, at reference wavelength, for ABO2 band |
| brdf_weight_uncert_strong_co2 | Float32 | Uncertainty of overall retrieved weight for the composite BRDF, at reference wavelength, for SCO2 band |
| brdf_weight_uncert_weak_co2 | Float32 | Uncertainty of overall retrieved weight for the composite BRDF, at reference wavelength, for WCO2 band |
| brdf_weight_weak_co2 | Float32 | Overall retrieved weight for the composite BRDF, at reference wavelength, for WCO2 band |

12.5 Dispersion Results

The DispersionResults group (see Table 12-5 below) contains detailed information about the dispersion properties in the L2 retrievals.

Table 12-5: Dispersion Results fields in Level 2 Standard Data file (L2Std) and Diagnostic file (L2Dia)

| Data Element | Type | Comments |
|--------------------------------------|---------|--|
| dispersion_offset_apriori_o2 | Float64 | a priori of retrieved dispersion offset term in ABO2 band |
| dispersion_offset_apriori_strong_co2 | Float64 | a priori of retrieved dispersion offset term in SCO2 band |
| dispersion_offset_apriori_weak_co2 | Float64 | a priori of retrieved dispersion offset term in WCO2 band |
| dispersion_offset_o2 | Float64 | Retrieved dispersion offset term in ABO2 band |
| dispersion_offset_strong_co2 | Float64 | Retrieved dispersion offset term in SCO2 band |
| dispersion_offset_uncert_o2 | Float32 | Uncertainty of retrieved dispersion offset term in ABO2 band |
| dispersion_offset_uncert_strong_co2 | Float32 | Uncertainty of retrieved dispersion offset term in SCO2 band |
| dispersion_offset_uncert_weak_co2 | Float32 | Uncertainty of retrieved dispersion offset term in WCO2 band |

| Data Element | Type | Comments |
|---------------------------------------|---------|--|
| dispersion_offset_weak_co2 | Float64 | Retrieved dispersion offset term in WCO2 band |
| dispersion_spacing_apriori_o2 | Float32 | a priori of retrieved dispersion spacing in ABO2 band |
| dispersion_spacing_apriori_strong_co2 | Float32 | a priori of retrieved dispersion spacing in SCO2 band |
| dispersion_spacing_apriori_weak_co2 | Float32 | a priori of retrieved dispersion spacing in WCO2 band |
| dispersion_spacing_o2 | Float32 | Retrieved dispersion spacing in ABO2 band |
| dispersion_spacing_strong_co2 | Float32 | Retrieved dispersion spacing in SCO2 band |
| dispersion_spacing_uncert_o2 | Float32 | Uncertainty of retrieved dispersion spacing in ABO2 band |
| dispersion_spacing_uncert_strong_co2 | Float32 | Uncertainty of retrieved dispersion spacing in SCO2 band |
| dispersion_spacing_uncert_weak_co2 | Float32 | Uncertainty of retrieved dispersion spacing in WCO2 band |
| dispersion_spacing_weak_co2 | Float32 | Retrieved dispersion spacing in WCO2 band |

12.6 L1BSc Sounding Reference Fields

The L1bScSoundingReference group (see Table 12-6 below) contains certain fields from the L1BSc data files.

Table 12-6: L1BSc sounding reference in Level 2 Standard Data file (L2Std) and Diagnostic file (L2Dia).

| Data Element | Type | Comments |
|-------------------------------------|---------------|---|
| packaging_qual_flag | UInt8 | Bit flags recording errors during packaging of L2 full physics and preprocessing output into retrieval arrays: <ul style="list-style-type: none"> • 0—Good • Non-zero—See documentation |
| retrieval_index | Int32 | The index into the Retrieval dimension of arrays in the RetrievalResults, RetrievedStateVector, and SpectralParameters groups for soundings associated with retrievals |
| selection_flag_sel (OCO-2 v11 only) | IntBitfield 8 | Bitfield qual flag (selected = all bits 0), bit pos: 0: preconditions not met, 1: exceeded max warn level, 2: exceeded warn level cutoff, 3: randomly deselected, 4: matched to 0 size bin, 5: invalid geolocation, 6: no matching bin, 7: no matching enhanced mode. |
| sounding_id_l1b | Int64 | Unique identifier for each sounding |
| sounding_qual_flag | UInt64 | Bit flags indicating the quality of the data in sounding: <ul style="list-style-type: none"> • 0—Good • Non-zero—See documentation |

12.7 L1BSc Spectral Parameter Fields

The L1BScSpectralParameters group (see Table 12-7 below) contains certain fields regarding spectral properties of OCO-2 from the L1BSc data files.

Table 12-7: L1BSc SpectralParameters in Level 2 Standard Data file (L2Std) and Diagnostic file (L2Dia).

| Data Element | Type | Comments |
|--------------------------------------|---------|--|
| max_declocking_factor_o2 | Float32 | Maximum clocking correction factor of the ABO2 spectrum |
| max_declocking_factor_strong_co2 | Float32 | Maximum clocking correction factor of the SCO2 spectrum |
| max_declocking_factor_weak_co2 | Float32 | Maximum clocking correction factor of the WCO2 spectrum |
| rad_continuum_o2 | Float32 | The mean signal of the good samples in ABO2 falling between the 98th and 99th percentile for signal level |
| rad_continuum_strong_co2 | Float32 | The mean signal of the good samples in SCO2 falling between the 98th and 99th percentile for signal level |
| rad_continuum_weak_co2 | Float32 | The mean signal of the good samples in WCO2 falling between the 98th and 99th percentile for signal level |
| rad_mean_spectra_o2 | Float32 | The mean radiance of the ABO2 spectrum |
| rad_mean_spectra_strong_co2 | Float32 | The mean radiance of the SCO2 spectrum |
| rad_mean_spectra_weak_co2 | Float32 | The mean radiance of the WCO2 spectrum |
| rad_stddev_spectra_o2 | Float32 | The standard deviation of the radiance of the ABO2 spectrum |
| rad_stddev_spectra_strong_co2 | Float32 | The standard deviation of the radiance of the SCO2 spectrum |
| rad_stddev_spectra_weak_co2 | Float32 | The standard deviation of the radiance of the WCO2 spectrum |
| snr_o2_11b | Float32 | The mean signal-to-noise ratio of the good samples in the band falling between the 98th and 99th percentile for signal level |
| snr_strong_co2_11b | Float32 | The mean signal-to-noise ratio of the good samples in the band falling between the 98th and 99th percentile for signal level |
| snr_weak_co2_11b | Float32 | The mean signal-to-noise ratio of the good samples in the band falling between the 98th and 99th percentile for signal level |
| sounding_color_slice_mean_o2 | Float32 | Mean radiance of the valid color slice pixels within the ABO2 footprint. |
| sounding_color_slice_mean_strong_co2 | Float32 | Mean radiance of the valid color slice pixels within the SCO2 footprint. |
| sounding_color_slice_mean_weak_co2 | Float32 | Mean radiance of the valid color slice pixels within the WCO2 footprint. |

| Data Element | Type | Comments |
|--|----------------|--|
| sounding_color_slice_noise_ratio_o2 (OCO-2 only) | Float32 | Ratio between the ABO2 footprint color slice radiance standard deviation, and the expected radiance noise level. |
| sounding_color_slice_noise_ratio_strong_co2 (OCO-2 only) | Float32 | Ratio between the SCO2 footprint color slice radiance standard deviation, and the expected radiance noise level. |
| sounding_color_slice_noise_ratio_weak_co2 (OCO-2 only) | Float32 | Ratio between the WCO2 footprint color slice radiance standard deviation, and the expected radiance noise level. |
| sounding_color_slice_o2_qual_flag (OCO-2 only) | IntBitfield 16 | Bitfield qual flag, bit pos: 0: has no valid ABO2 color slice radiance. |
| sounding_color_slice_quadratic_o2 (OCO-2 only) | Float32 | Quadratic coefficient of a quadratic fit of the radiances of the valid color slice pixels as a function of the 0-based pixel row number within the ABO2 footprint. |
| sounding_color_slice_quadratic_strong_co2 (OCO-2 only) | Float32 | Quadratic coefficient of a quadratic fit of the radiances of the valid color slice pixels as a function of the 0-based pixel row number within the SCO2 footprint. |
| sounding_color_slice_quadratic_weak_co2 (OCO-2 only) | Float32 | Quadratic coefficient of a quadratic fit of the radiances of the valid color slice pixels as a function of the 0-based pixel row number within the WCO2 footprint. |
| sounding_color_slice_slope_o2 (OCO-2 only) | Float32 | Slope coefficient of a linear fit of the radiances of the valid color slice pixels as a function of the 0-based pixel row number within the ABO2 footprint. |
| sounding_color_slice_slope_strong_co2 (OCO-2 only) | Float32 | Slope coefficient of a linear fit of the radiances of the valid color slice pixels as a function of the 0-based pixel row number within the SCO2 footprint. |
| sounding_color_slice_slope_weak_co2 (OCO-2 only) | Float32 | Slope coefficient of a linear fit of the radiances of the valid color slice pixels as a function of the 0-based pixel row number within the WCO2 footprint. |
| sounding_color_slice_stddev_o2 (OCO-2 only) | Float32 | Radiance standard deviation of the valid color slice pixels within the ABO2 footprint. |
| sounding_color_slice_stddev_strong_co2 (OCO-2 only) | Float32 | Radiance standard deviation of the valid color slice pixels within the SCO2 footprint. |
| sounding_color_slice_stddev_weak_co2 (OCO-2 only) | Float32 | Radiance standard deviation of the valid color slice pixels within the WCO2 footprint. |
| sounding_color_slice_strong_co2_qual_flag (OCO-2 only) | IntBitfield 16 | Bitfield qual flag, bit pos: 0: has no valid SCO2 color slice radiance. |
| sounding_color_slice_weak_co2_qual_flag (OCO-2 only) | IntBitfield 16 | Bitfield qual flag, bit pos: 0: has no valid WCO2 color slice radiance. |
| spike_eof_bad_colors_o2 | Int16 | Number of bad colors in the ABO2 spectrum |

| Data Element | Type | Comments |
|---------------------------------|-------|---|
| spike_eof_bad_colors_strong_co2 | Int16 | Number of bad colors in the SCO2 spectrum |
| spike_eof_bad_colors_weak_co2 | Int16 | Number of bad colors in the WCO2 spectrum |

12.8 L2 Preprocessing Fields

The PreprocessingResults group (see Table 12-8 below) contains fields from the Level 2 preprocessing results.

Table 12-8: Preprocessing Results data in Level 2 Standard Data file (L2Std) and Diagnostic file (L2Dia).

| Data Element | Type | Comments |
|-------------------------------------|---------|---|
| albedo_o2_abp | Float32 | O ₂ albedo at 785 and 755 nm |
| cloud_flag_abp | Signed8 | Indicator of whether the sounding contained clouds: 0—'Classified clear' 1—'Processing failed' 2—'Not classified' All other values undefined |
| cloud_flag_idp | Signed8 | Cloud flag derived from IMAP-DOAS algorithm: -2—'Measurement unusable' -1—'Did not converge' 0—'Definitely cloudy' 1—'Probably cloudy' 2—'Probably clear' 3—'Very clear' All other values undefined. |
| co2_column_strong_band_apriori_idp | Float32 | A priori CO ₂ vertical column density from meteorological data |
| co2_column_strong_band_idp | Float32 | CO ₂ vertical column density (from SCO2 band) |
| co2_column_strong_band_uncert_idp | Float32 | 1-sigma error in the CO ₂ vertical column density (from SCO2 band) |
| co2_column_weak_band_apriori_idp | Float32 | A priori CO ₂ vertical column density from meteorological data |
| co2_column_weak_band_idp | Float32 | CO ₂ vertical column density (from WCO2 band) |
| co2_column_weak_band_uncert_idp | Float32 | 1-sigma error in the CO ₂ vertical column density (from WCO2 band) |
| co2_ratio_idp | Float32 | Ratio of retrieved CO ₂ column (no scattering code) in WCO2 and SCO2 bands |
| co2_strong_band_processing_flag_idp | Int8 | Indicator of whether the SCO2 analysis succeeded: 0—'Processing succeeded' 1—'Processing failed' 2—'Processing skipped' All other values undefined |

| Data Element | Type | Comments |
|--|---------|--|
| co2_weak_band_processing_flag_idp | Int8 | Indicator of whether the WCO2 analysis succeeded: 0—'Processing succeeded' 1—'Processing failed' 2—'Processing skipped' All other values undefined |
| dispersion_multiplier_abp | Float64 | A number retrieved by the ABO2 algorithm that multiplies the dispersion coefficients as given in the L1B input file to get the effective wavelength of each channel to correct for the spacecraft-to-Earth Doppler shift. |
| dry_air_column_apriori_idp | Float32 | Integrated vertical column of dry airmass derived from meteorological data |
| fluorescence_offset_relative_757nm_idp | Float32 | Fraction of continuum level radiance explained by an additive offset term in the 757 nm spectral window (unitless). In the absence of instrumental errors, this will be only caused by fluorescence. Rotational Raman scattering should be negligible over typical vegetated surface and moderate solar zenith angles (<65 degrees). |
| fluorescence_offset_relative_771nm_idp | Float32 | Fraction of continuum level radiance explained by an additive offset term in the 771 nm spectral window (unitless). In the absence of instrumental errors, this will be only caused by fluorescence. Rotational Raman scattering should be negligible over typical vegetated surface and moderate solar zenith angles (<65 degrees). |
| fluorescence_qual_flag_idp | UInt8 | Indicator of the quality of the IMAP DOAS fluorescence retrieval for each sounding: 0—good 1—bad |
| fluorescence_radiance_757nm_idp | Float32 | Radiance generated by fluorescence at 757 nm |
| fluorescence_radiance_757nm_uncert_idp | Float32 | Standard deviation of the radiance generated by fluorescence at 757 nm |
| fluorescence_radiance_771nm_idp | Float32 | Radiance generated by fluorescence at 771 nm |
| fluorescence_radiance_771nm_uncert_idp | Float32 | Standard deviation of the radiance generated by fluorescence at 771 nm |
| h2o_ratio_idp | Float32 | Ratio of retrieved H ₂ O column (no scattering code) in WCO2 and SCO2 bands |
| h2o_ratio_uncert_idp | Float32 | 1-sigma error in the ratio of retrieved H ₂ O column (no scattering code) in WCO2 and SCO2 bands |
| noise_o2_abp | Float32 | O ₂ measurement noise retrieved by the ABO2 algorithm |
| o2_ratio_idp | Float32 | Ratio of retrieved and meteorological O ₂ column |
| reduced_chi_squared_o2_abp | Float32 | O ₂ reduced chi squared retrieved by ABO2 preprocessing |

| Data Element | Type | Comments |
|--------------------------------------|---------|--|
| reduced_chi_squared_o2_threshold_abp | Float32 | Threshold of O2 reduced chi squared used to set cloud_flag |
| sea_ice_flag_abp | Signed8 | Simple, unvalidated parameterization for determination of sea ice presence over a water surface based on continuum signals in bands 1 and 3; use with caution. 0=no sea ice, 1=sea ice, 2=undetermined |
| selection_priority | Signed8 | Indicator of the likelihood of generating a good retrieval from the sounding: 0 = most likely 20 = least likely |
| signal_o2_abp | Float32 | O2 measurement signal level retrieved by the ABO2 algorithm |
| snr_o2_abp | Float32 | O2 measurement SNR retrieved by the ABO2 algorithm |
| surface_pressure_abp | Float32 | Surface pressure retrieved by the ABO2 algorithm |
| surface_pressure_apriori_abp | Float32 | <i>a priori</i> surface pressure used by the ABO2 algorithm |
| surface_pressure_delta_abp | Float32 | The value of surface_pressure_abp minus surface_pressure_apriori_abp and surface_pressure_offset_abp |
| surface_pressure_offset_abp | Float32 | Empirically determined value to be added to the A band retrieved surface pressure, such that their sum is unbiased in clear scenes. It is modeled as a piecewise linear function of solar zenith angle; separate functions are used for land vs. ocean pixels. |
| temperature_offset_abp | Float32 | The offset to the prior meteorological temperature profile as retrieved by the ABO2 algorithm |

12.9 L2 Retrieval Geometry Fields

The RetrievalGeometry group (see Table 12-9 below) contains fields geographic properties of the OCO-2 and OCO-3 observations.

Table 12-9: Retrieval Geometry in Level 2 Standard Data file (L2Std).

| Data Element | Type | Comments |
|-----------------------------|---------|--|
| retrieval_altitude | Float32 | Altitude of the sounding based on Earth topography |
| retrieval_altitude_per_band | Float32 | Altitude of the per-spectrum footprint based on Earth topography |
| retrieval_altitude_uncert | Float32 | Uncertainty of the source Earth topography data |
| retrieval_aspect | Float32 | Orientation of the surface slope relative to the local North |
| retrieval_azimuth | Float32 | Angle between the LOS as defined from the sounding location to the spacecraft, and the sounding location local north direction |

| Data Element | Type | Comments |
|---|-----------|---|
| retrieval_center_offset_o2_weak_co2 | Float32 | Distance between the ABO2 band footprint center and the WCO2 band footprint center |
| retrieval_center_offset_strong_co2_o2 | Float32 | Distance between the SCO2 band footprint center and the ABO2 band footprint center |
| retrieval_center_offset_weak_co2_strong_co2 | Float32 | Distance between the WCO2 band footprint center and the SCO2 band footprint center |
| retrieval_land_fraction | Float32 | Percentage of land surface type within the sounding |
| retrieval_land_water_indicator | Int8 | Surface type at the sounding location: 0—Land 1—Water 2—Unused 3—Mixed land water |
| retrieval_latitude | Float32 | Geodetic latitude of the sounding based on Earth topography |
| retrieval_latitude_geoid | Float32 | Geodetic latitude of the sounding based on standard geoid |
| retrieval_longitude | Float32 | Longitude of the sounding based on Earth topography |
| retrieval_longitude_geoid | Float32 | Longitude of the sounding based on standard geoid |
| retrieval_los_surface_bidirectional_angle | Float32 | Angle between the LOS as defined from the sounding location to the spacecraft, and the sounding surface normal |
| retrieval_overlap | Float32 | Area of intersection of all three band footprints relative to average area of all three band footprints |
| retrieval_overlap_o2_weak_co2 | Float32 | Area of intersection of the footprints of ABO2 and WCO2 relative to the average area of the two footprint |
| retrieval_overlap_strong_co2_o2 | Float32 | Area of intersection of the footprints of ABO2 and SCO2 relative to the average area of the two footprints |
| retrieval_overlap_weak_co2_strong_co2 | Float32 | Area of intersection of the footprints of WCO2 and SCO2 relative to the average area of the two footprints |
| retrieval_pcs_data_source (OCO-3 only) | Signed8 | 0 = Estimator uses SRU, IMU, and GPS, 1 = Estimator uses SRU, and GPS, 2 = Estimator uses IMU, and GPS, 3 = Estimator uses SRU, IMU, and BAD position, 4 = Estimator uses SRU, and BAD position, 5 = Estimator uses IMU, and BAD position, 6 = Estimator uses BAD attitude, and GPS position, 7 = Estimator uses ISS BAD data only Else = no data available |
| retrieval_pcs_mode (OCO-3 only) | FixLenStr | The two-letter abbreviation of the Pointing Control System mode: PS, PA, PR, PC, PJ, PT, RN, ND, RG, GL, RT, TG, RA, AM |

| Data Element | Type | Comments |
|---|-------------|---|
| retrieval_plane_fit_quality | Float32 | Goodness-of-fit of surface slope: the standard deviation of the points, to which the plane is fitted, with the expected values taken as the orthogonal projection of the points onto the plane |
| retrieval_pma_azimuth (OCO-3 only) | Float32 | Pointing Mirror Assembly azimuth rotation angle in science reference |
| retrieval_pma_elevation (OCO-3 only) | Float32 | Pointing Mirror Assembly elevation rotation angle in science reference |
| retrieval_pma_motion_flag (OCO-3 only) | Signed8 | Motion flag for Pointing Mirror Assembly (0 = not moving, 1 = in motion, -1 = unknown) |
| retrieval_polarization_angle | Float32 | The angle between the accepted polarization axis of the instrument and the instrument reference plane for polarization, defined as the plane formed by the LOS and the ray from the sounding location to the local zenith |
| retrieval_relative_velocity | Float32 | Velocity of the spacecraft along the LOS: positive indicates spacecraft moving toward sounding location |
| retrieval_slant_path_diff_o2_weak_co2 | Float32 | Difference in slant path between ABO2 and WCO2 footprints |
| retrieval_slant_path_diff_strong_co2_o2 | Float32 | Difference in slant path between SCO2 and ABO2 footprints |
| retrieval_slant_path_diff_weak_co2_strong_co2 | Float32 | Difference in slant path between WCO2 and SCO2 footprints |
| retrieval_slope | Float32 | Slope of a plane fit to points within the sounding |
| retrieval_solar_azimuth | Float32 | Angle between the solar direction as defined from the sounding location to the Sun, and the sounding location local North direction |
| retrieval_solar_distance | Float64 | Distance between sounding location and the Sun |
| retrieval_solar_relative_velocity | Float32 | Velocity of the Sun along the sounding location/Sun vector: negative indicates Sun moving toward sounding location |
| retrieval_solar_surface_bidirectional_angle | Float32 | Angle between the solar direction as defined from the sounding location to the sun, and the sounding surface normal |
| retrieval_solar_zenith | Float32 | Angle between the solar direction as defined from the sounding location to the Sun, and the sounding location local zenith direction |
| retrieval_surface_roughness | Float32 | Standard deviation of the altitude within the sounding |
| retrieval_vertex_latitude | Float32 | Geodetic latitude of the footprint vertices using Earth topography |
| retrieval_vertex_longitude | Float32 | Longitude of the footprint vertices using Earth topography |

| Data Element | Type | Comments |
|------------------|---------|---|
| retrieval_zenith | Float32 | Angle between the LOS as defined from the sounding location to the spacecraft, and the sounding location local zenith direction |

12.10 L2 Retrieval Header Fields

The Retrieval Header group (see Table 12-10 below) contains fields information about the time and date of the OCO-2 observations.

Table 12-10: Retrieval Header data in Level 2 Standard Data file (L2Std).

| Data Element | Type | Comments |
|-------------------------|-----------|--|
| frame_index | Signed32 | Index of the frame dimension of the corresponding sounding in L1bScSoundingReference data elements |
| retrieval_time_string | FixLenStr | Data acquisition time for the retrieval based upon the three footprint times (yyyy-mm-ddThh:mm:ss.mmmZ) |
| retrieval_time_tai93 | Float64 | Data acquisition time for the retrieval based upon the three footprint times in seconds since Jan. 1, 1993 |
| sounding_id | Signed64 | The sounding_id of the sounding containing the spectra used to perform the retrieval |
| sounding_index | Signed32 | Index of the sounding dimension of the corresponding sounding in the L1bScSoundingReference data elements |
| sounding_operation_mode | FixLenStr | The two-letter abbreviation of the science AcquisitionMode: GL, ND, TG, XS |

12.11 L2 Retrieval Results

The RetrievalResults group (see Table 12-11 below) contains the retrieval results from the OCO-2 Level 2 data products.

Table 12-11: Retrieval Results data in Level 2 Standard Data file (L2Std).

| Data Element | Type | Comments |
|-------------------------------------|---------|-------------------------------------|
| apriori_o2_column | Float32 | a priori vertical column of O2 |
| co2_profile | Float32 | Vertical profile of CO2 |
| co2_profile_averaging_kernel_matrix | Float32 | Averaging kernel for CO2 profile |
| co2_profile_apriori | Float32 | Vertical a priori profile of CO2 |
| co2_profile_covariance_matrix | Float32 | Covariance matrix for CO2 profile |
| co2_profile_uncert | Float32 | Vertical profile of CO2 uncertainty |

| Data Element | Type | Comments |
|--------------------------------|---------|---|
| co2_vertical_gradient_delta | Float32 | The change from apriori to retrieved value of the vertical gradient in the CO ₂ profile. Indicates that the apriori CO ₂ profile was substantially different than that which was retrieved. |
| diverging_steps | Int16 | Number of iterations in which solution diverged |
| dof_co2_profile | Float32 | Degrees of freedom (X_{CO_2} only) |
| dof_full_vector | Float32 | Degrees of freedom (Full state vector) |
| eof_1_scale_apriori_o2 | Float32 | a priori of retrieved scale factor of first empirical orthogonal residual function in ABO2 band |
| eof_1_scale_apriori_strong_co2 | Float32 | a priori of retrieved scale factor of first empirical orthogonal residual function in SCO2 band |
| eof_1_scale_apriori_weak_co2 | Float32 | a priori of retrieved scale factor of first empirical orthogonal residual function in WCO2 band |
| eof_1_scale_o2 | Float32 | Retrieved scale factor of first empirical orthogonal residual function in ABO2 band |
| eof_1_scale_strong_co2 | Float32 | Retrieved scale factor of first empirical orthogonal residual function in SCO2 band |
| eof_1_scale_uncert_o2 | Float32 | Uncertainty of retrieved scale factor of first empirical orthogonal residual function in ABO2 band |
| eof_1_scale_uncert_strong_co2 | Float32 | Uncertainty of retrieved scale factor of first empirical orthogonal residual function in SCO2 band |
| eof_1_scale_uncert_weak_co2 | Float32 | Uncertainty of retrieved scale factor of first empirical orthogonal residual function in WCO2 band |
| eof_1_scale_weak_co2 | Float32 | Retrieved scale factor of first empirical orthogonal residual function in WCO2 band |
| eof_2_scale_apriori_o2 | Float32 | a priori of retrieved scale factor of second empirical orthogonal residual function in ABO2 band |
| eof_2_scale_apriori_strong_co2 | Float32 | a priori of retrieved scale factor of second empirical orthogonal residual function in SCO2 band |
| eof_2_scale_apriori_weak_co2 | Float32 | a priori of retrieved scale factor of second empirical orthogonal residual function in WCO2 band |
| eof_2_scale_o2 | Float32 | Retrieved scale factor of second empirical orthogonal residual function in ABO2 band |
| eof_2_scale_strong_co2 | Float32 | Retrieved scale factor of second empirical orthogonal residual function in SCO2 band |
| eof_2_scale_uncert_o2 | Float32 | Uncertainty of retrieved scale factor of second empirical orthogonal residual function in ABO2 band |

| Data Element | Type | Comments |
|-----------------------------------|---------|---|
| eof_2_scale_uncert_strong_co2 | Float32 | Uncertainty of retrieved scale factor of second empirical orthogonal residual function in SCO2 band |
| eof_2_scale_uncert_weak_co2 | Float32 | Uncertainty of retrieved scale factor of second empirical orthogonal residual function in WCO2 band |
| eof_2_scale_weak_co2 | Float32 | Retrieved scale factor of second empirical orthogonal residual function in WCO2 band |
| eof_3_scale_apriori_o2 | Float32 | a priori of retrieved scale factor of third empirical orthogonal residual function in ABO2 band |
| eof_3_scale_apriori_strong_co2 | Float32 | a priori of retrieved scale factor of third empirical orthogonal residual function in SCO2 band |
| eof_3_scale_apriori_weak_co2 | Float32 | a priori of retrieved scale factor of third empirical orthogonal residual function in WCO2 band |
| eof_3_scale_o2 | Float32 | Retrieved scale factor of third empirical orthogonal residual function in ABO2 band |
| eof_3_scale_strong_co2 | Float32 | Retrieved scale factor of third empirical orthogonal residual function in SCO2 band |
| eof_3_scale_uncert_o2 | Float32 | Uncertainty of retrieved scale factor of third empirical orthogonal residual function in ABO2 band |
| eof_3_scale_uncert_strong_co2 | Float32 | Uncertainty of retrieved scale factor of third empirical orthogonal residual function in SCO2 band |
| eof_3_scale_uncert_weak_co2 | Float32 | Uncertainty of retrieved scale factor of third empirical orthogonal residual function in WCO2 band |
| eof_3_scale_weak_co2 | Float32 | Retrieved scale factor of third empirical orthogonal residual function in WCO2 band |
| fluorescence_at_reference | Float32 | Retrieved fluorescence at 0.757 microns |
| fluorescence_at_reference_apriori | Float32 | <i>a priori</i> of retrieved fluorescence at 0.757 microns |
| fluorescence_at_reference_uncert | Float32 | Uncertainty of retrieved fluorescence at 0.757 microns |
| fluorescence_slope | Float32 | Retrieved fluorescence slope at 0.757 microns |
| fluorescence_slope_apriori | Float32 | <i>a priori</i> of retrieved fluorescence slope at 0.757 microns |
| fluorescence_slope_uncert | Float32 | Uncertainty of retrieved fluorescence slope at 0.757 microns |
| h2o_scale_factor | Float32 | Retrieved scale factor for H ₂ O profile |
| h2o_scale_factor_apriori | Float32 | <i>a priori</i> of retrieved scale factor for H ₂ O profile |
| h2o_scale_factor_uncert | Float32 | Uncertainty of retrieved scale factor for H ₂ O profile |
| iterations | Int16 | Number of iterations |

| Data Element | Type | Comments |
|--|---------|--|
| last_step_levenberg_marquardt_parameter | Float32 | Levenberg Marquardt parameter corresponding to last iteration |
| num_active_levels | Int16 | Number of levels in atmospheric model |
| outcome_flag | Int8 | Indicator of retrieval results: 1—'Passed internal quality check' 2—'Failed internal quality check' 3—'Reached maximum allowed iterations' 4—'Reached maximum allowed divergences' |
| retrieved_co2_column | Float32 | Retrieved vertical column of CO2 |
| retrieved_dry_air_column_layer_thickness | Float32 | Retrieved vertical column of dry air per atmospheric layer |
| retrieved_h2o_column | Float32 | Retrieved vertical column of H2O |
| retrieved_h2o_column_layer_thickness | Float32 | Retrieved vertical column of H2O per atmospheric layer |
| retrieved_o2_column | Float32 | Retrieved vertical column of O2 |
| retrieved_wet_air_column_layer_thickness | Float32 | Retrieved vertical column of wet air per atmospheric layer |
| specific_humidity_profile_met | Float32 | Meteorological specific humidity profile interpolated to observation location, time |
| surface_pressure_apriori_fph | Float32 | a priori surface pressure retrieved by full-physics algorithm |
| surface_pressure_fph | Float32 | Surface pressure retrieved by full-physics algorithm |
| surface_pressure_uncert_fph | Float32 | Uncertainty in the surface pressure retrieved by the full-physics algorithm |
| surface_type | String | Type of model used for the Earth's surface: 'Lambertian' 'Cox-Munk,Lambertian' |
| temperature_offset_apriori_fph | Float32 | a priori of retrieved offset of temperature profile |
| temperature_offset_fph | Float32 | Retrieved offset of temperature profile |
| temperature_offset_uncert_fph | Float32 | Uncertainty of retrieved offset of temperature profile |
| temperature_profile_met | Float32 | Meteorological temperature profile interpolated to observation location, time |
| tropopause_altitude | Float32 | Inferred tropopause altitude based on lapse rate |
| tropopause_pressure | Float32 | Inferred tropopause pressure altitude based on lapse rate |
| vector_altitude_levels | Float32 | Altitude corresponding to each atmospheric level |
| vector_altitude_levels_apriori | Float32 | A priori altitude corresponding to each atmospheric level |
| vector_pressure_levels | Float32 | Pressure altitude corresponding to each atmospheric level |
| vector_pressure_levels_apriori | Float32 | a priori pressure altitude corresponding to each atmospheric level |

| Data Element | Type | Comments |
|----------------------------------|---------|--|
| vector_pressure_levels_met | Float32 | Pressure altitude corresponding to each meteorological atmospheric level |
| wind_speed | Float32 | Retrieved Cox-Munk wind speed |
| wind_speed_apriori | Float32 | a priori of retrieved Cox-Munk wind speed |
| wind_speed_u_met | Float32 | Meteorological eastward wind interpolated to observation location, time |
| wind_speed_uncert | Float32 | Uncertainty of retrieved Cox-Munk wind speed |
| wind_speed_v_met | Float32 | Meteorological northward wind interpolated to observation location, time |
| xco2 | Float32 | Column-averaged CO ₂ dry air mole fraction |
| xco2_apriori | Float32 | a priori of column-averaged CO ₂ dry air mole fraction |
| xco2_avg_kernel | Float32 | Column averaging kernel |
| xco2_avg_kernel_norm | Float32 | Normalized column averaging kernel |
| xco2_pressure_weighting_function | Float32 | Pressure weighting function used to form X_{CO_2} |
| xco2_uncert | Float32 | Uncertainty in column averaged CO ₂ dry air mole fraction |
| xco2_uncert_interf | Float32 | Variance of X_{CO_2} due to interference |
| xco2_uncert_noise | Float32 | Variance of X_{CO_2} due to noise |
| xco2_uncert_smooth | Float32 | Variance of X_{CO_2} due to smoothing |

12.12 L2 Spectral Parameters Group

The SpectralParameters group (see Table 12-12 below) contains the retrieval results from the OCO-2 Level 2 data products.

Table 12-12: Spectral Parameters data in Level 2 Standard Data file (L2Std).

| Data Element | Type | Comments |
|--|---------|--|
| noise_o2_fph | Float32 | Aggregate noise in the ABO2 band |
| noise_strong_co2_fph | Float32 | Aggregate noise in the SCO2 band |
| noise_weak_co2_fph | Float32 | Aggregate noise in the WCO2 band |
| reduced_chi_squared_o2_fph | Float32 | Reduced chi squared of spectral fit of the ABO2 band |
| reduced_chi_squared_strong_co2_fph | Float32 | Reduced chi squared of spectral fit of the SCO2 band |
| reduced_chi_squared_weak_co2_fph | Float32 | Reduced chi squared of spectral fit of the WCO2 band |
| relative_residual_mean_square_o2 | Float32 | Mean square of the residuals divided by the signal for the ABO2 band |
| relative_residual_mean_square_strong_co2 | Float32 | Mean square of the residuals divided by the signal for the SCO2 band |
| relative_residual_mean_square_weak_co2 | Float32 | Mean square of the residuals divided by the signal for the WCO2 band |

| Data Element | Type | Comments |
|---------------------------------|-------------|--|
| residual_mean_square_o2 | Float32 | Mean of the squares of the residuals for the ABO2 band |
| residual_mean_square_strong_co2 | Float32 | Mean of the squares of the residuals for the SCO2 band |
| residual_mean_square_weak_co2 | Float32 | Mean of the squares of the residuals for the WCO2 band |
| signal_o2_fph | Float32 | Aggregate signal in the ABO2 band |
| signal_strong_co2_fph | Float32 | Aggregate signal in the SCO2 band |
| signal_weak_co2_fph | Float32 | Aggregate signal in the WCO2 band |

13 Full Data Tables for OCO-2 and OCO-3 Level 2 Lite Files (LtCO2)

With the v10 delivery of the OCO-2 and OCO-3 data products, we have released a version of the Lite data files similar to the OCO-2 Lite files from V9. The main differences between the Lite data file are that the files are aggregated on a daily basis, the files contain a streamlined set of output parameters (a subset of the full L2 data products) and they contain screened and bias corrected values for X_{CO_2} (see Section 3 for OCO-2 screening/bias correction details and Section 4 for OCO-3 details) for the retrievals. The unscreened/bias corrected values are included as well.

Table 13-1 Table 13-2, Table 13-3 and Table 13-4 provide a description of the variables available in the Lite data files. They are designed to be somewhat easier to use (smaller files, aggregated daily). The data included in these files are consistent with the Level 2 data products.

13.1 OCO-2 and OCO-3 Lite File Main Group Fields

The main group (see Table 13-1 below) contains the many of the geographic and retrieval related fields from the OCO-2 and OCO-3 Level 2 Lite data products

Table 13-1: Provides a description of the fields in the OCO-2 and OCO-3 Lite Data Product files.

| Element | Type | Comment |
|---------------------|---------|---|
| co2_profile_apriori | Float32 | Prior CO ₂ Prior assumed by L2 code; Defined on layer boundaries. These are oriented space-to-surface, so the first element defines the TOA, the last element defines the surface. |
| date | Float32 | Observation date and time matching sounding id. |
| File_index | Float32 | 1-Based Index of L2 File for each sounding |
| latitude | Float32 | Center latitude of the measurement |
| longitude | Float32 | Center longitude of the measurement |
| levels | Long | Level counter |
| pressure_levels | Float32 | Pressure at each level; Defined on layer boundaries. These are oriented space-to-surface, so the first element defines the TOA, the last element defines the surface |
| pressure_weight | Float32 | Pressure weighting function for each level; Defined on layer boundaries. These are oriented space-to-surface, so the first element defines the TOA, the last element defines the surface |
| sensor_zenith_angle | Float32 | Zenith angle of the satellite at the time of the measurement |
| solar_zenith_angle | Float32 | Solar zenith angle at the time of the measurement |
| sounding_id | Long | From scan start time in UTC |
| source_files | | Source L2 File Names for these soundings |
| time | Long | Seconds since 1970-01-01 00:00:00 |
| vertex_latitude | Float32 | Corner latitudes of the measurement FOV |
| vertex_longitude | Float32 | Corner longitudes of the measurement FOV |

| Element | Type | Comment |
|-----------------------|---------|---|
| xco2 | Float32 | Column-averaged dry-air mole fraction of CO ₂ (Bias corrected as described in Section 3 for OCO-2 and Section 4 for OCO-3) |
| xco2_apriori | Float32 | A priori X_{CO_2} value |
| xco2_averaging_kernel | Float32 | X_{CO_2} column averaging kernel |
| xco2_qf_bitflag | Byte | xco2_quality_flag bit flag |
| xco2_quality_flag | Byte | X_{CO_2} quality flag ("0=Good Retrieval, 1=Bad Retrieval) |
| xco2_uncertainty | Float32 | X_{CO_2} posterior error estimate |

13.2 OCO-2 and OCO-3 Lite File Preprocessor Group Fields

The Preprocessor group (see Table 13-2 below) contains the many of the key fields from the different preprocessing steps of the retrievals.

Table 13-2: Contains description of the fields in the "Preprocessor" folder of the Lite files.

| Element | Type | Comment |
|---|---------|---|
| co2_ratio | Float32 | Band 3 / Band 2 Ratio of retrieved Single-band X_{CO_2} using IMAP-DOAS algorithm |
| co2_ratio_offset_per_footprint (OCO-2 only) | Float32 | Per footprint offset subtracted from co2_ratio in the L2Std files to form co2_ratio in the lite files |
| dp_abp | Float32 | Retrieved-Prior Pressure from the fast O2A-band only preprocessor retrieval |
| h2o_ratio | Float32 | H ₂ O Ratio |
| h2o_ratio_offset_per_footprint (OCO-2 only) | Float32 | Per footprint offset subtracted from h2o_ratio in the L2Std files to form co2_ratio in the lite files |
| max_declocking_o2a | Float32 | ABS(MaxDeclockingFactor_O2A_Band - 1)*100 |
| max_declocking_sco2 (OCO-2 only) | Float32 | ABS(MaxDeclockingFactor_StrongCO2_Band - 1)*100 |
| max_declocking_wco2 (OCO-2 only) | Float32 | ABS(MaxDeclockingFactor_WeakCO2_Band - 1)*100 |
| xco2_strong_idp | Float32 | X_{CO_2} from Strong CO ₂ Band only, IMAP-DOAS algorithm |
| xco2_weak_idp | Float32 | X_{CO_2} from Weak CO ₂ Band only, IMAP-DOAS algorithm |

13.3 OCO-2 and OCO-3 Lite File Retrieval Group Fields

The Retrievals group (see Table 13-3 below) contains the many of the key fields from the L2 retrievals.

Table 13-3: Contains description of the fields in the "Retrievals" folder of the Lite files.

| Element | Type | Comment |
|------------|---------|---|
| albedo_o2a | Float32 | Retrieved Band 1 reflectance (land), or lambertian albedo component of BRDF (ocean) |

| Element | Type | Comment |
|---------------------------|---------|--|
| albedo_sco2 | Float32 | Retrieved Band 3 reflectance (land), or lambertian albedo component of BRDF (ocean) |
| albedo_quad_o2a | Float32 | Retrieved Band 1 reflectance quadratic component (land), n/a (ocean) |
| albedo_quad_sco2 | Float32 | Retrieved Band 3 reflectance quadratic component (land), n/a (ocean) |
| albedo_quad_wco2 | Float32 | Retrieved Band 2 reflectance quadratic component (land), n/a (ocean) |
| albedo_slope_o2a | Float32 | Retrieved Band 1 reflectance slope (land), or slope of lambertian albedo component of BRDF (ocean) |
| albedo_slope_sco2 | Float32 | Retrieved Band 3 reflectance slope (land), or slope of lambertian albedo component of BRDF (ocean) |
| albedo_slope_wco2 | Float32 | Retrieved Band 2 reflectance slope (land), or slope of lambertian albedo component of BRDF (ocean) |
| albedo_wco2 | Float32 | Retrieved Band 2 reflectance (land), or lambertian albedo component of BRDF (ocean) |
| aod_bc | Float32 | Retrieved Black Carbon Optical Depth at 0.755 microns |
| aod_dust | Float32 | Retrieved Dust Aerosol Optical Depth at 0.755 microns |
| aod_ice | Float32 | Retrieved Ice Cloud Optical Depth at 0.755 microns |
| aod_oc | Float32 | Retrieved Organic Carbon Optical Depth at 0.755 microns |
| aod_seasalt | Float32 | Retrieved Sea Salt Carbon Optical Depth at 0.755 microns |
| aod_strataer | Float32 | Retrieved Upper Trop+Stratospheric Aerosol Optical Depth at 0.755 microns |
| aod_sulfate | Float32 | Retrieved Sulfate Aerosol Optical Depth at 0.755 microns |
| aod_total | Float32 | Retrieved Total Cloud+Aerosol Optical Depth at 0.755 microns |
| aod_water | Float32 | Retrieved Water Cloud Optical Depth at 0.755 microns |
| chi2_o2a | Float32 | Reduced Chi-Squared for Band 1 (O2A band) of L2 spectral fit |
| chi2_sco2 | Float32 | Reduced Chi-Squared for Band 3 (Strong CO ₂ band) of L2 spectral fit |
| chi2_wco2 | Float32 | Reduced Chi-Squared for Band 2 (Weak CO ₂ band) of L2 spectral fit |
| co2_grad_del | Float32 | level 13 is at P/Psurf=0.631579 |
| defined_mode (OCO-2 only) | Byte | Prior surface pressure used in the retrieval, as determined by GEOS5-FP-IT short-term (0-9 hour) forecast |
| deltaT | Float32 | Retrieved Offset to Prior Temperature Profile in Kelvin |
| diverging_steps | Byte | No. of diverging steps taken in retrieval |
| dp | Float32 | Retrieved-Prior Pressure from the L2 Full-Physics retrieval |
| dp_o2a | Float32 | Delta Psurf from L2, O2A-band Prior |
| dp_sco2 | Float32 | Delta Psurf from L2, SCO2-band Prior |
| dpfrac | Float32 | $xco2_raw * (1 - \{Meteorology/psurf_apriori_band3\} / \{Retrieval/psurf\})$ |
| dws | Float32 | Retrieved AOD_dust+AOD_water+AOD_seasalt at 0.755 microns |
| eof3_3_rel (OCO-2 only) | Float32 | 3rd EOF of Band 3, relative to Signal |
| fs | Float32 | Simultaneous Fluorescence retrieval (at 757 nm) by L2 code; note this is different than the dedicated retrieval using only solar lines |
| h2o_scale | Float32 | Retrieved scale factor to Prior Water Vapor Profile |
| ice_height | Float32 | Retrieved Ice Cloud Height |

| Element | Type | Comment |
|-------------------|---------|---|
| iterations | Byte | No. of iterations used in retrieval |
| psurf | Float32 | Surface pressure retrieved by the Level-2 retrieval |
| psurf_apriori | Float32 | Prior surface pressure used in the retrieval, as determined by ECMWF short-term (0-9 hour) forecast |
| rms_rel_o2a | Float32 | RMS of the L2 fit residuals in the o2a band, relative to the continuum signal, times 100 [so it is in percent] |
| rms_rel_sco2 | Float32 | RMS of the L2 fit residuals in the strong CO ₂ band, relative to the continuum signal, times 100 [so it is in percent] |
| rms_rel_wco2 | Float32 | RMS of the L2 fit residuals in the weak CO ₂ band, relative to the continuum signal, times 100 [so it is in percent] |
| s31 | Float32 | Ratio of Band 3 to Band 1 signal level |
| s32 | Float32 | Ratio of Band 3 to Band 2 signal level |
| SigmaB | Float32 | Multiply Psurf by these values to get the pressure layer boundaries (= pressure levels) |
| surface_type | Byte | Surface type used in the retrieval: 0=ocean and corresponds to a Cox-Munk+Lambertian surface; 1=land and corresponds to a pure Lambertian surface |
| T700 | Float32 | Temperature at 700 hPa (from ECMWF) |
| tcwv | Float32 | Retrieved TCWV obtained by multiplying retrieved h2o _o scale factor to prior (ECMWF) TCWV |
| tcwv_apriori | Float32 | Prior TCWV (from ECMWF prior profile) |
| tcwv_uncertainty | Float32 | Retrieved TCWV Posterior Uncertainty |
| water_height | Float32 | Retrieved Water Cloud Height |
| windspeed | Float32 | Surface wind speed retrieved by the Level-2 retrieval |
| windspeed_apriori | Float32 | Surface wind speed retrieved by the Level-2 retrieval |
| xco2_raw | Float32 | Raw value of Retrieved X _{CO2} (not bias corrected) |

13.4 OCO-2 and OCO-3 Lite File Sounding Group Fields

The Sounding group (see Table 13-4 below) contains the many of the geographic fields from the L2 retrievals.

Table 13-4: Contains description of the fields in the "Sounding" folder of the Lite files.

| Element | Type | Comment |
|----------------------|---------|---|
| airmass | Float32 | Airmass, computed as $1/\cos(\text{solar_zenith_angle}) + 1/\cos(\text{sensor_zenith_angle})$ |
| altitude | Float32 | Surface Altitude in meters above sea level |
| altitude_stddev | Float32 | Standard deviation of surface elevation within the FOV |
| footprint | Byte | Index of OCO-2 (OCO-3) Sounding 1-8 |
| glint_angle | Float32 | Angular distance from viewing along the perfect glint direction |
| land_fraction | Int8 | Fraction of the footprint that contains land in percent |
| land_water_indicator | Int8 | 0=Land;1=Ocean;2=Inland Water;3=Mixed |
| operation_mode | Int8 | OCO-2 Operation Mode: 0=Nadir, 1=Glint, 2=Target, 3=Transition |
| orbit | Int8 | OCO-2 orbit number since mission start |

| Element | Type | Comment |
|----------------------------------|-----------|---|
| Path (OCO-2 Only) | Int8 | OCO-2 fixed orbit path number ranging from 1-233 |
| polarization_angle (OCO-2 Only) | Float32 | Polarization angle |
| pcs_data_source (OCO-3 Only) | Byte | Sounding pcs data source |
| pma_azimuth_angle (OCO-3 Only) | Float32 | Azimuth angle PMA |
| pma_elevation_angle (OCO-3 Only) | Float32 | Elevation angle PMA |
| polarization_angle (OCO-3 Only) | Float32 | Sounding_polarization_angle |
| sensor_azimuth_angle | Float32 | azimuth angle of the satellite at the time of the measurement |
| snr_o2 | Float32 | O2A-Band Continuum Signal-to-Noise Ratio |
| snr_strong_co2 | Float32 | Strong CO2-Band Continuum Signal-to-Noise Ratio |
| snr_weak_co2 | Float32 | Weak CO2-Band Continuum Signal-to-Noise Ratio |
| solar_azimuth_angle | Float32 | solar azimuth angle at the time of the measurement |
| target_id (OCO-3 Only) | Int8 | OCO-3 Target (or SAM) ID |
| target_name (OCO-3 Only) | VarLenStr | OCO-3 Target (or SAM) Name |

13.5 OCO-2 and OCO-3 Lite File Meteorology Group Fields

The Sounding group (see Table 13-5 below) contains the meteorology fields from the L2 retrievals.

Table 13-5: Fields in the "Meteorology" folder of the OCO-2, OCO-3 Lite files.

| Element | Type | Comment |
|--------------------|---------|---|
| psurf_apriori_o2a | Float32 | Prior surface pressure for Band 1 location, as determined by GEOS5-FP-IT short-term (0-9 hour) forecast |
| psurf_apriori_sco2 | Float32 | Prior surface pressure for Band 3 location, as determined by GEOS5-FP-IT short-term (0-9 hour) forecast |
| psurf_apriori_wco2 | Float32 | Band 2 Prior Surface Pressure |
| windspeed_u_met | Float32 | Apriori Surface Wind Speed, U Component from GEOS-5 FPIT in the N-S direction, m/s |
| windspeed_v_met | Float32 | Apriori Surface Wind Speed, V Component from GEOS-5 FPIT in the E-W direction, m/s |

14 Tools and Data Services

14.1 HDFView

HDFView is a Java based graphical user interface created by the HDF Group that can be used to browse all ACOS HDF products. The utility allows users to view all objects in an HDF file hierarchy, which is represented as a tree structure. HDFView can be downloaded or support found at: <https://portal.hdfgroup.org/display/support/Download+HDFView>

14.2 Panoply

Panoply is a tool from the Goddard Institute for Space Studies (GISS). It plots geo-referenced and other arrays from NetCDF, HDF, GRIB, and other datasets. Panoply is a cross-platform application that runs on Macintosh, Windows, Linux and other desktop computers. A particularly convenient feature of Panoply is its ability to communicate with remote Hyrax (xml) catalogues and thus plotting datasets without the need to download the data files. Apart from the on-line archive, Goddard DAAC serves ACOS and OCO data through Hyrax (OPeNDAP) as well, and this path to data can be discovered in the ACOS and OCO dataset landing pages (see below). Panoply is available for free download from the [GISS website](#).

14.3 Goddard DAAC user interface.

The NASA Goddard Earth Sciences Data and Information Services Center (GES DISC) provides temporal and spatial searches, as well as variable and spatial subsets, through its [user interface](#). Dataset landing pages provide basic summary and data access points for all datasets curated by the GES DISC. A simple keyword search would suffice to discover all OCO-2 or OCO-3 datasets:

<https://disc.gsfc.nasa.gov/datasets?keywords=OCO-2&page=1>

<https://disc.gsfc.nasa.gov/datasets?keywords=OCO-3&page=1>

Apart from the direct access to the online archive and Hyrax (OPeNDAP) directories, the interface ultimately provides the search results as lists of data links. Goddard DAAC requires **user registration** before any data can be downloaded. Detailed instructions on how to register and how to use wget and curl with the data download links, as well as other advanced methods, are provided on the interface:

<https://disc.gsfc.nasa.gov/data-access#>

14.4 NASA Earth Data Search Client

In a similar manner, information and data access can be found from the NASA Earth Data Search Client:

<https://search.earthdata.nasa.gov/search?q=oco-2>

<https://search.earthdata.nasa.gov/search?q=oco-3>

All NASA data centers from the Earth Science Data Information System (ESDIS) report their data collections to this system. It is a convenient one-stop shop for discovery of all NASA Earth Science Missions data.

15 Contact Information

For the most up-to-date contact information, please refer to the JPL mission sites (which provides a link to the official mission sites:

OCO-2: <https://www.jpl.nasa.gov/missions/orbiting-carbon-observatory-2-oco-2>

OCO-3: <https://www.jpl.nasa.gov/missions/orbiting-carbon-observatory-3-oco-3>.

16 Acknowledgements and References

16.1 Acknowledgements

This research was carried out at the Jet Propulsion Laboratory, California Institute of Technology, under a contract with the National Aeronautics and Space Administration.

16.2 Additional Resources

There are a number of other project documents that the user should refer to as they work with the data.

1. Solar Induced Chlorophyll Fluorescence Data User's Guide – provide guidance for using the OCO-2 and OCO-3 SIF data products. It is available at the GES DISC [here](#).
2. L1B ATBD – this algorithm theoretical basis document describes the process used to take the uncalibrated spectrum to calibrated radiance spectra. The document is available [here](#).
3. L2 ATBD – this ATBD steps through the physics and implementation of the Level 2 algorithm. Available at the OCO-2 Level 2 data page [here](#).
4. ATBDs for IMAP-DOAS and ABO2 – these ATBD documents describe the two methods of identifying potentially cloudy footprints, in what we refer to as the prescreening step. These data are then used for setting data quality and data selection levels.
5. Published papers—in addition to the references in the next section, there are a number of published papers describing the algorithm, application to GOSAT, prescreening steps, etc. Please see the most up to date list of publications on the [OCO-2](#) or [OCO-3](#) web sites.

16.2.1 Links

- OCO-2 Mission [site](#)
- OCO-3 Mission [site](#)
- [OCO-2 data summary](#) page at the Goddard DISC
- [OCO-3 data summary](#) page at the Goodard DISC
- JPL retrievals using the radiances from the Japanese GOSAT satellite, known as the Atmospheric CO2 Observations from Space (ACOS) data at the Goddard DISC summary page: https://disc.gsfc.nasa.gov/datasets/ACOS_L2S_9r/summary

17 References

17.1.1 OCO-2 Mission

- Canadell, J.G., C. Le Quere, M.R. Raupach, C.B. Field, E.T. Buitenhuis, P. Ciais, T.J. Conway, N.P. Gillett, R.A. Houghton, and G. Marlan (2007), Contributions to accelerating atmospheric CO₂ growth from economic activity, carbon intensity, and efficiency of natural sinks, *Proceedings of the National Academy of Sciences*, 47, 18866–18870.
- Conway, T.J., P.M. Lang, and K.A. Masarie (2011), Atmospheric carbon dioxide dry air mole fractions from the NOAA ESRL carbon cycle cooperative global air sampling network, 1968–2010, Version: 2011-10-14, <http://www.esrl.noaa.gov/gmd/ccgg/trends/global.html>
- Buchwitz, M., Schneising, O., Burrows, J. P., Bovensmann, H., Reuter, M., and Notholt, J. (2007), First direct observation of the atmospheric CO₂ year-to-year increase from space, *Atmos. Chem. Phys.*, 7, 4249–4256, <https://doi.org/10.5194/acp-7-4249-2007>,
- Crisp, D., R.M. Atlas, F.-M. Breon, L.R. Brown, J.P. Burrows, P. Ciais, B.J. Connor, S.C. Doney, I.Y. Fung, D.J. Jacob, C.E. Miller, D. O'Brien, S. Pawson, J.T. Randerson, P. Rayner, R.J. Salawitch, S.P. Sander, B. Sen, G.L. Stephens, P.P. Tans, G.C. Toon, P.O. Wennberg, S.C. Wofsy, Y.L. Yung, Z. Kuang, B. Chudasama, G. Sprague, B. Weiss, R. Pollock, D. Kenyon, S. Schroll (2004), The Orbiting Carbon Observatory (OCO) mission, *Advances in Space Research* 34 700–709, <https://doi.org/10.1016/j.asr.2003.08.062>.
- Crisp, D., C. E. Miller, and P. L. DeCola (2008), NASA Orbiting Carbon Observatory: Measuring the column averaged carbon dioxide mole fraction from space, *Journal of Applied Remote Sensing* 2, 023508, <https://doi.org/10.1117/1.2898457>.
- Frankenberg, C., Chris O'Dell, Joseph Berry, Luis Guanter, Joanna Joiner, Philipp Köhler, Randy Pollock, Thomas E. Taylor (2014a), Prospects for chlorophyll fluorescence remote sensing from the Orbiting Carbon Observatory-2, *Remote Sensing of Environment*, 147, 1–12, <https://doi.org/10.1016/j.rse.2014.02.007>.
- Frankenberg, C., R. Pollock, R. A. M. Lee, R. Rosenberg, J.-F. Blavier, D. Crisp, C.W. O'Dell, G. B. Osterman, C. Roehl, P. O. Wennberg, and D. Wunch (2015), The Orbiting Carbon Observatory (OCO-2): spectrometer performance evaluation using prelaunch direct Sun measurements, *Atmos. Meas. Tech.*, 7, 1–10, <https://doi.org/10.5194/amt-8-301-2015>.
- Hamazaki, T., Kaneko, Y., Kuze, A., and Kondo, K. (2005), Fourier transform spectrometer for greenhouse gases observing satellite (GOSAT), in: *Proceedings of SPIE*, vol. 5659, p. 73–80, doi: 10.1117/12.581198.
- Kieffer H. H. and T. C. Stone (2005), The spectral irradiance of the Moon. *Astronom. J.*, 129: 2887–2901, <https://doi.org/10.1086/430185>.
- Kuze. A., Suto. H., Nakajima, M., and Hamazaki, T. (2009), Thermal and near infrared sensor for carbon observation Fourier-transform spectrometer on the Greenhouse Gases Observing Satellite for greenhouse gases monitoring, *Appl. Opt.*, 48, 6716–6733, 15 <https://doi.org/10.1364/AO.48.006716>.
- Kuze, A, T. E. Taylor, F. Kataoka, C. J. Bruegge, D. Crisp, M. Harada, M. Helmlinger, M. Inoue, S. Kawakami, N. Kikuchi, Y. Mitomi, J. Murooka, M. Naitoh, D. M. O'Brien, C. W. O'Dell, H. Ohyama, H. Pollock, F. M. Schwandner, K. Shiomi, H. Suto, T. Takeda, T. Tanaka, T. Urabe, T. Yokota, and Y. Yoshida, (2014), Long-Term Vicarious Calibration of GOSAT Short-Wave Sensors: Techniques for Error Reduction and New Estimates of

- Radiometric Degradation Factors, IEEE Transactions On Geoscience and Remote Sensing, 52, 3991-4004, <https://doi.org/10.1109/TGRS.2013.2278696>.
- Le Quéré, C., G. P. Peters, R. J. Andres, R. M. Andrew, T. A. Boden, P. Ciais, P. Friedlingstein, R. A. Houghton, G. Marland, R. Moriarty, S. Sitch, P. Tans, A. Arneeth, A. Arvanitis, D. C. E. Bakker, L. Bopp, J. G. Canadell, L. P. Chini, S. C. Doney, A. Harper, I. Harris, J. I. House, A. K. Jain, S. D. Jones, E. Kato, R. F. Keeling, K. Klein Goldewijk, A. Körtzinger, C. Koven, N. Lefèvre, F. Maignan, A. Omar, T. Ono, G.-H. Park, B. Pfeil, B. Poulter, M. R. Raupach,*, P. Regnier, C. Rödenbeck, S. Saito, J. Schwinger, J. Segsneider, B. D. Stocker, T. Takahashi, B. Tilbrook, S. van Heuven, N. Viovy, R. Wanninkhof, A. Wiltshire, and S. Zaehle, (2014), Global carbon budget 2013, *Earth Syst. Sci. Data*, 6, 235–263, <https://doi.org/10.5194/essd-6-235-2014>
- P.J. Rayner and D.M. O'Brien (2001), The utility of remotely sensed CO₂ concentration data in surface source inversions, *Geophys. Res. Lett.* 28, 175-178, <https://doi.org/10.1029/2000GL011912>.
- Yoshida, Y., Ota, Y., Eguchi, N., Kikuchi, N., Nobuta, K., Tran, H., Morino, I., and Yokota, T.: (2011), Retrieval algorithm for CO₂ and CH₄ column abundances from short-wavelength infrared spectral observations by the Greenhouse Gases Observing Satellite, *Atmos. Meas. Tech.*, 4, 717–734, <https://doi.org/10.5194/amt-4-717-2011>.

17.1.2 Algorithms and Retrievals

- Crisp, D., B. M. Fisher, C.W. O'Dell, C. Frankenberg, R. Basilio, H. Bösch, L. R. Brown, R. Castano, B. Connor, N. M. Deutscher, A. Eldering, D. Griffith, M. Gunson, A. Kuze, L. Mandrake, J. McDuffie, J. Messerschmidt, C. E. Miller, I. Morino, V. Natraj, J. Notholt, D. O'Brien, F. Oyafuso, I. Polonsky, J. Robinson, R. Salawitch, V. Sherlock, M. Smyth, H. Suto, T. Taylor, P. O. Wennberg, D. Wunch, and Y. L. Yung (2012), The ACOS X_{CO_2} retrieval algorithm, Part 2: Global X_{CO_2} data characterization. *Atmos Meas. Tech.*, 5, 687-707, <https://doi.org/10.5194/amt-5-687-2012>.
- Frankenberg, C., Platt, U., and Wagner, T. (2005), Iterative maximum *a posteriori* (IMAP-) DOAS for retrieval of strongly absorbing trace gases: Model studies for CH₄ and CO₂ retrieval from near- infrared spectra of SCIAMACHY onboard ENVISAT, *Atmos. Chem. Phys.*, 5, 9–22, <https://doi.org/10.5194/acp-5-9-2005>.
- Jacobs N. et al. (2024), The importance of digital elevation model accuracy in X_{CO₂} retrievals: improving the Orbiting Carbon Observatory 2 Atmospheric Carbon Observations from Space version 11 retrieval product, *Atmos Meas. Tech.*, 17, 1375-1401, <https://doi.org/10.5194/amt-17-1375-2024>.
- Lee, R.A.M, C.W. O'Dell, D. Wunch, C. Roehl, G.B. Osterman, J.F. Blavier, R. Rosenberg, L. Chapsky, C. Frankenberg, S.L. Hunyadi-Lay, B.M. Fisher, D.M Rider, D. Crisp and R. Pollock (2017), Preflight Spectral Calibration of the Orbiting Carbon Observatory-2, *IEEE Trans. Geosci. Remote Sens.*, 55, 5, 2499-2508, <https://doi.org/10.1109/TGRS.2016.2645614>.
- Mandrake, L., C. Frankenberg, C. W. O'Dell, G. Osterman, P. Wennberg and D. Wunch (2013), Semi-autonomous sounding selection for OCO-2, *Atmos. Meas. Tech.*, 6, 2851-2864, <https://doi.org/10.5194/amt-6-2851-2013>.
- O'Dell, C.W., B. Connor, H. Bösch, D. O'Brien, C. Frankenberg, R. Castano, M. Christi, D. Crisp, A. Eldering, B. Fisher, M. Gunson, J. McDuffie, C. E. Miller, V. Natraj, F. Oyafuso, I. Polonsky, M. Smyth, T. Taylor, G. C. Toon, P. O. Wennberg, and

- D. Wunch, (2012), The ACOS CO₂ retrieval algorithm, Part 1: Description and validation against synthetic observations. *Atmos. Meas. Tech.*, 5, 99-121, <https://doi.org/10.5194/amt-5-99-2012>.
- O'Dell, C. W. et al (2018): Improved retrievals of carbon dioxide from Orbiting Carbon Observatory-2 with the version 8 ACOS algorithm, *Atmos. Meas. Tech.*, 11, 6539–6576, <https://doi.org/10.5194/amt-11-6539-2018>.
- Rodgers, C. (2000) *Inverse Methods for Atmospheric Sounding: Theory and Practice*. World Scientific Publishing Co Pte Ltd.
- Taylor, T.E., C. O'Dell, D.M. O'Brien, N. Kikuchi, T. Yokota, T. Nakajima, H. Ishida, D. Crisp, and T. Nakajima (2012), Comparison of cloud screening methods applied to GOSAT near-infrared spectra, *IEEE Trans. Geosci. Rem. Sens.*, <https://doi.org/10.1109/TGRS.2011.2160270>.
- Taylor, T.E., C.W. O'Dell, C. Frankenberg, P.T. Partain, H.W. Cronk, A. Savtchenko, R.R. Nelson, E.J. Rosenthal, A.Y. Chang, B.M Fisher, G.B. Osterman, H.R. Pollock, D. Crisp, A. Eldering, and M.R. Gunson, (2016), Orbiting Carbon Observatory-2 (OCO-2) cloud screening algorithms: validation against collocated MODIS and CALIOP data, *Atmospheric Measurement Techniques*, 9, 3, 973-989, <https://doi.org/10.5194/amt-9-973-2016>.
- Taylor, T. E. et al (2023), Evaluating the consistency between OCO-2 and OCO-3 XCO₂ estimates derived from the NASA ACOS version 10 retrieval algorithm, *Atmos. Meas. Tech.*, 16, 3173–3209, <https://doi.org/10.5194/amt-16-3173-2023>.

17.1.3 Chlorophyll Fluorescence

- Frankenberg, C., Fisher, J., Worden, J., Badgley, G., Saatchi, S., Lee, J.-E., et al. (2011), New global observations of the terrestrial carbon cycle from GOSAT: Patterns of plant fluorescence with gross primary productivity. *Geophysical Research Letters*, 38(17), <https://doi.org/10.1029/2011GL048738>.
- Frankenberg, C., O'Dell, C., Guanter, L., & McDuffie, J. (2012), Remote sensing of near-infrared chlorophyll fluorescence from space in scattering atmospheres: implications for its retrieval and interferences with atmospheric CO₂ retrievals. *Atmospheric Measurement Techniques*, 5(8), 2081–2094, <https://doi.org/10.5194/amt-5-2081-2012>.
- Joiner, J., Y. Yoshida, A. P. Vasilkov, Y. Yoshida³, L. A. Corp4, and E. M. Middleton (2011), First observations of global and seasonal terrestrial chlorophyll fluorescence from space, *Biogeosciences*, 8, 637–651 <https://doi.org/10.5194/bg-8-637-2011>.

17.1.4 Validation

Papers related to validation of the ACOS data product, plans for OCO-2 data validation or the TCCON network:

- Deutscher N. et al. (2010), Total column CO₂ measurements at Darwin, Australia - site description and calibration against in situ aircraft profiles, *Atmos. Meas. Tech.*, 3, 947–958, <https://doi.org/10.5194/amt-3-947-2010>.
- Frankenberg C. et al. (2016), Using airborne HIAPER Pole-to-Pole Observations (HIPPO) to evaluate model and remote sensing estimates of atmospheric carbon dioxide, *Atmos. Chem. Phys.*, 16, 7867-7878, <https://doi.org/10.5194/acp-16-7867-2016>.

- Jacobs N. et al. (2024), The importance of digital elevation model accuracy in X_{CO2} retrievals: improving the Orbiting Carbon Observatory 2 Atmospheric Carbon Observations from Space version 11 retrieval product, *Atmos Meas. Tech. Discuss.*, 17, 1375-1401, <https://doi.org/10.5194/amt-17-1375-2024>.
- Keppel-Aleks G. et al. (2011), Sources of variations in total column carbon dioxide, *Atmospheric Chemistry and Physics*, 11, 3581–3593, <https://doi.org/10.5194/acp-11-3581-2011>.
- Kiel M. et al. (2019), How bias correction goes wrong: measurement of X-CO₂ affected by erroneous surface pressure estimates, 12, <https://doi.org/10.5194/amt-12-2241-2019>.
- Kulawik, S. et al: Consistent evaluation of ACOS-GOSAT, BESD-SCIAMACHY, CarbonTracker, and MACC through comparisons to TCCON, *Atmos. Meas. Tech.*, 9, 683–709, <https://doi.org/10.5194/amt-9-683-2016>, 2016.
- Lindqvist H. et al. (2015), Does GOSAT capture the true seasonal cycle of carbon dioxide?, *Atmos. Chem. Phys.*, 15, 13023-13040, [doi:10.5194/acp-15-13023-2015](https://doi.org/10.5194/acp-15-13023-2015).
- Messerschmidt, J. et al: Calibration of TCCON column-averaged CO₂: the first aircraft campaign over European TCCON sites, *Atmos. Chem. Phys.*, 11, 10765–10777, <https://doi.org/10.5194/acp-11-10765-2011>, 2011.
- Washenfelder R. et al. (2006), Carbon dioxide column abundances at the Wisconsin Tall Tower site, *J. Geophys. Res.*, 111, D22305, <https://doi.org/10.1029/2006JD007154>.
- Wunch D. et al. (2010), Calibration of the Total Carbon Column Observing Network using aircraft profile data, *Atmospheric Measurement Techniques*, 3, 1351–1362, <https://doi.org/10.5194/amt-3-1351-2010>.
- Wunch D. et al. (2011a), The Total Carbon Column Observing Network, *Phil. Trans. R. Soc. A*, 369, 2087–2112, <https://doi.org/10.1098/rsta.2010.0240>.
- Wunch, D. et al: A method for evaluating bias in global measurements of CO₂ total columns from space, *Atmos. Chem. Phys.*, 11, 12317–12337, <https://doi.org/10.5194/acp-11-12317-2011>, 2011.
- Wunch, D. et al: Comparisons of the Orbiting Carbon Observatory-2 (OCO-2) XCO₂ measurements with TCCON, *Atmos. Meas. Tech.*, 10, 2209–2238, <https://doi.org/10.5194/amt-10-2209-2017>, 2017.

18 Acronyms

| | |
|------------------|--|
| ABO2 | O ₂ -A band cloud screening algorithm |
| ACOS | Atmospheric CO ₂ observations from space |
| AFE | Analog front-end electronics |
| aod | Aerosol optical depth |
| ARP | Ancillary radiometric product |
| ATBD | Algorithm theoretical basis document |
| CO ₂ | Carbon dioxide |
| CSU | Colorado State University |
| DN | Data number |
| DOAS | Differential optical absorption spectroscopy |
| ECMWF | European Centre for Medium-Range Weather Forecasts |
| EOS | Earth Observing System |
| EOS A-Train | EOS Afternoon Constellation |
| FP | Full physics (algorithm) |
| FPA | Focal plane array (or assembly) |
| FWHM | Full width at half maximum |
| GES DISC | Goddard Earth Sciences Data and Information Services Center |
| GOSAT | Greenhouse Gases Observing Satellite |
| GSFC | Goddard Space Flight Center |
| H ₂ O | Water |
| HDF | Hierarchical data format |
| ILS | Instrument line shape |
| IMAP-DOAS | Iterative maximum <i>a posteriori</i> differential optical absorption spectroscopy |
| JPL | Jet Propulsion Laboratory |
| L (0,1,..) | Level 0, 1, etc. data product |
| LOS | Line of sight |
| NASA | National Aeronautics and Space Administration |
| O ₂ | Oxygen |
| OCO | Orbiting Carbon Observatory |
| OCO-2 | Orbiting Carbon Observatory-2 |
| OCO-3 | Orbiting Carbon Observatory-3 |
| SAA | South Atlantic Anomaly |
| SCO2 | Strong CO ₂ band |
| SIF | Solar-induced chlorophyll fluorescence |
| SNR | Signal-to-noise ratio |
| TAI | International atomic time |
| TCCON | Total Carbon Column Observing Network |
| UTC | Coordinated universal time |
| VCD | Vertical column density |
| VMR | Volume mixing ratio |
| WCO2 | Weak CO ₂ band |
| WMO | World Meteorological Organization |

X_{CH_4} Column-averaged dry air mole fraction of atmospheric methane
 X_{CO_2} Column-averaged dry air mole fraction of atmospheric carbon dioxide